

**TECHNOLOGICAL INSTITUTE OF COSTA RICA**

**SCHOOL OF BIOLOGY**

**The University of Texas at Austin  
Molecular Cell and Developmental Biology  
The Gross Lab**



**THE ROLE OF CUGBP1 IN THE DEVELOPMENT OF  
ZEBRAFISH LENS**

**Report of Final Graduation Work  
In Partial fulfillment of the Requirements for the Degree of  
Bachelor of Biotechnology Engineering**

**Linette Pérez-Campos**

**Cartago April, 2012**

# THE ROLE OF CUGBP1 IN THE DEVELOPMENT OF ZEBRAFISH LENS

## Abstract

The lens is a transparent tissue in the anterior of the eye and its main role is to refract light on the retina. The lens consists of two types of cells: epithelial cells and fibers. Epithelial cells surround the anterior and lateral limits of the lens, remain proliferative and at the equator of the lens they differentiate into lens fibers. In this process newly generated lens fibers elongate and gradually lose their organelles, enabling transparency. Cataracts are any opacification of the lens that compromises its ability to refract light onto the retina, and can be genetic or environmentally induced.

Since it has been demonstrated that the zebrafish (*Danio rerio*) is an ideal organism to study human ocular disorders, this model system was utilized to study gene products that regulate normal lens development and that in pathological states contribute to cataracts. CUGBP1 is an mRNA binding protein that has been implicated in the multisystemic disease Myotonic Dystrophy 1 (DM1). DM1 is caused by a (CTG)<sub>n</sub> repeat expansion within the 3'UTR region of the *DMPK* gene. Its mechanism implies a toxic gain of function where expanded CUG mRNA repeats increase steady state levels of CUGBP1 protein among other effects. Patients with DM1 develop cataracts. So, it can be hypothesized that CUGBP1 disrupted expression in lenses from DM1 patients can be, at least, one of the causes that leads to cataracts in this disease.

*In situ* hybridization results show that *cugbp1* is expressed in the zebrafish lens at early embryonic development in newly formed lens fibers. Transgenic embryos expressing nuclear or membrane localized-EGFP under the control of a 1.2kb *cugbp1* promoter further demonstrate its expression in the lens. Knocking down expression of *cugbp1* with a splice-altering morpholino results in cataracts as early as 3dpf. Hence, the latter reveals that *cugbp1* expression is a requirement for normal lens early development. In morphant embryos, lens fiber compaction is disturbed. In addition, these cells retain nuclei. Lens overall shape and size is also affected. Furthermore, the defective phenotype includes a general developmental delay, little mobility and dilated cardiomyopathy, symptoms that are also observed in DM1 patients.

**Key words:** Cugbp1, Lens development, Lens fiber differentiation, Zebrafish.

# EL ROL DE CUGBP1 EN EL DESARROLLO DEL CRISTALINO DEL PEZ CEBRA

## Resumen

El cristalino (lente del ojo) es un tejido transparente en la región anterior del ojo y su rol principal es refractar la luz sobre la retina. El cristalino está constituido por dos tipos de células: células epiteliales y fibras. Las células epiteliales rodean la parte anterior y los límites laterales de la lente del ojo, mantienen su capacidad de proliferación y en el ecuador del cristalino se diferencian para generar fibras. En este proceso, las fibras recién generadas se elongan y gradualmente pierden sus organelas, permitiendo así la transparencia. Las cataratas se refieren a cualquier opacificación del cristalino que comprometa su habilidad de refractar la luz hacia la retina y pueden ser inducidas por la genética o el ambiente.

Debido a que se ha demostrado que el pez cebra (*Danio rerio*) es un organismo ideal para estudiar desordenes oculares humanos, este sistema modelo se utilizó para estudiar productos génicos que regulan el desarrollo normal de la lente y que en estados patológicos contribuyen a la aparición de cataratas. CUGBP1 es una proteína de unión a ARNm que ha sido implicada en la enfermedad multisistémica Distrofia Miotónica 1 (DM1). La DM1 es causada por la expansión de la repetición (CTG)<sub>n</sub> localizada en la región 3'UTR del gen *DMPK*. Su mecanismo implica una ganancia de función que es tóxica donde la expansión de las repeticiones CUG del ARNm estabilizan la proteína CUGBP1 provocando un aumento de sus niveles, entre otros efectos. Pacientes con DM1 desarrollan cataratas. Entonces, se puede plantear la hipótesis de que una expresión defectuosa de CUGBP1 en el cristalino de pacientes con DM1 puede ser, por lo menos, una de las causas que conllevan a la formación de cataratas en esta enfermedad.

Resultados de ensayos de hibridación *in situ* muestran que *cugbp1* se expresa en la lente del ojo del pez cebra durante el desarrollo embrionario temprano en fibras recién formadas. Embriones transgénicos que expresan la proteína verde fluorescente co-localizada en el núcleo o la membrana celular bajo el control de una región promotora de 1.2kb del gen *cugbp1* evidencian aún más su expresión en el cristalino. El disminuir la expresión (knock down) de *cugbp1* con un morfolino que altera el proceso de corte y empalme (splicing) resulta en la formación de cataratas a partir de los 3 días después de la fertilización. Por lo tanto, lo anterior revela que la expresión de *cugbp1* es un requerimiento para el desarrollo temprano normal de la lente del ojo. En embriones inyectados con el morfolino, la compactación de las fibras del cristalino se ve perturbada. Además, estas células retienen el núcleo. La forma y el tamaño generales de la lente del ojo también se ven afectados. Asimismo, el fenotipo defectuoso incluye un retraso general en el desarrollo, poca movilidad y miocardiopatía dilatada, síntomas que también se observan en pacientes con DM1.

**Palabras clave:** Cugbp1, Desarrollo del cristalino, Diferenciación de las fibras del cristalino, Pez cebra.

# **THE ROLE OF CUGBP1 IN THE DEVELOPMENT OF ZEBRAFISH LENS**

## **Accreditation**

**Report of final graduation work presented to the School of Biology**

**Costa Rica Institute of Technology**

**In partial fulfillment of the requirements for the Degree of**

**Bachelor of Biotechnology Engineering**

### **Tribunal Members**

---

**M.Sc. María Clara Soto-Bernardini**  
**Professor Costa Rica Institute of Technology**

---

**Ph.D. Jeffrey Gross**  
**Professor University of Texas at Austin**

---

**M.Sc. Olga Rivas-Solano**  
**Lector**

\*Signed accreditation is shown at Annex 1.

## Dedication

To my mother, that even though we think very differently,  
she has always been there to support me.

## **Acknowledgements**

I would like to thank Dr. Jeffrey Gross for allowing me to perform this amazing and interesting project in his laboratory.

Thank you to Julie Hayes for always guiding me in the experimental procedures of this project, teaching me how to work in a laboratory and always having a good and helpful attitude.

Thank you to Professor María Clara Soto-Bernardini for guiding me through the steps of the writing process of this project.

To Richard Nuckels, Julie Hayes and Jeffrey Gross thank you for performing previous valuable work in this project.

To Rosa Uribe thank you for always helping me and teaching me experimental procedures.

Thank you to all The Gross Lab members for always answering my questions and helping me along the way.

Thank you to Professor Olga Rivas-Solano for being the lector of this project.

Thank you to all my academic professors at the Biology School for teaching me theoretical and basic scientific knowledge.

Thank you to my mother and father for always supporting me and being helpful throughout my school years. I love you both.

## **General Index**

<b>Abstract</b>	2
<b>Resumen</b>	3
<b>Accreditation</b>	4
<b>Dedication</b>	5
<b>Acknowledgements</b>	6
<b>General Index</b>	7
<b>Index of Figures</b>	10
<b>Index of Annexes</b>	11
<b>Chapter 1. Introduction</b>	12
<b>Chapter 2. Research Aims</b>	14
2.1 General objective	14
2.2 Specific objectives	14
<b>Chapter 3. Theoretical Framework</b>	15
3.1 Zebrafish lens early development	15
3.2 Differences between mammalian and zebrafish lens development and early morphology	19
3.3 Lens fiber cells differentiation	21
3.3.1 Aquaporin0 (AQP0) expression and function	22
3.3.2 Lens actin cytoskeleton	24
3.3.3 Organelle degradation in lens fibers: emphasis in nuclei	29
3.4 CUG binding protein 1 (CUGBP1): an mRNA binding protein	32
3.5 Myotonic dystrophy 1 (DM1)	33
3.5.1 CDM phenotype	33
3.5.2 DM1 phenotypes	34
3.5.3 Molecular mechanisms of Myotonic dystrophy 1	36
3.5.4 CUGBP1 and its involvement in DM1 models and tissues	40
3.6 CUGBP1 and early development	41
3.7 DM1 and the lens	48

<b>Chapter 4. Materials and Methods</b>	<b>55</b>
4.1 RNA <i>in situ</i> hybridization with digoxigenin-labeled probe	55
4.1.1 <i>cugbp1</i> cDNA cloning	55
4.1.2 cDNA sequencing and protein sequence alignment	55
4.1.3 Digoxigenin-labeled probe synthesis	56
4.1.4 <i>In situ</i> hybridization	56
4.2 <i>cugbp1</i> promoter activity in microinjected and transgenic zebrafish embryos	57
4.2.1 Search and cloning of a zebrafish <i>cugbp1</i> promoter region	58
4.2.2 Location of the <i>cugbp1</i> promoter region in the zebrafish genome	58
4.2.3 Plasmids construction	59
4.2.4 Transposase mRNA synthesis	60
4.2.5 Injections	60
4.2.6 Immunohistochemistry on transverse cryosections from embryonic zebrafish eyes	61
4.3 <i>cugbp1</i> down regulation by splice-altering morpholino injections	61
4.3.1 Splice-altering morpholino injections	61
4.3.2 Test of morpholino activity by reverse transcription PCR (RT-PCR)	62
4.3.3 Observation of the phenotypes and behaviors of <i>cugbp1</i> -MO and <i>cugbp1</i> -MM injected embryos	63
4.3.4 BrdU incorporation assay, immunohistochemistry on transverse cryosections from embryonic eyes of previously injected <i>cugbp1</i> -MO and <i>cugbp1</i> -MM embryos and statistical analysis	63
4.3.5 Aquaporin0 (Aq0) immunohistochemistry on transverse cryosections from embryonic eyes of previously injected <i>cugbp1</i> -MO and <i>cugbp1</i> -MM embryos	64
4.3.6 F-actin staining on transverse cryosections from embryonic eyes of previously injected <i>cugbp1</i> -MO and <i>cugbp1</i> -MM embryos	64
4.3.7 Nuclei staining on transverse cryosections from embryonic eyes of previously injected <i>cugbp1</i> -MO and <i>cugbp1</i> -MM embryos	65
<b>Chapter 5. Results</b>	<b>66</b>
5.1 RNA <i>in situ</i> hybridization with digoxigenin-labeled probe	66
5.1.1 <i>cugbp1</i> cDNA sequencing and protein sequence alignment	66
5.1.2 <i>In situ</i> hybridization to detect mRNA expression	66
5.2 <i>cugbp1</i> promoter activity in microinjected and transgenic zebrafish embryos	70
5.2.1 Identification of the location of the <i>cugbp1</i> promoter region in the zebrafish genome	70
5.2.2 EGFP expression driven by a 1.2kb <i>cugbp1</i> promoter region	70
5.3 <i>cugbp1</i> down regulation by splice-altering morpholino injections in	74

zebrafish embryos	
5.3.1 Splice-altering morpholino activity tested by RT-PCR	74
5.3.2 Morphant vs. control embryos phenotype and behavior	75
5.3.3 Cell proliferation analysis by BrdU incorporation assay in lens cells after <i>cugbp1</i> down regulation	75
5.3.4 Expression of lens fiber membrane protein Aquaporin0 as a marker of early fiber differentiation after <i>cugbp1</i> down regulation	75
5.3.5 F-actin organization in the lens after knocking down <i>cugbp1</i> expression	80
5.3.6 Lens fibers nuclei degradation in <i>cugbp1</i> -MM vs. <i>cugbp1</i> -MO embryos	80
<b>Chapter 6. Discussion and Conclusions</b>	<b>84</b>
6.1 <i>cugbp1</i> expression on zebrafish early lens development	84
6.1.1 <i>cugbp1</i> cDNA sequencing and protein sequence alignment	84
6.1.2 <i>cugbp1</i> mRNA expression and promoter activity	84
6.2 <i>cugbp1</i> down regulation by splice-altering morpholino injections in zebrafish embryos	91
6.2.1 Splice-altering morpholino activity tested by RT-PCR.	91
6.2.2 Morphant (MO) vs. control (MM) embryos phenotype and behavior	94
6.2.3 Cell proliferation and differentiation analysis in the lens of <i>cugbp1</i> knock down in zebrafish embryos	102
6.2.4 F-actin organization in the lens of <i>cugbp1</i> -MO zebrafish embryos	105
6.2.5 Nuclei degradation in <i>cugbp1</i> -MM embryos vs. <i>cugbp1</i> -MO embryos	106
<b>Chapter 7. Recommendations and Future Directions</b>	<b>109</b>
7.1 Identification of Cugbp1 RNA targets at the developing zebrafish lens	109
7.2 Reversal of <i>cugbp1</i> morpholino phenotype by RNA rescue	112
7.3 Other experiments	113
<b>References</b>	<b>114</b>
<b>Annexes</b>	<b>128</b>

## Index of Figures

<b>Figure 5.1.1</b>	Amino acid sequence alignment of <i>cugbp1</i> cDNA with previously reported <i>cugbp1</i> sequence DDBJ AB032726.	67
<b>Figure 5.1.2a</b>	Diagram representing a transverse section of the zebrafish lens.	68
<b>Figure 5.1.2b</b>	Transverse sections of zebrafish eyes show expression of <i>cugbp1</i> mRNA in the lens by <i>in situ</i> hybridization assay.	69
<b>Figure 5.2.1</b>	EGFP expression driven by a 1.2kb <i>cugbp1</i> promoter in F0 zebrafish embryos.	71
<b>Figure 5.2.2a</b>	Transverse sections at the eye region from zebrafish F1 stable transgenic line embryos carrying the 1.2kb <i>cugbp1</i> :pME-nlsEGFP-polyA transgene.	72
<b>Figure 5.2.2b</b>	Transverse sections at the eye region from zebrafish F1 stable transgenic line embryos carrying the 1.2kb <i>cugbp1</i> :pME-EGFPCAAX-polyA transgene.	73
<b>Figure 5.3.1</b>	Knock down of <i>cugbp1</i> function in zebrafish embryonic development by a splice-altering morpholino results in a cataract phenotype and other features that resemble DM1 disease.	76
<b>Figure 5.3.3</b>	BrdU incorporation assay at 24-26 or 72-74hpf showed that there were no differences in the total number of proliferative cells in the lens between <i>cugbp1</i> -MO and <i>cugbp1</i> -MM embryos.	78
<b>Figure 5.3.4</b>	Lens fibers express differentiation marker Aqp0 in <i>cugbp1</i> -MO embryos.	79
<b>Figure 5.3.5</b>	F-actin organization in the lens mass shows differences between <i>cugbp1</i> -MO and <i>cugbp1</i> -MM embryos.	81
<b>Figure 5.3.6</b>	Nuclei staining (Sytox Green) exhibits a flawed lens fiber late differentiation after knocking down <i>cugbp1</i> expression.	82
<b>Figure 6.2.1</b>	Splice-altering <i>cugbp1</i> morpholino activity generates a frameshift and a premature stop codon by removing exon5.	92

## Index of Annexes

<b>Annex 1.</b>	Signed accreditation	128
<b>Annex 2.</b>	CS10R plasmid	129
<b>Annex 3.</b>	Sequence alignment of <i>cugbp1</i> cDNA used for probe synthesis	130
<b>Annex 4.</b>	Amino acid sequence from <i>cugbp1</i> cDNA used for probe synthesis	132
<b>Annex 5.</b>	Protocol for <i>cugbp1</i> probe synthesis	133
<b>Annex 6.</b>	Whole mount RNA <i>in situ</i> hybridization protocol	134
<b>Annex 7.</b>	Immunohistochemistry protocol	137
<b>Annex 8.</b>	<i>cugbp1</i> promoter sequence and location	140
<b>Annex 9.</b>	RT-PCR Morpholino Activity	
	<b>A.</b> Morpholino disrupted splicing by removing exon4	141
	<b>B.</b> Mismatch morpholino did not disrupt splicing	142
<b>Annex 10.</b>	BrdU+ cell counts	143

## **Chapter 1. Introduction**

The lens is a transparent and avascular tissue in the anterior of the eye and its main role is to refract light onto the retina where light is transduced into neural signals. Afterwards, these signals are transmitted to the brain. The vertebrate lens consists of two types of cells: epithelial cells and fibers. Epithelial cells surround the anterior and lateral limits of the lens, remain proliferative and at the equator of the lens, or near to it, they differentiate into lens fibers (Chow and Lang 2001; Tsang and Gouras 2006; Greiling and Clark 2009). In this process newly formed lens fibers elongate and gradually lose their organelles, enabling transparency (Bassnett 2009).

Cataracts are defined as any opacification of the lens that compromises its ability to refract light onto the retina (Graw 1999). According to the World Health Organization, the latest estimates (Oct., 2011) say there are 285 million people visually impaired worldwide and about 90% of them live in developing countries. Cataracts account for 33% of global visual impairment ( $VI = VA < 0.3$ ) and are still the main cause of blindness in third world nations (WHO 2011). Visual acuity (VA) is the ability to distinguish details and shapes of objects. Any visual deprivation, such as lens opacities, will result in a decrease of VA. In humans, VA develops from birth to adolescence and a VA of 1.0 is reached by 5-6 years of age (Ekström 2009). Cataracts can be genetic and/or environmentally induced and can happen via many different cellular and molecular mechanisms. Therefore, it is necessary to investigate the cellular and molecular basis of lens development and physiology to be able to understand the reasons that cause cataracts. This will lead to aim for new and better therapeutic treatments (Gross and Perkins 2007; Wormstone and Wride 2011).

The zebrafish (*Danio rerio*) has emerged as an ideal model to study early development and disease of the visual system, including the lens of the eye. Some of the zebrafish advantages to study overall embryonic development are: external fertilization, their rapid development compared to other vertebrate model organisms, embryonic development occurs *ex utero*. The embryo is transparent which facilitates visual identification of morphogenetic movements and organogenesis with a standard dissection microscope. Zebrafish are easily adapted to laboratory settings and can be maintained in a relatively small space compared to

other vertebrate model systems. These freshwater fish reach sexual maturity in just 3-4 months and a single pair of fish can produce >200 fertilized eggs per mating. These characteristics have made zebrafish embryos ideal for the discovery of the function of genes implicated in regulating embryonic development, including lens morphogenesis (Glass and Dahm 2004; Fadool and Dowling 2008; Greiling and Clark 2009).

Zebrafish are very visually oriented and their lenses show much the same morphology as other vertebrates, including humans (Glass and Dahm 2004). Their visual system is first identified as a functional structure between the third and fourth days post fertilization (dpf; Easter and Nicola 1996). Moreover, the lens shape and overall structure suggests it is a functional optical element in the visual pathway as early as 3dpf (Greiling and Clark 2009). All the aspects mentioned above make zebrafish well suited for examining lens development, function and disease.

## **Chapter 2. Research aims**

### **2.1 General objective**

- Identify and investigate the role of Cugbp1 protein in early zebrafish (*Danio rerio*) lens development.

### **2.2 Specific objectives**

- Detect if there is *cugbp1* mRNA expression in zebrafish early lens development, and if so, where inside the lens and at what developmental stages is it expressed.
- Identify a promoter at the *cugbp1* gene that directs expression at the zebrafish lens to estimate Cugbp1 protein expression.
- Identify if a specific *cugbp1* morpholino alters splicing of *cugbp1* mRNA.
- Identify phenotypical defects in whole embryos, at first sight, due to down regulation of *cugbp1* and compare them with defects previously reported at DM1 disease where *cugbp1* expression is also disrupted.
- Observe if lens development is affected when *cugbp1* expression is down regulated and recognize a role for Cugbp1 protein in zebrafish early lens development.
- Detect if Cugbp1 is necessary for zebrafish lens cell proliferation.
- Identify if Cugbp1 is required for the expression of Aqp0 protein to detect if Cugbp1 is necessary for zebrafish lens fibers early differentiation.
- Recognize if *cugbp1* has a role in F-actin distribution and/or arrangement in zebrafish lens fibers.
- Identify if Cugbp1 is involved in nuclei degradation in zebrafish lens fibers to recognize if Cugbp1 is needed for lens fibers maturation.

## **Chapter 3. Theoretical Framework**

### **3.1 Zebrafish lens early development**

Zebrafish lens establishment starts at the 14-15 somite stage (~16hpf; hours post fertilization) with a contact between the surface cranial ectoderm and an evaginating solid mass of cells that comes from the diencephalon (more posterior and ventral part of the forebrain) and constitutes the optic primordium. The optic primordium is a solid mass of cells that emerges from the anterior portion of the neural tube and will eventually give rise to the retina. The forebrain or prosencephalon refers to the most anterior region of the brain and it includes the diencephalon (Schmitt and Dowling 1994; Kimmel *et al.* 1995; Soules and Link 2005; Dahm *et al.* 2007; Greiling and Clark 2008).

The surface ectoderm-optic primordium interaction results in the thickening of the lens placode and in zebrafish, this occurs at 16hpf. This thickening starts as a columnar epithelium by doubling of the basal to apical height of cells from simple cuboidal epithelium of the cranial surface ectoderm (Schmitt and Dowling 1994; Greiling and Clark 2008; Greiling and Clark 2009). The lens placode is defined as the ectodermal primordium of the lens and it overlies the center of the developing retina (Kimmel *et al.* 1995; Dahm *et al.* 2007; Greiling and Clark 2009).

When observed from the surface the lens placode, from 16hpf zebrafish embryos, looks circular, of approximately 8 cells in diameter, and it is composed of columnar cells relatively uniform in size and shape. At this point, the lens placode of the zebrafish resembles the mammalian or avian placode (Greiling and Clark 2009).

By 18hpf, many of the cells in the lens placode have more than double in height as compared to 16hpf, and look as a solid mass of cells ordered as a flattened spheroid (plate-like thickening organization). The lens mass is two or three cell-layers thick at the center with a single layer remaining laterally. The change in morphology has made elongated cells of the lens placode clearly distinguishable from cuboidal cells of the surface ectoderm. In the anteromedial region of the lens mass, cells are shorter and more rounded than the elongated cells present at the posterior and lateral lens borders (Greiling and Clark 2009). At the analogous moment in development, the mammalian and avian single layered lens placodes

start to invaginate instead of undergoing a delamination growth process as in zebrafish embryos (Fadool and Dowling 2008; Greiling and Clark 2008).

At 20hpf the thickness of the lens mass increases bulging towards the retina and narrows in the equatorial dimension. At this moment, it is quite obvious that the lens placode has changed from a plate-like structure to a lentoid solid mass of cells that will eventually acquire a more spherical shape (Fadool and Dowling 2008; Greiling and Clark 2008; Greiling and Clark 2009). Elongated fiber-like cells appeared along the deep and lateral boundaries of the lens mass surrounding a central core of rounded, undifferentiated cells. Three distinct cell morphologies can be seen at this stage: (1) cells at the posterior and lateral surfaces are tall and similar in height to the elongated cells at 18hpf. These cells formed a single layer that establishes a posterior and lateral border of the lens and have a basal cell surface 2-3 times wider than the apical surface. (2) Cells in the center of the elongated lens mass with round or ovoid shape and irregularly clustered in the center of the lens core and stalk (region located in the anterior-middle). (3) Cells at the anterior lens border in contact with the surface epithelium are elongated and with a more parallel orientation to the surface ectoderm (Greiling and Clark 2009).

At 22hpf cells attached to the surface ectoderm narrow to form a stalk 2 to 3 cells wide connecting the developing cornea with the developing lens. At this moment of development the shape of the lens mass is rounded. Three morphologically distinct cell types are clearly present: (1) the lateral and posterior borders of the lens are formed by a single-layer of tall columnar cells with wider basal than apical cell surfaces. These cells radiated out from the central core. (2) The central core is a cluster of cells in the middle of the lens; these cells appear to have a tear-drop shape with their narrow edges facing towards the center. (3) Cells at the anterior-middle of the lens and the surface ectoderm in contact with the lens are rounded or cuboidal in shape with an irregular arrangement. These 3 cell types correspond to the primary fiber cells, the embryonic nucleus, and undifferentiated cells of the original lens mass, respectively (Greiling and Clark 2009). The analogous lens developmental stage of mammals and birds shows a different formation pattern. In these superior vertebrates the lens placode continues its invagination process forming a cavity that pinches off from the surface ectoderm

as a fluid-filled lens vesicle surrounded by a single layer of epithelial cells (Reza and Yasuda 2004; Soules and Link 2005; Greiling and Clark 2008).

The lens mass remains connected to the surface ectoderm at 23hpf by a stalk that is only one cell wide. The surface ectoderm is a single-layer of flat, cuboidal epithelium above the lens except where it is still attached to the lens in the very anterior-middle border. Fiber-like cells begin to curve and appear to wrap around the central core. Cells in the central core of the lens mass remain large and tear-drop shaped with their narrow edges facing the lens center. The cells at the anterior-middle of the lens remained rounded or cuboidal in shape and in an irregular arrangement (Greiling and Clark 2009).

At 24hpf the lens mass separates completely from the surface ectoderm which remains a continuous single layer of epithelial cells at the surface of the head of the fish. Cells in the posterior-middle region continue to enlarge and take on a rounded shape forming an organizing center around which primary fiber cells elongate and migrate. Lateral columnar cells elongate further to form arcs or layers of primary lens fibers surrounding the nucleus. Cells at the anterior border organize into a single-layer of epithelium and cells deep to the developing anterior epithelium are still disorganized and undifferentiated (Schmitt and Dowling 1994; Greiling and Clark 2009).

The morphology of the differentiated lens cells at 28hpf represents the cell types expected in the adult lens: (1) A single-layer of tall, cuboidal epithelium that covers the entire anterior hemisphere of the lens and that in zebrafish, but not mammals, extends posteriorly beyond the lens equator, but not in the posterior-most surface of the lens. (2) Primary fiber cells that wrap around the large round cells in the core of the lens nucleus. (3) Secondary fiber cells that elongate and migrate from a developing transition region (Dahm *et al.* 2007; Greiling and Clark 2009). In the zebrafish lens, this transition region is located more posteriorly as compared to the mammalian and avian lenses that possess this region at their equator. This type of region in the lens is common among vertebrates and it is where epithelial cells exit the cell cycle and start differentiating into secondary lens fibers (Soules and Link 2005; Griep 2006; Weber and Menko 2006b; Greiling and Clark 2008).

By 36hpf the lens seems spherical in the equatorial dimension and lentoid in the anterior-posterior dimension. Newly added fiber cells are smaller and more compact than at

28hpf and the height of the anterior epithelial cells is decreased by half. Cell membranes between the central cells look jagged like establishing shallow interdigitations between them (Greiling and Clark 2009).

By 2dpf zebrafish embryos start their hatching period (Kimmel *et al.* 1995; Easter and Nicola 1996; Easter and Nicola 1997). At 48hpf, the lens still appears spherical at the equator and lentoid in the anterior-posterior direction. By 2days the lens has increased in size and cells of the anterior epithelium continue to decrease in height and form a flat cuboidal epithelium. Fiber cells in the cortex are narrow and elongated. The posterior tips of newly added elongating fiber cells meet at the midline establishing a posterior suture. Borders between cells in the lens mass are increasingly jagged (Greiling and Clark 2009).

At 72hpf (3dpf; first day post hatch; Kimmel *et al.* 1995), the width of the lens increases at the equator making the lens shape spherical in all dimensions. An umbilical suture (point-like) can be seen at both the anterior and posterior poles (Greiling and Clark 2009). A thin extracellular capsule is apparent, which is an uninterrupted basement membrane completely enclosing and protecting the lens. Newly generated lens fibers possess interdigitations that have not yet achieve an eventual ball and socket organization (Soules and Link 2005; Danysh and Duncan 2009). Between the third and fourth dpf the still growing zebrafish visual system is first identified as a functional structure (Easter and Nicola 1996). By 4dpf the lens is a larger spherical version of the 3dpf lens, that increases in size by additional layers of secondary fiber cells (Greiling and Clark 2009).

As lens development and growth proceeds through embryogenesis into postnatal (mice) or larval (zebrafish) and subsequently throughout adult life a distinguished organization of regions with high or low proliferative index arises at the lens epithelium. This epithelial tissue has 4 distinct subpopulations: (1) a central zone (CZ) that comprises the biggest portion of lens epithelial tissue covering most of the anterior surface of the lens. This region has a low proliferative index with most of its cells in a quiescent state (G0); although they retain their proliferative potential. (2) A pregerminative zone (PGZ) that constitutes cells comprising a narrow, latitudinal band or ring peripheral to and limiting the CZ. A small portion of these cells undergo mitosis to add to the lens epithelial mono-layer as the lens increases in size throughout life. Only rarely, the daughter cells differentiate into lens fibers. (3) Cells in the

germinative zone (GZ) are located at a narrow, latitudinal band peripheral and posterior to the PGZ. In the GZ cells have a high proliferative index. Daughter cells from the GZ migrate into the transition region of the lens. (4) A transition zone (TZ) is found posterior to the GZ at the equatorial (mice) or posterior to the equatorial (zebrafish) arc or bow region of the lens. This zone is a narrow ring of cells where proliferation does not happen. Cells in this place exit the cell cycle, elongate and differentiate into secondary lens fibers as they form concentric layers around previously formed lens fibers. This summarizes how cells are continuously added to the differentiated fiber cell mass that originates from the epithelium (Graw 1999; Soules and Link 2005; Griep 2006; Kuszak and Costello 2006; Mathias *et al.* 2010).

In addition, it is important to mention that as the lens matures, its fiber cells become flattened and band-like shaped with a width to thickness ratio between 10:1 and 15:1. Lens fibers develop interdigitating lateral membrane protrusions at their narrow edges and ball and socket-like joints on their broad surfaces (Dahm *et al.* 2007).

### **3.2 Differences between mammalian and zebrafish lens development and early morphology**

Although the mammalian, bird and zebrafish lens are all derived from surface ectoderm, zebrafish early lens development possess noteworthy differences compared to mammals and birds. During embryonic development, the mammalian and avian lens placode invaginates to form a hollow lens vesicle bordered by a monolayer of ectoderm that constitutes epithelial cells. Instead, in zebrafish the lens placode delaminates as a solid cluster of cells from the surface ectoderm (Schmitt and Dowling 1994; Easter and Nicola 1996; Soules and Link 2005; Dahm *et al.* 2007).

In birds and mammals, primary lens fibers are formed from epithelial cells located in the posterior half of the lens vesicle. These posterior epithelial cells elongate in a posterior to anterior direction and a parallel-like way. They differentiate to fill the lens vesicle cavity as primary fibers. In contrast, in zebrafish primary lens fibers differentiate from cells in the center of the delaminated solid cluster of cells by elongating in a circular fashion. Thus, giving rise to concentrically arranged primary lens fibers. In both cases, primary lens fibers give rise to the lens nucleus (Dahm *et al.* 2007; Greiling and Clark 2008; Greiling and Clark 2009).

Cells in the anterior half of the still fluid-filled lens vesicle in birds and mammals as well as cells in the anterior-most border of the lens solid mass in zebrafish become the lens anterior epithelium. These epithelial cells exhibit a high mitotic activity to form a mono-layer of epithelial cells that extends along the anterior and equatorial surface of the lens. However, in contrast to birds and mammals, in zebrafish the epithelial single layer extends farther towards the posterior-lateral surface of the lens. And, like birds and mammals, the epithelial cell layer does not extend to the most-posterior border area in zebrafish lenses. At this region, lens fibers are in direct contact with the lens capsule (Dahm *et al.* 2007; Greiling and Clark 2008).

As mentioned before, another difference corresponds to the location of the transition region where epithelial cells differentiate to give rise to secondary lens fibers. In mammals and birds this region is located at the lens equator; whereas in zebrafish, this transition zone is at a more posterior region compared with the lens equator (Soules and Link 2005; Griep 2006; Weber and Menko 2006b; Greiling and Clark 2008).

Lens suture formation as fibers elongate and meet at their narrow edges with another fiber is another variant. Zebrafish, as well as avian lenses exhibit two umbilical sutures (point-like), one at the center of the anterior pole and the other one at the center of the posterior pole. In these types of sutures fiber cells are meridians and taper at the ends as they extend from pole to pole. All fibers are sequentially overlaid onto existing growth shells of fibers, resulting in radial cell columns that extend from the center (at the transitional zone) to both the anterior and posterior poles of the lens. These fibers are seen as straight meridians (circular arcs) that extend from pole to pole (Al-Ghoul *et al.* 2003). Dahm *et al.* (2007) have shown that when the lens capsule, the monolayer of epithelial cells and some of the outer-most fiber cells are removed the umbilical anterior lens suture, from zebrafish whole lens samples becomes visible. Scanning electron microscopy micrograph pictures show that the secondary lens fibers converge in a single point at each lens pole.

In contrast, the fibers of other superior vertebrates are not meridians. These lens fibers possess ends that flare (spread gradually outward) and curve away from the poles in opposite directions. As a result the end-to-end arrangement, where opposing fibers meet produces lens suture branches instead of just a suture point in the lens as a whole. Lenses with line sutures

(e.g., rabbit and frog lenses), feature two anterior branches oriented at 180° to each other to form a vertical line-like suture. Opposite end curvature results in two posterior branches forming a horizontal line-like suture (Al-Ghoul *et al.* 2003).

Other vertebrates (e.g., mice, rat, pig, cat, dog, bovine and primates at birth) have lenses with Y-like sutures. In this type of lenses three anterior branches orient at 120° to each other to form a Y-like suture. Opposite end curvature results in three posterior branches that form an inverted Y-like suture. In primates, the overall type of suture changes over time. During fetal development the previously described Y-like sutures form. During infancy an anterior and posterior six branch suture, referred as simple star develops. At adolescence, both sutures evolve to become nine branch sutures, known as star. Later on, at the adult stage the sutures are gradually transformed and become 12 branch sutures, referred as complex star (Al-Ghoul *et al.* 2003; Kuszak *et al.* 2004).

These differences must be taken into account when interpreting results of molecular biology studies (Dahm *et al.* 2007). The present work is an example of this type of studies in which the purpose is to try to identify the function of a gene (*cugbp1*) in early zebrafish lens development. The results obtained have the ultimate goal to try to understand what can happen if the pathway of the human ortholog *CUGBP1* is interrupted in embryonic development and unravel its early function in lens formation.

### **3.3 Lens fiber cells differentiation**

At the TZ of the lens, epithelial cells initiate their differentiation to become fibers, a process that comprises dramatic changes in gene expression as well as in cell shape. It has been observed that actin filament reorganization is necessary for both types of changes to happen (Weber and Menko 2006a). In the cortical region (outer layers, which are comprised of differentiating lens fibers that still have not lost their organelles) of the embryonic lens, the fiber cells elongation process occurs in parallel with the accumulation of lens differentiation-specific proteins (e.g., AQP0; Varadaraj *et al.* 2007).

In fact, lens fibers can elongate more than 1,000 fold to reach the lens sutures. The stretched fiber cells are arranged as a series of concentric layers in which they appear as flattened hexagons in sections along the equator (Nowak *et al.* 2009) with two broad and four

narrow lateral faces. The broad lateral faces are oriented parallel to the lens surface (Kuszak and Costello 2006). After the morphogenetic changes associated with elongation have happened, the maturing fiber cells lose their organelles, including nuclei to enable transparency (Weber and Menko 2006a).

### **3.3.1 Aquaporin0 (AQP0) expression and function**

Epithelial cells at the transition bow of the lens initiate a change in the pattern of gene expression as they start to differentiate into lens fibers. The new pattern includes the expression of structural proteins that can be soluble (e.g. crystallins) and also membrane proteins (e.g. water channels) in the lens fibers. Crystalline proteins contribute to the transparency and appropriate refractive index of the lens. This happens due to the crystallins elevated concentration and short-range interaction. Membrane proteins maintain the architecture needed for lens appropriate function, also contributing to lens transparency (Chepelinsky 2009). Aquaporin proteins (AQPs) are transmembrane water channels that mediate the permeation of water across cell membranes (Agre *et al.* 1998).

The lens lacks blood vessels since they would scatter the incident light (deviate light from its original trajectory). Hence, this avascular region of the eye has evolved a standing and efficient circulatory current known as microcirculatory system. This current enters at both the anterior and posterior poles of the lens; then passes into and through the lens fibers. Finally, the current exists at the equatorial region of the lens. This circulatory system depends on water channels (Mathias *et al.* 2010).

In mice, it has been observed that Aquaporin0 (*Aqp0*; previously known as *Mip*) mRNA as well as protein expression is observed in the lens. It begins at embryonic day 11.25 (E11.25) when the posterior lens epithelial cells simultaneously start to differentiate into primary lens fibers. This expression continues throughout lens development and in the adult lens. AQP0 protein is exclusively expressed at the cell membranes of primary and secondary lens fibers since their early cell differentiation. This membrane location remains permanently (Varadaraj *et al.* 2007).

It has also been shown that a second aquaporin gene, Aquaporin1 (*Aqp1*) is expressed in mice lens. However, this protein is expressed in lens epithelial cell membranes and not at

lens fibers. AQP1 expression at the lens starts at E17.5, 7.25 hours later than AQP0 expression begins at lens fibers. This happens even though lens anterior epithelium develops earlier than primary and secondary lens fibers. Secondary lens fibers that differentiate from epithelial cells that have already expressed AQP1 show progressive decrease of AQP1 protein expression as they differentiate (Varadaraj *et al.* 2007).

The temporal pattern of expression between AQP0 (E11.5) and AQP1 (E17.5) suggests that as the lens body increases in size by the addition of new lens fibers, there is a growing demand for higher epithelial membrane water permeability to establish the microcirculatory system. In addition, the lens switch from AQP1 expression in epithelial cells, located at the transitional ring of the lens, to AQP0 in the differentiating secondary lens fibers. This indicates that AQP0 may have other important membrane functions. AQP0 might also function as an adhesion protein to join adjacent fiber cells. AQP0 probably contributes to reduce the extracellular space between lens fibers and to diminish light scattering (Varadaraj *et al.* 2007).

It is thought that after the two principal evolutionary radiations of jawed vertebrate life that separated the ray-finned fish (class Actinopterygia; includes the zebrafish) and the sarcopterygian lineage (from where the land vertebrates evolved), a genome-wide duplication event happened in a zebrafish early ancestor (Meyer and Schartl 1999). This possible incident might explain why many single copy genes in mammals can be observed as duplicates in zebrafish where the function and temporal-spatial expression of the single-copy mammalian gene can be split up between both duplicates (Postlethwait *et al.* 2004).

Indeed, it has been shown that the zebrafish genome has two *aqp0* genes referred as *aqp0a* and *aqp0b*. Both genes are expressed during lens development in fiber membranes and persist in the adult lens (Froger *et al.* 2010; Tingaud-Sequeira *et al.* 2010). Moreover, knocking down *aqp0a* and/or *aqp0b* in zebrafish embryos by translation altering morpholino results in an obvious cataract phenotype as early as 3dpf (Froger *et al.* 2010). Morpholinos are chemically modified oligonucleotide analogous with a morpholino moiety instead of a ribose. They also possess a non-ionic phosphorodiamidate linkage instead of an anionic phosphodiester bond resulting in a neutrally charged backbone. These mentioned variations form a modified and highly soluble polymer that hybridizes RNA molecules with high affinity

and little cellular toxicity. Moreover, morpholinos are resistant to digestion by nucleases (Ekker 2000; Corey and Abrams 2001).

Froger *et al.* (2010) experiments have indicated that both *aqp0a* and *aqp0b* are needed for lens transparency. Nevertheless, water permeability assays suggest that Aqp0a protein functions as a water channel, whereas Aqp0b does not. Aqp0b might supply adhesion and/or interactions with other lens components. Mammalian *Aqp0* functions might be distributed between *aqp0a* and *Aqp0b* in zebrafish. However, additional work is needed to figure out *aqp0b* function on the zebrafish lens.

The unique eye expression of Aqp0 protein in lens fibers as they start their differentiation process from initial epithelial cells makes this protein an excellent marker to assess for early fiber cell differentiation in the lens.

### **3.3.2 Lens actin cytoskeleton**

During fibrogenesis, epithelial cells undergo elongation, with the anterior and posterior tips of the elongating lens fibers sliding along the epithelium and capsule at the anterior and posterior direction, respectively and as these cells migrate inward. Lens fibers finally detach from the epithelium and capsule when they reach the anterior and posterior sutures. At the sutures, fiber cells form contacts with their counterparts from the opposite side of the lens. All these cellular movements are greatly coordinated through actin cytoskeleton remodeling events (Rao and Maddala 2006). Thus, the actin cytoskeleton plays an important role in regulating fiber cell elongation, migration, lens capsule-cell and intercellular interactions, cell packing, overall geometry and in the maintenance of fiber cell symmetry. Therefore, the activities of the actin cytoskeleton are critical for the establishment of lens overall shape, symmetry and ultimately, for lens optical properties (Rao and Maddala 2006).

The actin cytoskeleton is composed of F-actin (actin filaments or microfilaments) and other accessory proteins that vary depending on the type of structure formed. F-actin represents a helical protein filament formed by polymerization of globular actin molecules (G-actin). During remodeling of the actin cytoskeleton, F-actin undergoes disassembly and reassembly (Alberts *et al.* 2008).

Studies performed in Quails (*Coturnix japonica*; class Aves) during embryonic lens development by Weber and Menko (2006a) have shown that a disassembly of actin stress fibers (contractile large bundle/parallel arrays of F-actin crosslinked by  $\alpha$ -actinin) happens as lens fiber differentiation is initiated. In central epithelial cells at the anterior region of the lens, actin stress fibers are organized along these cells basal surfaces (face linked to the lens capsule). Indeed, actin stress fibers are the primary actin filament structures of the undifferentiated lens epithelium and are most possibly linked to extracellular matrix components of the lens capsule through integrin receptors. In general, integrins are transmembrane adhesion proteins that play part in cell-matrix junctions. The extracellular domains of integrins bind to components of the extracellular matrix (in these case: lens capsule), while the cytoplasmic tail binds indirectly to F-actin. This type of cell-extracellular matrix junction in which there is an intracellular coupling to F-actin is called focal adhesion (Cooper 2000; Alberts *et al.* 2008). Lamellipodial-like extensions are broad membrane protrusions that contain a three-dimensional network of F-actin and can contribute in focal adhesion formation (Cooper 2000; Lodish *et al.* 2000). These extensions were observed at the central epithelial cells basal edges. At the apicolateral (apical: faces the center of the lens) aspects of these cells in the region of tight junctions (physical attachments that seal the gaps between cells in the apical side of epithelia making the sheet an impermeable or selectively permeable barrier), F-actin had a cortical arrangement (Weber and Menko 2006a).

However, at the equatorial epithelium where differentiation has started, a different F-actin organization was observed. In the anterior-most region of the equatorial epithelium, F-actin staining in the cells basal and basolateral aspects was amorphous and diffused indicating that actin stress fibers were no longer present. This loss of actin stress fibers was concomitant with lens cell differentiation. At the cells lateral borders (region of cell to cell interfaces) few F-actin was detected. F-actin at the apical domain remains cortical. At the very center of the equator, F-actin staining was disorganized and diffuse in the basal surfaces. The latter is indicative of a transition due to actin filament reorganization as cells moved through the transition region. As cells moved to the posterior-most aspects of the equatorial epithelium, F-actin became localized at the cell to cell interfaces at their basal surfaces as well as along the lateral sides. Moreover, dense clusters of F-actin in the center of the cell that radiated out to

the cell borders were evident at the basal surfaces of these cells. Cortical F-actin at the cells lateral borders is consistent with their function in the assembly of stable N-cadherin cell-cell junctions (Weber and Menko 2006a). Cadherins are transmembrane proteins that mediate contacts between cells to form adherence junctions. Inside the cell, cadherins bind indirectly to F-actin (Cooper 2000; Alberts et al. 2008).

At the most cortical fiber cell region in the posterior pole of the lens, F-actin was present at the basal tips of lens fibers and organized in a dense meshwork pattern. The basal tips of these newly formed cortical lens fibers correspond to the surface in contact with the lens basement membrane/capsule at the posterior region of the lens. At the basal and basolateral aspects, F-actin is present along all sides of the already hexagonal cells, but is missing from the vertices (region where three cells meet). At the lateral surfaces of these lens fibers, cortical F-actin extended around the entire perimeter of the cells and along the length of these elongating lens fibers. Cortical F-actin became much more organized than at earlier moments of differentiation probably helping to stabilize lens elongated and hexagonally packed morphology (Weber and Menko 2006a).

In summary, Weber and Menko (2006a) have demonstrated that the initiation of lens cells differentiation is coincident with the disassembly of the cellular projections (lamellipodia) and actin stress fibers that provide cell attachment between the extracellular matrix (capsule) and the undifferentiated lens epithelia. F-actin is reorganized as cortical actin in the differentiating lens fibers. Indeed, stress fibers disassembly is sufficient to induce lens fibers differentiation. Actin filaments organized as stress fibers interact with integrin receptors at focal adhesion complexes where they mediate integrin/matrix adhesion. The lens epithelium is the only region of the embryonic lens that expresses high levels of  $\alpha 5\beta 1$  integrin and fibronectin (extracellular matrix ligand of  $\alpha 5\beta 1$  integrin). The interaction of both molecules promotes actin stress fibers organization and their loss could signal stress fibers disassembly that activates lens cell differentiation.

Moreover, lens cell culture studies have evidenced that actin stress fiber disassembly as well as cortical F-actin organization are dependent on the assembly of N-cadherin cell-cell adhesions. However, in the undifferentiated epithelium adhesion corresponds primarily to integrin/matrix interactions. Epithelial cells lose their tight associations with the lens capsule

(integrin/matrix adhesions) as they differentiate and cadherin based cell-cell junctions become the principal form of adhesion as lens fibers develop. This switch may promote the disassembly of actin stress fibers and induces lens fibers differentiation (Weber and Menko 2006a).

In addition, Fischer *et al.* (2000) experiments realized in chick lens cell cultures determined that in undifferentiated epithelial cells F-actin was organized in polygonal arrays of actin stress fibers that intersect with an adhesion belt (a type of cadherin cell-cell junction in epithelial cells located just below the tight junctions and forming a continuous belt-like structure around each cell in which an underlying contractile bundle of actin filaments is linked to the plasma membrane; Cooper 2000; Alberts *et al.* 2008). As cells elongated to form lentoid bodies (lens fiber-like cells) the arrays of stress fibers were lost. Actin filaments in differentiated lentoid cells were predominantly associated with membranes in a reticular pattern. Moreover, in late-stage differentiated lentoid cells, F-actin colocalized with N-cadherin molecules in complex curvilinear patterns outlining membranes (Fischer *et al.* 2000).

Cortical actin filaments are also part of a complex structure in lens fibers, besides N-cadherin cell-cell adhesions, referred as membrane skeleton. The membrane skeleton is a highly cross-linked network of spectrin (a long thin flexible rod protein) tetramers linked to short F-actin, and together they are associated with membrane attachment and actin regulatory proteins. The membrane skeleton is associated with the inner surface of the lens fiber plasma membrane. In this complex structure, F-actin stability depends on capping proteins at filament ends that prevent assembly as well as disassembly, and on tropomyosins (TMs). TMs bind along the sides of microfilaments blocking severing and reducing subunit dissociation. Tropomodulins (Tmods) are actin pointed end-capping proteins that bind to TMs and cap TM-coated F-actin preventing polymerization and depolymerization in post-mitotic cells like lens fibers. Thus, Tmods and TMs regulate actin filament lengths and provide stability to the membrane skeleton (Alberts *et al.* 2008; Nowak *et al.* 2009).

A *Tmod1* viable knock out mice line with no detectable TMOD1 protein in the lens indicated that the membrane skeleton is necessary for maintenance of fiber cell hexagonal shape, packing geometry during maturation of lens fibers and radial column organization in the lens cortex. Patches of disordered fiber cells were observed in *Tmod1* knock out mice

lenses in comparison with hexagonally packed geometry of controls. These patches exhibited polygonal and often somewhat rounded fiber cell shapes with variable numbers of vertices per cell and irregular lengths of connecting membranes, rather than regular flattened hexagonal shapes. The fibers are also not arranged in precise radial columns as seen in normal equatorial sections. At the transition zone of the lens (equator), regions displaying disordered fiber cell packing tended to be located 20-30 cell layers in from the epithelium; in the region where TMOD1 normally assembles on the fiber membranes. The latter showed that the absence of TMOD1 affects geometry of maturing lens fibers, rather than initial elongation and organization (Nowak *et al.* 2009).

Nowak *et al.* (2009) determined that TMOD1 appears to selectively stabilize the subset of F-actin that belongs to the membrane skeleton, which corresponds to a part of the F-actin in lateral broad and narrow sides, but not the vertices of maturing fibers. Absence of TMOD1 (and consequently a disrupted membrane skeleton) does not affect fiber cell initial differentiation or cell shape morphogenesis. Instead, TMOD1 protein stabilizes F-actin in the membrane skeleton during cortical fiber cell maturation before organelle loss. This indicates a role in maintaining cell shape and packing geometry.

In addition, Quail lens cell culture experiments have proven that the actin cytoskeleton also supports cell survival, and a prolonged disruption of the latter induces apoptotic events that result in cell death. Depolymerization of F-actin in lens epithelial cell cultures for a prolonged time (48h) induces extensive membrane blebbing and cell rounding, indicative of late stage apoptosis. Induced loss of cortical F-actin in cell cultures containing differentiating lentoid cells also resulted in blebbing of the plasma membrane. The latter proved that F-actin provides an essential survival signal to both lens epithelial and differentiating fiber cells (Weber and Menko 2006a).

Furthermore, a short-term induced F-actin disassembly on lens epithelial cell cultures does not induce apoptosis. Rather, it triggers the expression of fiber cell differentiation specific markers, cell cycle withdrawal and the loss of actin stress fibers with a subsequent reorganization into cortical F-actin as fibers differentiate. In addition, *BCL-2* (a suppressor of apoptosis) expression is increased in lens cell cultures that lose their actin stress fibers but also

organize actin as cortical filaments and survive. The latter suggests that the F-actin survival signal in differentiating lens fibers may be conveyed by *BCL-2* (Weber and Menko 2006a).

### **3.3.3 Organelle degradation in lens fibers: emphasis in nuclei**

During lens fibers differentiation, all structures large enough to scatter light including nuclei, mitochondria, Golgi apparatus and endoplasmic reticulum are broken down and removed from the developing fiber cells (Greiling and Clark 2008; Bassnett 2009). Despite all these changes, lens fibers survive and are maintained within the lens throughout the life span of the individual (Counis *et al.* 1998).

Chicken studies have demonstrated that in embryonic lenses organelles are present initially throughout all the cells in the developing tissue. Then, in a specific moment in early development (embryonic day 12 in chick embryos) organelles are eliminated in cells located at the center of the lens (primary lens fibers). The latter results in the formation of a central area without membrane-bound organelles, including nuclei, termed organelle free zone (OFZ). After its initial establishment, the OFZ becomes larger as the lens grows and new fibers are continuously added. Then, organelles are present only in those fiber cells located at the periphery of the lens (Bassnett and Mataic 1997). The only cells in the lens located in the visual axis that do not lose their organelles are cells in the central-anterior epithelium. Nevertheless, they constitute a very thin layer. So, since light scattering is proportional to path length, the light scattering due to organelles in the lens epithelium is insignificant (Bassnett 2009).

It has been observed that during epithelial cell differentiation into lens fibers, the shape of nuclei changes along the course of this process. In lens epithelial cells, nuclei appear to be round and relatively large. In superficial lens fibers, nuclei appear ovoid, and as lens fibers mature nuclei seem to elongate along with fiber elongation. However, just prior to disintegration, nuclei remnants assume a much smaller and more spherical shape (Bassnett and Beebe 1992; Counis *et al.* 1998; De María and Arruti 2004).

Nucleated fiber cells can perform transcription and this process might be stopped until sometime prior to remodeling of the nuclear lamina (thin sheet-like meshwork beneath the

inner nuclear membrane). Afterwards, chromatin disintegration occurs. This order of events has been reported in bovine and chick lenses (Bassnett and Mataic 1997; Bassnett 2009).

It has been suggested that the nuclei degradation process might be different in primary and secondary lens fibers. Although, the only difference observed in nuclei degradation is that in primary lens fibers denucleation occurs simultaneously in a cluster of cells during early development. Afterwards, nuclei degradation in secondary lens fibers occurs as each cell differentiates (Bassnett 2009).

Nuclear breakdown happens at the same time as other organelles are rapidly being disintegrated. However, it is believed that organelle disintegration occurs through independent pathways (Bassnett 2009). Mitochondria degenerate more rapidly than nuclei. In lens epithelial cells, mitochondria are present in perinuclear (around the nucleus) clusters. When lens fibers are differentiating, mitochondria become elongated and distributed throughout the cytoplasm. Prior to disintegration, mitochondria become swollen and fragmented in cells bordering the organelle free zone (OFZ; Bassnett and Beebe 1992).

Most lens mutations that led to cataracts affect organelle degradation to some extent. Some of these mutations can directly affect organelle breakdown. However, any mutation that disrupts lens homeostasis sufficiently may have the potential to disrupt organelle degradation indirectly due to its obvious complex series of interdependent steps (Bassnett 2009).

DNase II $\beta$  (aka DLAD; DNase II-like group: acidic and with no cation dependence) is an enzyme expressed at significant levels at the lens and liver (Counis *et al.* 1998). DNase II $\beta$  knock out mice retain undigested DNA in the lens nuclear fibers leading to nuclear cataracts. This implies that DNase II $\beta$  has a fundamental role in lens fiber denucleation. DNase II $\beta$  cleaves DNA producing 3'-phosphoryl and 5'-hydroxy ends. Since 3'-hydroxy ends rather than 5'-hydroxy ends accumulate when lens fibers denucleation takes place, it has been suggested that endogenous phosphatases might convert 3'-phosphoryl ends in 3'-hydroxy ends (Appleby and Modak 1977; Bassnett 2009).

DNase II $\beta$  is up regulated in differentiating lens fibers. Moreover, it is believed that most of the acid nuclease activity in lens fiber cells is due to DNase II $\beta$  activity as a lysosomal enzyme. This enzyme might gain access to the nuclear compartment by fusion of lysosomes to the nuclear envelope and a subsequent release of DNase II $\beta$  in the nuclear compartment.

However, even though DNase II $\beta$  is critical for lens fibers denucleation, it might not be the only nuclease in lens fibers. DNase II $\beta$  null mice lens exhibit persistent nuclei but chromatin fragmentation and clumping is still observed suggesting that there might be other nucleases involved (Bassnett 2009).

De María and Arruti (2004) studied the presence of DNase I (DNase I-like: absolute Ca<sup>2+</sup>, Mg<sup>2+</sup> dependence; Counis *et al.* 1998) in lens fibers from adult bovine eyes. In lens epithelial cells, DNase I is present at the cytoplasm. In epithelial cells from the proliferative zone and in cells at the onset of fibrogenesis in the transition region DNase I is still located in the cytoplasmic fraction. In more elongated fibers, DNase I is mainly concentrated in close proximity to the cell membrane, but it also starts to be observed in the nuclear territory. Indeed, as fibers elongate DNase I becomes concentrated in patches distributed at the nuclear surface. Then, it becomes tightly associated with highly condensed and fragmented chromatin as lens differentiation proceeds. Furthermore, at the last stages of nuclei degradation DNase I is still associated to nuclear remnants. The obtained results suggest that DNase I might have a role in DNA degradation during the last stages of nuclei degeneration (De María and Arruti 2004).

At the bovine lens secondary fiber nuclear breakdown, the following sequence is observed: onset of chromatin condensation, production of DNA breaks having 3-OH free ends in condensed chromatin, spreading of condensation and fragmentation through the whole chromatin. Then, beginning of nuclear envelope (lamina) degradation and association of DNase I with condensed and fragmented chromatin happens. Lastly, nuclear remnants that remain associated with DNase I are evident at the final stages of nuclear breakdown (De María and Arruti 2004). In addition, regulation of DNase activities might also need the effect of post-translational modifications, mitochondrial release molecules and growth factors (Counis *et al.* 1998).

When lens fibers reach the organelle free zone, they lose their ability to perform protein synthesis, intracellular membrane trafficking, oxidative phosphorylation and all functions realized by organelles. Alongside, terminal differentiation occurs (Bassnett 2009). However, lens fibers retain their cytoplasm (Counis *et al.* 1998).

### 3.4 CUG binding protein 1 (CUGBP1): an mRNA binding protein

CUGBP1 is an mRNA binding protein and a founding member of the CELF (CUGBP1 and ETR-3 like factors) protein family. Members of this family regulate gene expression at the nuclear as well as the cytoplasmic levels. Their main nuclear function corresponds to the regulation of pre-mRNA alternative splicing. In the cytoplasm, they are implicated in the control of mRNA translation and stability. CUGBP1 performs all these functions (Barreau *et al.* 2006).

What characterizes a RNA binding protein is the presence of at least one RNA-binding domain (RBD), also known as ribonucleoprotein (RNP) domain or RNA recognition motif (RRM). This domain is sufficient for RNA binding with a wide range of specificities. Moreover, RRM possess two consensus sequences. In this paper, we will refer to the domain as RRM and to the consensus sequences within the RRM as RNPs. The first RNP consensus sequence identified is referred as RNP1; and it is an octamer positioned at the center of the RRM domain. A second RNP sequence, RNP2 is a hexamer and is located at the N-terminus region of the RRM. The RRM consists of a four-stranded anti-parallel  $\beta$ -sheet packed against two  $\alpha$ -helices ( $\beta\alpha\beta\alpha\beta$ ) topology. The two conserved motifs, RNP2 and RNP1 correspond to the first and third  $\beta$ -strands, respectively. In eukaryotes, RRM are often found as multiple copies within a protein (Maris *et al.* 2005; Tsuda *et al.* 2009; Teplova *et al.* 2010).

CELF proteins are highly similar in their structural organization. They possess three RRM, two in the N-terminal region (RRM1, RRM2) and one in the C-terminal site (RRM3) of the protein. They also have a less well conserved linker region between the second and third RRM (Barreau *et al.* 2006).

Human CUGBP1 was first identified using a band shift assay. By this technique, it was determined that this protein (extracted from cytoplasmic extracts of Hela cells, fibroblasts and myotubes) binds to (CUG)<sub>8</sub> RNA repeats (Timchenko *et al.* 1993). This specific binding activity led to the correlation of CUGBP1 with Myotonic Dystrophy 1 (DM1) pathology, which is a neuromuscular disease. This association was derived from the observation that DM1 is a genetic disease characterized by a (CUG)<sub>n</sub> trinucleotide repeat expansion in the 3'-untranslated region (UTR) of the dystrophia myotonica protein kinase (DMPK) gene (Timchenko *et al.* 1996).

### **3.5 Myotonic Dystrophy 1 (DM1)**

DM1 is an autosomal dominant, multisystemic disease. The human mutation lies on the long arm of chromosome 19, band 13q as an expansion of CTG repeats in the 3' UTR of the dystrophina myotonica protein kinase gene (DMPK) that encodes a serine/threonine protein kinase that contains coiled-coil, C-terminal membrane association and autoregulatory domains. A CTG expansion from ~80 to 4000 repeats results in DM1 disease. DM1 exists in four basic forms depending on the age of appearance of the symptoms: CDM (Congenital Myotonic Dystrophy), childhood onset, classical/adult and late-onset/asymptomatic; the last three forms are commonly referred as DM1 (Harmon *et al.* 2008; Schoser and Timchenko 2010; Turner and Hilton-Jones 2010).

#### **3.5.1 CDM phenotype**

At the congenital form of DM1, referred as Congenital Myotonic Dystrophy (CDM) the largest CTG repeat expansions (> 1,500) have been identified. CDM patients may be born as premature infants due to these large repeat expansions. Polyhydramnios (excess of amniotic fluid in amniotic sac) and the reduction of fetal movements have been reported during the pregnancies of infants with CDM. After the patient is born, first symptoms include postnatal hypotonia (diminished resistance of muscles to passive stretching) and immobility (Leyenaar *et al.* 2005; Schoser and Timchenko 2010; Turner and Hilton-Jones 2010). In up to 50% of affected patients, bilateral talipes (also known as club feet; feet appear rotated internally at their ankles) and other contractures are present at birth. Facial diplegia (paralysis affecting symmetrical parts of the body) is another characteristic feature of CDM. Newborns have an open mouth with a tent-formed upper lip and a high-arched palate. A weak cry and the inability to suck are present in nearly 75% of affected babies. These latter features are due to weakness of facial jaw and palatal muscles. In the patients that survive, hypotonia improves steadily and is only rarely prominent after 3-4 years of age. However, facial diplegia becomes more apparent leading to a typical facial carp-mouth appearance. Speech development is delayed. The latter is caused by hypotonia of the facial, palatal and jaw muscles (Schara and Schoser 2006; Schoser and Timchenko 2010).

Despite the severe muscular phenotype of this disorder, myotonia (muscle stiffness and delayed relaxation after muscle contraction) is not present at the neonatal period in CDM patients and it is seldom present before school age. However, in CDM survivors myotonia becomes a more prominent feature at the second decade of life (Schara and Schoser 2006; Ekström 2009; Schoser and Timchenko 2010).

Neonatal respiratory complications are frequent and in severe cases that require ventilation for more than four weeks; this symptom will most likely result in death. At postnatal stages, delayed motor development is very common; however most children that survive become able to walk independently. Although normal mental development is possible, mental retardation is observed to a variable degree in a great number of patients. Depression, attention deficit hyperactivity, autism and anxiety disorders have been reported in childhood, but not commonly (Schoser and Timchenko 2010).

Other CDM associated abnormalities of high frequency include: inguinal (at the groin) or hiatus (at superior part of the stomach) hernia (protrusion of an organ or tissue through an abnormal opening in the body), undescended testis, congenital dislocation of the hip and torticollis (stiff neck). Congenital heart defect (as elevated diaphragm), hydrocephalus (abnormal accumulation of cerebrospinal fluid in the cavities of the brain), spasticity (excessive contraction of muscles leading to stiff or rigid muscles, blocked nasolacrimal duct and cleft lip (Schara and Schoser 2006; Schoser and Timchenko 2010).

### **3.5.2 DM1 phenotypes**

Childhood-onset DM1 is defined by the beginning of symptoms approximately after one year of age (Longman 2006). Early motor development is normal or only slightly delayed. Neuromuscular problems may be weakness of facial and neck muscles but without the typical features of CDM (e.g., carp-mouth). Distal weakness, audiologic problems and recurrent abdominal pain have been reported. Mental handicap leading to speech and learning difficulties is most commonly recognized during school age. Motor disabilities or respiratory difficulties are no prominent features (Schara and Schoser 2006). Myotonia and distal limb muscle weakness develop during the teenage years (Longman 2006).

Cardiologic problems may become important in later life as how it can also happen in CDM survivors. It has been reported that cardiac arrhythmias (abnormal rate or rhythm of the heartbeat) or cardiomyopathy (deterioration of the heart muscle) may occur in the second decade of life in childhood onset DM1. These problems could lead to sudden death. When growing older, childhood onset patients may show symptoms of the adult onset form in their twenties (Schara and Schoser 2006).

Adult onset DM1 is the most common form of Myotonic Dystrophy and is frequently referred as the classical form. Facial weakness with bilateral mild ptosis (dropping of the eyelid) and distal muscle weakness are the most common features. Grip (when difficulty in releasing grip or opening the hand after making a fist) and percussion myotonias (after a brief mechanical stimulation) are regular features, but myotonia also affects other muscles like bulbar (muscles that control speech, swallowing and chewing), facial and tongue muscles. The latter causes problems with swallowing, chewing and talking. Cardiac defects include dilated cardiomyopathy (the heart becomes enlarged and debilitated and cannot pump blood efficiently), conduction abnormalities with arrhythmia and conduction blocks up to cardiac death (Schara and Schoser 2006).

The central nervous system is also affected (e.g., mental retardation, affected personality traits and excessive daytime sleepiness). Pigmentary retinal degeneration has been reported, but the most common eye defects are posterior subcapsular cataracts (starting at the cortical fibers situated at the posterior pole). There are also gastrointestinal problems like irritable bowel syndrome and symptomatic gall stones. Testicular atrophy, hypotestosteronism (low levels of testosterone activity) and insulin resistance with usually mild type 2 diabetes (insulin resistance) are other features (Schara and Schoser 2006; Schoser and Timchenko 2010; Turner and Hilton-Jones 2010).

Furthermore, there are patients that have a late-onset/asymptomatic form of DM1. The presence of cataracts in middle or older age is its characteristic feature. Signs of muscle weakness or myotonia can be present, but these symptoms are very rare. No major cognitive impairment has been detected, other than mild verbal memory dysfunction (Ekström 2009). One of the most important reasons in detecting the repeat expansion mutation, in these late-onset carriers, is to identify other affected family members and enable genetic counseling to

more affected patients due to the genetic anticipation (successive generations inherit increasing disease severity with decreasing age of onset) phenomenon observed in this disease (Cho and Tapscott 2007; Turner and Hilton-Jones 2010). Anticipation has been suggested to occur as the trinucleotide expansions are highly unstable resulting in a progressive increase in the repeat length during gametogenesis. This eventually leads to an infant with CDM as this affected group of patients has been reported to possess the longest CTG expansions (Campbell *et al.* 2004; Ekström 2009). Besides, germ-line instability, the mutant expanded repeats exhibit somatic mosaicism, in which variable repeat size in different tissues of a single patient has been observed. In addition, increasing expansion in the length of the mutant CTG repeats with increasing age, in a single patient, has also been observed (Ekström 2009).

### **3.5.3 Molecular mechanisms of Myotonic dystrophy 1**

Although some of the symptoms of DM1 may be attributed to decreased levels of DMPK protein, a much more complex mechanism takes place. As DM1 is a multisystemic disease with variable expressivity of its symptoms, the features are unlikely to be explained by a defect in the *DMPK* gene alone (Winchester *et al.* 1999). Hence, three distinct mechanisms have been proposed to contribute simultaneously with DM1 pathogenesis: (1) Haploinsufficiency of *DMPK*, (2) altered expression of neighboring genes and (3) RNA toxicity. These mechanisms link the trinucleotide repeat expansion with DM1 disease (Kaliman and Llagostera 2008; Ekström 2009). In all, the trinucleotide repeat expansions are suggested to disturb normal cellular processes at the RNA, protein and/or chromatin level (Cho and Tapscott 2007).

Haploinsufficiency happens when a normal phenotype needs a protein product from both alleles of a particular gene. If one gene copy is flawed, the reduction by half of the gene product will result in a defective phenotype. Initial research was aimed to identify the function of DMPK protein since several studies showed that cytoplasmic amounts of this protein were reduced in DM1 patients. In DM1, the *DMPK* gene with the triplet repeat expansion in its 3' UTR is transcribed into non-decreased mRNA with the CUG repeats. However, a part of the mRNAs containing CUG repeats tends to be retained in nuclear foci (ribonucleoprotein precipitates) preventing transport to the cytoplasm (Berul *et al.* 1999; Cho and Tapscott 2007;

Kaliman and Llagostera 2008; Ekström 2009). These aggregated forms reduce the processing of mutant DMPK mRNA by the CUG repeat tract. Hence, there is a reduction in the translation of DMPK protein (Ekström 2009).

To test if decreased DMPK protein translation may account for DM1 phenotype several studies have observed what happens if DMPK function is eliminated in mice. *Dmpk* null mice developed late onset mild myopathy. In addition, mice heterozygous and homozygous for disrupted *Dmpk* gene also exhibited cardiac conduction defects (Berul *et al.* 1999; Cho and Tapscott 2007). Hence, haploinsufficiency of DMPK protein may contribute to DM1 features specially in skeletal and cardiac muscles but does not account for all the clinical spectrum of DM1 (Cho and Tapscott 2007; Ekström 2009).

The expanded CTG repeats in the *DMPK* gene may affect the expression of other genes. The CTG mutation is a strong nucleosome-binding site that could modify chromatin structure having regional effects on the expression of *DMPK* and other genes close to *DMPK*. In fact, *SIX5/DMAHP* (homeodomain-containing transcription factor) has been implicated as a second candidate for DM1 pathogenesis. This because the mutant *DMPK* (CTG)<sub>n</sub> repeat overlaps not only the 3'end of the *DMPK* gene, but also a 5' promoter (or more strictly speaking, enhancer-promoter) region of the downstream neighboring gene *SIX5* (Winchester *et al.* 1999; Ranum and Day 2004).

In more detail, first it was demonstrated that a DNase I hypersensitive site was positioned adjacent and downstream the CTG repeat at the wild type *DMPK* gene. Expanded CTG repeats seen in DM1 eliminate this hypersensitive site and transform the region that surrounds the repeats into a more condensed chromatin structure (Otten and Tapscott 1995). This hypersensitive site contains a promoter element that regulates transcription of *SIX5*. Allele-specific analysis of *SIX5* expression demonstrated that steady-state transcript levels from the allele with the CTG repeat expansion were significantly reduced in comparison to those from the wild type allele. Hence, CTG repeat expansions can suppress local gene expression of *SIX5* in DM1 disease (Klesert *et al.* 1997). *SIX5* mRNAs are expressed in DM1 affected tissues such as brain, eye, heart and skeletal muscle (Ekström 2009).

In addition, another target gene which its disrupted expression due to altered chromatin structure may contribute to DM1 is *DMWD*. *DMWD* is located immediately upstream of

*DMPK*. In mice, Northern blotting and RNA *in situ* hybridization assays have revealed ubiquitous low expression in all tissues of the mouse embryo. Strong RNA expression has been detected in the brain and testis of adult mice; thus it has been suggested that *DMWD* gene could be involved in the mental and testicular symptoms observed in severe cases of DM1 (Jansen *et al.* 1995). Moreover, Alwazzan *et al.* (1999) have demonstrated that levels of cytoplasmic *DMWD* RNA from the allele adjacent to mutant *DMPK* (with expanded CTG repeats) are reduced in DM1 cells. This model explains some but not all disrupted features of DM1 (Ekström 2009).

Even though it has been proven that expanded CTG repeats affect translation of *DMPK* protein and the transcription of other genes in the *DMPK* locus; pathological features of DM1 disease are mainly linked with the accumulation of non-coding CUG repeats (Ekström 2009). As previously mentioned, posttranscriptional *DMPK* mRNAs containing expanded CUG repeats accumulate in large nuclear foci. The latter was first observed by Taneja *et al.* (1995) in DM1 primary skin fibroblast cells from two affected patients and a DM1 adult muscle tissue. Large amounts of mutant *DMPK* transcripts were also detected in the cytoplasm of DM1 fibroblasts, but in smaller complexes and not as large aggregated forms. However, data for the cytoplasmic as well as for nuclear localization of mutant *DMPK* mRNA in DM1 has been controversial. Different studies have observed that mutant *DMPK* transcripts are blocked and present only in nuclei. But, it has also been suggested that non-aggregated mutant *DMPK* transcripts are also present in nuclei. Other studies found that aggregated forms are found in both the nucleus and cytoplasm of DM1 cells (Schoser and Timchenko 2010).

Despite the discrepancies related to the locations of mutant *DMPK* mRNA inside the cell, Junghans (2009) has proposed a DM1 model based on previously obtained data. In this viewpoint mechanism, foci are not the only forms of mutant RNA in DM1 cells. There are also smaller complexes of soluble mutant *DMPK* mRNA. In addition, CUGBP1 and MBNL1 (zinc finger protein and mammalian homologue of *Drosophila* muscle-blind which is required for muscle and photoreceptor development; Fardaei *et al.* 2002; Huang *et al.* 2008) are RNA-binding proteins that regulate post-transcriptional processes. Binding of CUGBP1 and MBNL1 proteins to different forms of expanded CUG repeats causes DM1 pathology because

the regulation of gene expression of both proteins (especially alternative splicing) is disrupted upon mutant *DMPK* mRNA binding (Junghans 2009).

Mutant expanded CUG repeats in *DMPK* mRNA form double stranded (duplex) hairpins in nuclei. First, MBNL1 protein binds to the double stranded regions of these hairpin regions and these fusions lead to insoluble foci (aggregated form). Indeed, binding of each MBNL1 clamps the adjacent duplex to facilitate the binding of the next MBNL1 protein. Each bound MBNL1 gives the duplex more stability by a closing zipper-like mechanism. Hence, MBNL1 binding stabilizes these hairpins. In addition, this zipper-like mechanism excludes CUGBP1 from binding to insoluble foci. As MBNL1 is coprecipitated with mutant *DMPK* RNA into insoluble foci, free MBNL1 in solution is gradually depleted and less able to exclude CUGBP1 protein from binding to expanded CUG repeats. Then, CUGBP1 binds to soluble single stranded mutant *DMPK* CUG repeats. In addition, CUGBP1 protein binds to single stranded tails at the hairpin bases (Junghans 2009).

Binding to soluble single stranded mutant CUG repeats protects CUGBP1 protein from normal rapid catabolism, prolonging the normally short half-life of CUGBP1 protein. The latter induces higher CUGBP1 protein concentrations and increased CUGBP1-dependent splice variants. In cytoplasm, there are also un-aggregated expanded CUG repeats in DM1 cells. Hence, in cytoplasm, CUGBP1 also binds mutant *DMPK* mRNA and its protein levels are also increased. The elevated CUGBP1 protein also alters normal translation and stability of its cytoplasmic mRNA targets in DM1. Differently, binding to double stranded insoluble mutant RNAs leads to sequestration of MBNL1 and, thus, leading to decreased MBNL1-dependent splice variants. In addition, there are transcription factors (TF) that also bind to soluble ssCUG repeats; this leads to TF leaching (depletion) from chromatin and diminished transcription of specific genes in DM1 (Junghans 2009; Schoser and Timchenko 2010). Hence, transcriptional and post transcriptional expression mechanisms are disrupted in cells expressing mutant *DMPK* mRNA with expanded CUG repeats leading to DM1 clinical features.

### 3.5.4 CUGBP1 and its involvement in DM1 models and tissues

Transient expression of RNAs containing *Dmpk* 3'-UTR with 960 CUG repeats (*Dmpk*-CUG<sup>960</sup> mRNA) in COS M6 cells (monkey cell line) induced hyper-phosphorylation of nuclear, but not cytoplasmic CUGBP1 protein. These cells also exhibited CUGBP1 increased steady state levels in nuclear fractions. DM1 cell cultures of skin fibroblasts converted to muscle cells and DM1 heart tissues also exhibited elevated CUGBP1 protein levels compared to controls. CUGBP1 was also hyper-phosphorylated in both types of DM1 samples. However, these samples were not separated in nuclear and cytoplasmic extracts (Kuyumcu-Martínez *et al.* 2007).

A bitransgenic inducible (by tamoxifen) and heart-specific DM1 mice model expressing 960 CUG repeats in the context of the *Dmpk* 3'-UTR was created. These transgenic mice develop cardiac features of DM1 disease after tamoxifen administration including dilated cardiomyopathy (weakened and enlarged heart). They demonstrated elevated CUGBP1 protein levels specifically in nuclei containing foci of CUG repeat RNA. Bitransgenic mice exhibited colocalization of MBNL1 with RNA foci and increased CUGBP1 as early as 6 hours after tamoxifen administration. These observations indicate that up regulation of CUGBP1 is an early and primary response to expression of expanded CUG repeats (Wang *et al.* 2007). Besides CUGBP1 increased steady state levels in induced heart tissues; these tissues demonstrated CUGBP1 hyperphosphorylation. These results indicate that CUGBP1 hyperphosphorylation induces protein stabilization and is also a direct effect of *Dmpk*-CUG expanded repeat expression (Kuyumcu-Martínez *et al.* 2007).

Numerous assays performed with *Dmpk*-CUG<sup>960</sup> COS M6 cells and heart tissues from *Dmpk*-CUG<sup>960</sup> heart-specific mice model and DM1 patients have shown that PKC (protein kinase C) is activated (by phosphorylation) when there is expression of *DMPK*-CUG expanded repeats. PKC activation (induced by these mRNA mutant repeats) is required for CUGBP1 hyperphosphorylation and its subsequently steady state levels (Kuyumcu-Martínez *et al.* 2007).

Additionally, Koshelev *et al.* (2010) demonstrated that 2-6 month old bitransgenic mice overexpressing CUGBP1 in hearts (tetracycline inducible and heart-specific) reproduce functional and molecular abnormalities observed in DM1 patients and DM1 mice models,

including the line previously described developed by Wang *et al.* (2007). These bitransgenic mice exhibited dilated cardiomyopathy and reproduce histopathological abnormalities observed in Wang *et al.* (2007) transgenic mice line (DMPK-CTG<sup>960</sup>) and DM1 patient tissues. These abnormalities included necrosis, degeneration and loss of myocardial fibers (Koshelev *et al.* 2010).

Since it is well known that DM1 impairs skeletal muscle function, an inducible and skeletal muscle-specific CUGBP1 transgenic mice line was created by Ward *et al.* (2010). This phenotype aimed to determine whether CUGBP1 overexpression in skeletal muscle from adult mice reproduces features of DM1 patients and of a DM1 mice model (DMPK-CTG<sup>960</sup> inducible and skeletal muscle-specific) previously created by Orengo *et al.* (2008). At 2-3 months of age, these transgenic mice were induced to express CUGBP1 protein. These mice had a strong observable phenotype by 2 weeks of inducing CUGBP1 overexpression. They exhibited impaired movement, abnormal gait, an 18% reduction in total body weight and histology characteristic features observed in DM1 including a large number of myofibers containing central nuclei. Furthermore, during the periods of time with high CUGBP1 induction (1-4 weeks) transgenic mice exhibited a significant reduction in muscle function. However, muscle performance improved by 8 weeks of induction when it was shown that CUGBP1 expression levels were significantly reduced. The latter suggests a tight correlation between the severity of muscle function and CUGBP1 protein levels of expression during DM1 (Ward *et al.* 2010).

### **3.6 CUGBP1 and early development**

The zebrafish *CUGBP1* ortholog: *cugbp1*, formerly known as *Bruno-like (brul)* was first identified as a maternal factor (Suzuki *et al.* 2000). Maternal factors are gene products present in the egg at and before fertilization. They are synthesized during oogenesis and are crucial before zygotic genome activation which occurs at a developmental moment referred as midblastula transition (MBT). In zebrafish, the MBT occurs gradually between the beginning of cell cycle 10 (512 cells) and the ending of cycle 13 (sphere stage; Kane and Kimmel 1993; Pelegri 2003).

In zebrafish, maternal *cugbp1* mRNA expression has been observed during oogenesis as well as at early embryonic development. At oogenesis, *cugbp1* mRNA was distributed ubiquitously at stage IB (primary growth, oocytes reside within a definitive follicle). At stage II (cortical alveolus stage), mRNA expression was observed at the vegetal cortex. By the stage III (vitellogenesis), *cugbp1* mRNA was still accumulated at the vegetal cortex, although it was also located around the germinal vesicle (nucleus; Suzuki *et al.* 2000).

Once the egg has been fertilized, maternal *cugbp1* mRNA was observed in the vegetal pole at the onset of embryogenesis. Then, streaming of *cugbp1* mRNA towards the blastodisc was observed as early as 30 minutes post fertilization (minpf, 1 cell stage; Suzuki *et al.* 2000). At the 4 cell stage (1hpf), *cugbp1* mRNA was detected at the cytoplasm of the distal ends of cleavage furrows; hence suggesting a role as a germ lineage determinant. In addition, it was still apparent at the vegetal pole and a weaker signal was observed in the blastomeres. At the sphere stage (4hpf), *cugbp1* mRNA was concentrated in a four-cell/cluster pattern that is reminiscent of primordial germ cells. In addition, a ubiquitous mRNA weaker signal was observed in the blastomeres (Hashimoto *et al.* 2004). Afterwards, the maternal mRNA gradually decreased during successive cleavage stages. Then, at 24hpf, zygotic *cugbp1* mRNA was observed at the lens specifically in lens fiber cells. Zygotic *cugbp1* mRNA expression was reported to be uniform throughout zebrafish embryos before 24hpf, although no specific moments of first appearance were specified (Suzuki *et al.* 2000).

Later on, immunostaining assays showed that zebrafish Cugbp1 protein is distributed all over the embryo from the 1 cell stage to 28hpf (not including the yolk). At the 1 cell period, Cugbp1 accumulated at the animal pole followed by a distribution throughout the whole blastomere. At 28hpf, Cugbp1 expression was observed at the whole embryo with stronger signals at the lens and somites (Hashimoto *et al.* 2006).

In *Xenopus* (genus of highly aquatic frogs), the ortholog of human *CUGBP1*, *eden-bp* (Embryo deadenylation element binding protein) has been identified as a maternal factor that recognizes a short element referred as EDEN on the 3'UTR of maternal mRNAs. The core motif of this element is a U(G/A) repeat. *eden-bp* protein activity is turned on at, or just after, fertilization triggering deadenylation [poly(A) tail shortening] and subsequent translational

repression and degradation of mRNAs bearing an EDEN (Paillard *et al.* 1998; Graindorge *et al.* 2008).

Gautier-Courteille *et al.* (2004) have monitored *eden-bp* mRNA and eden-bp protein expression by *Xenopus* whole-mount *in situ* hybridization and immunohistochemistry assays, respectively. Both *eden-bp* mRNA and protein expression were found to have very similar patterns of expression. At the blastula and gastrula stages, *eden-bp* was expressed homogeneously in whole *Xenopus* embryos. By the neurula stage, expression was more concentrated in the paraxial mesoderm (which gives rise to somites, facial muscle and cartilage) flanking the neural tube. In early tailbuds (stage 20-44, including beginning of hatching at stage 35-36), *eden-bp* was more abundant in the dorsal mesoderm and in the head area (including the eye). This preferential expression in the dorsal mesoderm and in the head was more marked in late tailbud and tadpole embryos. *eden-bp* expression in dorsal mesoderm is particularly obvious in the posterior presomitic mesoderm (PSM). *eden-bp* mRNA and protein relocation to preferred regions at the neurula and tailbud stages most likely relies on zygotic transcription and translation.

Moreover, *eden-bp* down regulation in *Xenopus* embryos by antisense morpholino or anti eden-bp antibody impairs somitic segmentation. The latter was evidenced by a lack of a periodic pattern of somites separated by chevron-shaped borders. Hence, eden-bp is required for the metamerization of the somites during embryonic development (Gautier-Courteille *et al.* 2004).

*etr-1*, identified in the nematode *Caenorhabditis elegans*, is the ortholog of human *CUGBP1* which whom it shares 74% identity within the RRM domains. A promoter element within *etr-1* gene linked to the GFP (green fluorescent protein) showed an expression pattern with high muscle specificity. By 300minpf, embryos exhibited GFP expression in the muscle sheet. The muscle sheet, in early embryos, is the term used to refer to the muscle cells that are initially seen as a continuous sheet on the lateral side of the embryo. Between 300-350minpf, the muscle sheet begins to separate, starting from the anterior, as the cells move to form two dorsal and two ventral muscle quadrants. By 430minpf, GFP expression is present at these four quadrants along the length of the embryo. Moreover, expression is evident in adult animals. GFP is observed in striated body-wall muscles along the length of the animal,

especially in the head. Expression was also seen in the intestinal and sphincter muscles, the sex-specific muscles of the male tail and the vulval muscles (vulva: hermaphrodite reproductive structure that serves to allow eggs to be laid and male sperm to be deposited; Milne and Hodgkin 1999).

Inactivation of *etr-1* caused embryonic lethality. First, embryos could not elongate and became paralyzed, a phenotype characteristic of a mutant line defective in muscle formation and function. ETR-1 protein is essential for muscle development and it may play a role in post-transcriptional regulation of some muscle components. Hence, a possible conservation of gene function between *etr-1* and *CUGBP1* was suggested (Milne and Hodgkin 1999).

The mice *CUGBP1* ortholog has also been implicated in early embryonic development. Kress *et al.* (2007) developed a *Cugbp1* null mice line (*Cugbp1*<sup>-/-</sup>) by homologous recombination. These homozygous mutants were viable, but a significant portion of them did not survive after their first few days of being born. They were smaller and their growth deficiency was already apparent just before birth. *Cugbp1*<sup>-/-</sup> mice weighted significantly less than controls. These differences remained stable throughout life and the null mice never reached the size and weight of controls. Impaired fertility was another feature observed in most *Cugbp1*<sup>-/-</sup> males and females. A more thorough analysis of male infertility showed an arrest of spermatogenesis (Kress *et al.* 2007).

*Cugbp1* expression was also tested in whole mice embryos by two different approaches: measurement of *Cugbp1* promoter activity by  $\beta$ -galactosidase; and protein detection by immunohistochemistry. *Cugbp1* promoter activity starts at the two-cell stage (time of first main zygotic activation) and it continues at least until the blastocyst stage. The promoter activity was also present in the oocyte; this expression was very strong and sustained during the preimplantation period. Evaluation of *Cugbp1* expression pattern later on development showed wide expression at 10 and 11 days post coitum (dpc). The highest expression levels were seen in the limb buds, cephalic structure, tail region and somites. Immunohistochemistry assay revealed the same temporal and spatial pattern. *Cugbp1* promoter activity in internal tissues from 12dpf embryos revealed that the expression was extensive and variable in intensity (Kress *et al.* 2007).

Furthermore, Kuyumcu-Martínez *et al.* (2007) examined endogenous levels of CUGBP1 protein from heart muscles of embryonic day 16 and 17 (E16, E17) and from heart and skeletal muscles of newborn and adult (6 months old) normal mice. This was done to try to identify a relationship between CUGBP1 phosphorylation and regulation of protein steady state levels during early development. Results indicated that CUGBP1 was more acidic in e17 and newborn tissues examined compared to adult tissues. This acidic shift was proved to be due to hyper-phosphorylation. In addition, there was an increase of CUGBP1 protein steady state levels due to hyperphosphorylation in adults from Wang *et al.* (2007) DM1 mice model (DMPK-CUG<sup>960</sup>) and DM1 patient tissues, as explained previously. Also, the abundance of CUGBP1 in normal embryonic and newborn cardiac and skeletal muscle was due to its hyperphosphorylation. There was no sign of CUGBP1 hyperphosphorylation in normal adult tissues.

These results lead Kuyumcu-Martínez *et al.* (2007) to conclude that a developmental change in the phosphorylation state of CUGBP1 in heart and skeletal muscle correlates directly with its steady state levels. This developmental normal change might not occur in DM1 patients leading to abnormal increased steady state levels of CUGBP1; and ultimately contribute to the abnormal pathogenic phenotype.

More specifically, it has been widely observed that the expanded CUG repeats in DM1 disrupt an alternative splicing program (Cooper *et al.* 2009). Alternatively spliced mRNAs can be regulated according to cell type, in response to external cues or depending on the developmental stage. RNA binding proteins, like CUGBP1, are involved in this regulation by binding to specific regions within pre-mRNAs. Additionally, it has been proven that alternative splicing regulation can involve the activities of antagonistic factors by promoting different pathways (Ranum and Cooper 2006).

In DM1, an alternative splicing transition mechanism regulated antagonistically by MBNL1 and CUGBP1 in striated (skeletal and heart) muscle is disrupted. In normal conditions, this mechanism is dependent on the developmental stage. First, CUGBP1 protein is up regulated in early embryonic development and as development proceeds CUGBP1 is down regulated; concomitantly MBNL1 is up regulated. CUGBP1 and MBNL1 reproduce embryonic and postnatal/adult alternatively spliced expression patterns, respectively. Since

DM1 is characterized by an elevation of CUGBP1 protein levels and sequestration of MBNL1 protein, the disruption of this mechanism results in an inappropriate expression of embryonic rather than adult splice variants in adult tissues. This results in DM1 pathogenesis (Kalsotra *et al.* 2008; Cooper *et al.* 2009; Schoser and Timchenko 2010).

Ladd *et al.* (2001) have also detected developmentally regulated expression of CUGBP1 protein. They showed that the abundance of CUGBP1 from mice skeletal muscle decreased significantly from strong expression during embryonic development (E14), NB (new born) and PN4 (postnatal day 4) to very low levels in adult thigh muscles. But, this stage-dependent pattern of expression was not limited to skeletal muscle. CUGBP1 protein expression stayed constant throughout early stages of mice brain development (E14, NB, and PN4) and decreased to a very low but still detectable level in the adult brain. In addition, Western Blot assays also revealed CUGBP1 expression in diaphragm, uterus, spleen, mammary gland, lung and adipose mice adult tissues. However, a possible change in CUGBP1 levels of expression throughout development was not studied in these last mentioned tissues.

To determine if increased CUGBP1 expression is sufficient to reproduce disrupted alternative splicing activity observed in DM1, Ho *et al.* (2005) generated transgenic mice that specifically express human *CUGBP1* (MCKCUG-BP1; MCK: creatine kinase promoter) in striated muscle tissues. Transgenic mice with CUGBP1 expression 4-6 fold above endogenous levels in neonatal heart and skeletal muscle were stillborn (it is likely that its mutant founder was chimeric).

To find out if *CUGBP1* alternative splicing activity was disrupted in neonatal hearts from MCKCUG-BP1 transgenic mice, Ho *et al.* (2005) compared splicing of *Tnnt2* (the mice ortholog of human *CTNT*: Cardiac Troponin T) in transgenic vs. WT (wild type) littermates. CTNT is a striated muscle protein that plays an important role in the regulation of muscle contraction. This protein contains different isoforms that are stage-dependent and regulated by alternative splicing (Cooper and Ordahl 1985; Filatov *et al.* 1999). Transgenic mice (~74%) exhibited increased levels of *Tnnt2* exon5 inclusion when compared with non-transgenic neonates (~35%). In DM1 patients, cardiac tissues show an inappropriate retention of the *CTNT* fetal exon5. Hence, increased *Tnnt2* exon5 inclusion in MCKCUG-BP1 mice is consistent with disrupted splicing and CUGBP1 increased steady state levels in DM1 (Ho *et*

*al.* 2005). In addition, it has been proven that MBNL1 protein has an antagonistic role in *Tnnt2* and *CTNT* alternative splicing as MBNL1 represses inclusion of exon5 (Kanadia *et al.* 2003; Ho *et al.* 2004).

Human myotubularin-related 1 gene (*MTMR1*) and its mice ortholog *Mtmr1* belong to a highly conserved family of eukaryotic phosphatases. At differentiation of muscle cells in culture (mouse myoblast cell line C2C12 and human fetal myoblasts) two major *MTMR1* isoforms (A and B) were identified in myoblasts prior to fusion into myotubes. After early induction of myoblast differentiation, a third isoform (C) was detected and its levels increased to become the major isoform when myotubes were predominant. At normal heart as well as skeletal muscle development, it has been proven that *MTMR1* undergoes a transition from the fetal (A and B) to the postnatal/adult (C) isoform (Buj-Bello *et al.* 2002; Ho *et al.* 2005).

Analysis of splicing in neonatal hearts and skeletal muscle samples revealed that mice overexpressing *CUGBP1* express more of the fetal *MTMR1* isoforms. In contrast, the predominant isoform in neonatal WT mice is C and adult WT mice express only the adult isoform suggesting that *MCKCUG-BP1* transgenic mice display a delay in the expression of the adult isoform (Ho *et al.* 2005). Furthermore, the splicing pattern of *MTMR1* mRNA was studied in congenital myotonic dystrophy muscle cells. Human fetal congenital DM1 myoblast cultures were induced to differentiate, and as myogenesis took place *MTMR1* isoform C decreases instead of increasing as shown in normal cell cultures. Additionally, after medium-induced differentiation, an abnormal *MTMR1* transcript isoform (G) appears in human congenital DM1 cell cultures. The G isoform was not detected in control cultures. Skeletal muscle tissues from congenital DM1 fetuses (aged 15-37weeks) also revealed the presence of the abnormal G isoform, suggesting that disrupted splicing of *MTMR1* also happens in human muscle affected by congenital myotonic dystrophy (Buj-Bello *et al.* 2002). However Ho *et al.* (2005) do not mention any studies performed to find out if *MTMR1* isoform G is present in *MCKCUG-BP1* transgenic mice.

In addition, sections of mice skeletal muscle from neonates overexpressing *CUGBP1* displayed abnormalities that resembled features of congenital myotonic dystrophy. Light and electron microscopy observations showed myofibers with chains of centrally located nuclei, degenerating muscle fibers surrounded by nuclei and irregularly shaped nuclei. When

compared with controls, WT neonatal tissues displayed small fibers with central nuclei consistent with normal still immature skeletal muscle. In contrast, transgenic animals possessed increased number of internal nuclei in individual fibers. In congenital myotonic dystrophy, skeletal muscle development is impaired, several of its abnormalities include: chains of centrally located nuclei, large variations in muscle fiber size and poor fiber type differentiation. The results in transgenic mice suggest that mice overexpressing human CUGBP1 in skeletal muscle display pathological features observed in DM1 disease (Ho *et al.* 2005).

### **3.7 DM1 and the lens**

To date, most of the efforts to try to understand the causes and features of DM1 disease have been oriented to the study of heart and skeletal muscle defects (Schoser and Timchenko 2010). The study of the mechanisms underlying the development of cataracts, in DM1, needs further investigation.

Adult lens samples from individuals who had suffered DM1 have been studied to observe the cataract morphology in this disease. The first lesion of the lens has been described as fine points mixed with colored crystals or iridescent-like dust in a thin band of anterior and posterior cortex beneath the capsule. The second and more advanced lesion is a stellate grouping of opacities at the posterior pole along the posterior suture lines of the lens. The stellate arrangement of opacities is considered a later stage than that of the colored crystals due to a condensation of the point-like opacities along the sutures (Eshaghian *et al.* 1978).

By transmission electron microscopy imaging, Eshaghian *et al.* (1978) observed numerous small, round globular bodies at the posterior pole of DM1 cataractous lenses. The accumulation of these abnormal bodies was associated with swirling membrane configurations that resembled myelin-like figures (whorls). Small amounts of cytoplasm were layered between the whorls. Hence, it was proposed that plasma membranes may wind around themselves to form the myelin-like figures. And that these whorls could correspond to the iridescent crystals seen in DM1 cataracts of adult patients at slit lamp views. If this is true, then there are no crystals, but derivatives of the plasma membrane which refract light to give the appearance of colored crystals. The accumulation of the myelin-like bodies along the

posterior suture could account for the stellate opacity observed. These observations suggest that the plasma membranes of lens fibers in DM1 may be defective. In addition, the general morphology of the anterior lens structure in adult DM1 patients was not normal. Central and peripheral epithelial cells contained nuclei with clumped chromatin, degenerating mitochondria and enlarged intercellular clefts or cisternae.

One of the first steps to try to identify what causes cataracts in DM1 was to determine if the *DMPK* gene is expressed in the lens. Dunne *et al.* (1996) probed that *DMPK* RNA is expressed in normal adult human lenses by RT-PCR (Reverse Transcriptase PCR). The same type of samples was used to demonstrate that DMPK protein is expressed at adult human lenses by Western Blot. The same size band had been previously detected in both human cardiac and skeletal muscles.

Immunohistochemistry assays with anti-DMPK antibody were performed on sagittal sections (vertical cut from front to rear, divides human body into right and left; equals to transverse sections in zebrafish lenses) from normal and DM1 human adult lenses. Normal adult lenses showed cytoplasmic staining with increased intensity in the perinuclear region (cytoplasmic region just around the nucleus) in epithelial cells. A more uniform cytoplasmic labeling was observed in anterior and posterior subcapsular cortical lens fibers. Nuclei were not labeled in any type of normal cell. The depth of fiber cells staining varied, it was most shallow at the posterior pole and it had the greatest depth in the equatorial region. Mature organelle-free nuclear lens fibers were not stained (Dunne *et al.* 1996).

One human adult lens sample from a DM1 patient with cataracts exhibited a significantly different distribution of DMPK protein. Staining was primarily detected inside the cell nucleus in epithelial cells. The difference in DMPK labeling between normal and a DM1 lens, although tentative due to limited samples, is consistent with an alteration in the localization of DMPK protein as a gain of function effect in DM1 (Dunne *et al.* 1996).

*DMPK* mRNA and protein expression in adult human lenses and Eshaghian *et al.* (1978) observation that whorls of multilaminate membranes were present at the posterior pole in DM1 lens samples; led Dunne *et al.* (1996) to hypothesized that altered expression of DMPK protein in DM1 could alter the regulation of organelle loss during normal lens fiber

maturation. An abnormal presence of membrane-enclosed organelles could produce these whorls in lenses from DM1 patients.

*DMPK* expression at the lens was further studied by Winchester *et al.* (1999). Three adult human eyes and two fetal eyes (12 weeks old) were used for RT-PCR (Reverse transcriptase-PCR) analyses and western blotting. *DMPK* mRNA was not detected at human adult lens samples, but it was present at the fetal eyes; however this last assay does not give specific information of the fetal lens. Analysis of *DMPK* protein by western blot did not show expression at adult lenses or fetal eyes extracts. *DMPK* mature mRNA and protein expression results disagree with the previously mentioned results since Dunne *et al.* (1996) did observe expression at both the protein and transcriptional levels in normal adult human lenses.

*In situ* hybridization results showed no *DMPK* mature mRNA expression in adult lenses from 8 human samples. *DMPK* protein expression was also not detected in any specific regions of 8 human adult lenses by immunodetection experiments on lens sections (Winchester *et al.* 1999). These observations were incongruent with earlier results. Dunne *et al.* (1996) obtained positive results in *DMPK* protein expression at human adult lenses, specifically at both the lens epithelial cells and cortical lens fibers. Unfortunately, this paper did not publish any positive or negative *in situ* hybridization results of *DMPK* transcripts or immunodetection assays of *DMPK* protein in fetal lenses (Winchester *et al.* 1999).

More recently, Harmon *et al.* (2008) have produced a highly specific and sensitive monoclonal antibody against the coiled-coil region of *DMPK* protein. With this antibody *DMPK* protein was detected at the mice embryo ocular lens. In addition, specific *DMPK* staining in the chick embryo revealed expression restricted to postmitotic lens fiber cells (stage 26; 4.5-5 days). *DMPK* protein expression in both the murine and avian embryos lenses suggests a conserved function for *DMPK* in early development. Expression in postmitotic cells further suggests a possible role for *DMPK* during cell differentiation (Harmon *et al.* 2008).

To try to identify what possible role does *DMPK* protein have in lens cells, Jin *et al.* (2000) overexpressed coding regions of human *DMPK* (20-fold increase compared to endogenous *DMPK*) in the human lens epithelial cell line known as B3. After 24-40hours after transient transfection multiple blebs and protrusions from near the plasma membrane were

observed. This cellular phenotype (blebbing) resembled the protrusions observed in the execution stage of apoptosis. Moreover, immunohistochemistry assays proved that the localization of DMPK completely overlapped with the formed blebs. Overexpression of cytoplasmic DMPK protein induced the apoptotic-like blebs where it was concentrated. The blebs also contained markers of the ER lumen and the outer membrane of the blebs exhibited a marker of the plasma membrane. This observations were consistent with the condensation of cytoplasm and the generation of outer membranes (forming the protrusions) from the plasma membrane, characteristics seen in apoptotic blebs.

Although DMPK overexpression induced blebbing formation, there were other behaviors that did not mimic the classical model of apoptosis. In conjunction with blebbing (24h post transfection), chromatin condensation and DNA fragmentation were monitored as these are two hallmarks of classical apoptosis (Mills *et al.* 1998; Jin *et al.* 2000). These two characteristics were not significantly observed in the blebbing cells. Moreover, a negative regulator transgene of classical apoptosis was co-transfected with the DMPK transgene. This bi-transgenic cell cultures did not show a decrease in blebbing. These results suggested that DMPK overexpression participates in a mechanism that is different from the classical model of apoptosis (Jin *et al.* 2000).

To identify if apoptotic-like blebbing was an effect produced by biological actions of DMPK protein or by recombinant protein nonphysiological dominant negative interactions, two B3 derived transgenic cultures were created. One of the lines was generated by transfecting a mutant *DMPK* transgene with blocked kinase activity. The other transgenic line was transfected with wild type *DMPK*. Striking differences were observed between these lines. Cells expressing WT *DMPK* possessed significant blebbing. These cells also exhibited enhanced labeling of F-actin-containing structures and increased organization of the actin cytoskeleton as evident stress fibers or cortical rings. The surrounding cells in the same culture that were not expressing wild type DMPK showed more diffuse and less intense F-actin signals (Jin *et al.* 2000).

On the other hand, cells expressing enzymatically inactive DMPK did not show blebbing. F-actin labeling did not exhibit any enhancement. There were no differences in F-actin staining between cells expressing mutant DMPK and the cells in the same culture that

did not express flawed DMPK protein. These results suggest that kinase activity from DMPK is needed for the induction of apoptotic-like blebbing in lens epithelial cells (Jin *et al.* 2000).

Due to the later results, DMPK overexpression in lens epithelial cell line B3 was related with the organization of F-actin cytoskeleton and membrane dynamics in the lens. Hence, *RHOA* was transiently transfected in the B3 cell line. RHOA is a GTPase that activates protein kinases structurally similar to DMPK in their catalytic protein kinase domain (Jin *et al.* 2000). RHOA promotes bundling of actin filaments with myosin II filaments to form stress fibers and focal adhesions (Ridley and Hall 1992; Chrzanowska-Wodnicka and BurrIDGE 1996) and apoptotic membrane blebbing (Milles *et al.* 1998). Hence, a comparison between the effects of RHOA when transiently transfected and expressed in B3 cells and the previous results of wild type DMPK overexpression was done. Indeed, overexpression of RHOA produced both blebbing and the changes in actin cytoskeleton seen after DMPK overexpression in lens epithelial cell cultures. Control experiments and the latter results suggested that the similar effects observed due to DMPK and RHOA expression are due to the fact that DMPK may function as well in regulating the organization of F-actin cytoskeleton and membrane dynamics in the lens. The functions of both proteins (DMPK and RHOA) might overlap in lens cells (Jin *et al.* 2000).

Jin *et al.* (2000) concluded that although other pathogenetic mechanisms such as a gain-of function from the abnormal properties of expanded CTG repeats cannot be ruled out; decreased expression and activity of normal DMPK may be at least one of the causes of cataracts in DM1. Overexpression of DMPK induces apoptotic-like processes. So, this protein may be part of the regulatory network that promotes apoptotic-like mechanisms to remove membrane organelles within developing lens fibers.

As mentioned before, *SIX5* has also been directly implicated as a candidate gene of DM1 since *DMPK* CTG repeat expansions decrease the expression of *SIX5* (Klesert *et al.* 2000). Hence, expression assays have been performed to identify if *SIX5* disrupted expression might trigger a cataract phenotype. RT-PCR (Reverse transcriptase-PCR) experiments were done in three adult human eyes and two fetal eyes (12 weeks old). *SIX5* mRNA was present in adult lens samples, but absent in whole eye fetal samples. *SIX5* mRNA expression by *in situ*

hybridization was observed in the lens epithelium of 8 adult human eyes, but not in any location in 6 samples of human fetal lenses (6-14 weeks; Winchester *et al.* 1999).

To determine if *SIX5* deficiency is at least in part responsible of DM1 features; a *Six5* deficient mice line was created. The *Six5* gene was disrupted by replacing its first exon with a  $\beta$ -galactosidase reporter. This made transgenic embryos to exhibit  $\beta$ -galactosidase expression driven by the *Six5* promoter. At 12.5 and 14.5dpc (days post coitum) faint staining was visualized at the lens fibers. In addition, few scattered spots of more intense staining at lens fibers were present at 14.5dpc (Klesert *et al.* 2000).

Klesert *et al.* (2000) also examined *Six5* knock out mice aged 5-7 and 8-10 months for presenile cataracts development under slip-lamp illumination. At both periods of time tested homozygous mutants had a higher grade of lens opacities compared to wild type littermates. Heterozygous mutants showed a trend toward a higher-grade cataract phenotype that augmented with age. However, the differences between heterozygous and wild type mice were not statistically significant at both periods of time analyzed. Anterior views of 10-month old *Six5* mutant mice lenses showed concentric refractile rings in the lens of null mice. Slit-lamp views revealed light scattering in the lens nucleus of homozygous mice. There were no differences observed between wild type and the heterozygous littermates. Hence, Klesert *et al.* (2000) hypothesized that the increased incidence of cataracts in mice deficient in *SIX5* indicates that a deficit of this protein in DM1 patients may be the reason of cataracts. However, Ranum and Day (2004) have questioned the latter since the cataracts observed in *Six5* knock out mice do not possess the typical iridescent opacities and the posterior location that is observed in DM1.

As stated before, MBNL1 protein expression is altered in DM1 tissues due to its sequestration by mutant mRNAs with expanded CUG repeats into nuclear foci (Jiang *et al.* 2004; Cardani *et al.* 2006). Hence, to observe if MBNL1 protein sequestration contributes to the DM1 defective phenotype, Kanadia *et al.* (2003) developed a *Mbnl1* knock out mice line. Data showing 18-week-old mutants lenses revealed the development of dust-like opacities. Anterior sections evidenced disorganized and cleft-like abnormalities in the anterior region of the lens mass. However, this study did not display a full description about the morphology and

progression of the development of cataracts in these mutants. Sections of the posterior region of *Mbnl1* mutant lenses were not shown either.

In all forms of DM1 (including CDM), the lens appears clear at birth and cataracts have not been described in anyone younger than at least 10 years old (Rhodes, unpublished). Ekström (2009) performed an ophthalmic study on 49 individuals with congenital (n=30) and childhood-onset (n=19) myotonic dystrophy 1 (females: n=20, 7.3-21.4 years; males: n=29, 1.6-21.9 years). Although, no true cataracts were reported in all individuals; bilateral subtle haze or condensation in the posterior lens pole was found in 39% of the individuals. The latter abnormality in the lens is suggestive of early stages of cataract development.

In the present literature review, the only identified published data directly relating *cugbp1* and the lens of the eye corresponds to early embryonic mRNA and protein expression in the zebrafish lens (Suzuki *et al.* 2000; Hashimoto *et al.* 2006). Hence, an important role of CUGBP1 at early lens development can be hypothesized. In addition, DMPK expression has been identified in embryonic development in chick and mice lenses (Harmon *et al.* 2008). Cataracts are a common feature in DM1 patients and the accumulation of mutant *DMPK* mRNA with expanded CUG repeats has been implicated in DM1 features; in part because soluble repeats lead to an augment in steady state levels of CUGBP1 increasing its post-transcriptional activity (Schoser and Timchenko 2010). So, it seems logical to think that *DMPK* mutant mRNA retention in lens cells may affect lens embryonic development by altering CUGBP1 levels and functions. Although cataracts are not present at birth in DM1 (Rhodes, unpublished), disrupted CUGBP1 expression could lead to lens lesions that may affect lens structure and clarity in posterior life. Other disrupted pathways could also contribute to the development of cataracts (i.e. MBNL1 depletion; Kanadia *et al.* 2003) in addition to CUGBP1 in DM1 patients.

## **Chapter 4. Materials and Methods**

All experiments were realized at The Gross Lab, Molecular Cell and Developmental Biology, University of Texas at Austin. DNA sequencing was performed at the Institute for Cellular and Molecular Biology (ICMB) Core Facilities, University of Texas at Austin.

Wild-type AB and TL Zebrafish (*Danio rerio*) strains were used and maintained at 28.5°C on a 14hour light/10hour dark cycle. Animals were treated in accordance with University of Texas at Austin, Institutional Animal Care and Use Committee (IACUC) provisions.

### **4.1 RNA *in situ* hybridization with digoxigenin-labeled probe**

An *in situ* hybridization assay was performed to try to identify the temporal and spatial *cugbp1* mRNA expression in the lens during early zebrafish development.

#### **4.1.1 *cugbp1* cDNA cloning**

Previously, zebrafish *cugbp1* mRNA was isolated and Reverse Transcriptase PCR (RT-PCR) was performed to obtain *cugbp1* cDNA. The *cugbp1* cDNA was cloned into CS10R plasmid (4.1kb; Annex 2). Afterwards, the *cugbp1*-CS10R construct was stored in The Gross Lab bacterial stock as D4 *cugbp1* CS10R.

(4.1.1 Section was performed by Dr. Jeffrey Gross, Principal Investigator).

#### **4.1.2 cDNA sequencing and protein sequence alignment**

To confirm that the cloned cDNA indeed encodes a zebrafish Cugbp1 protein and that it was produced by reverse transcription of *cugbp1* mature messenger RNA (mRNA), the previously cloned cDNA was sequenced. D4 *cugbp1* CS10R plasmid DNA was sequenced at the DNA Sequencing Facility of the ICBM at The University of Texas at Austin.

With the cDNA sequencing results (Annex 3, Probe), the amino acid sequence was deduced (Annex 4) to compare it with previously reported protein sequences. This was performed by using the translate application from the Molecular Toolkit online site (Colorado State University). The amino acid sequence obtained in the present study was aligned with a

501aa zebrafish Cugbp1 protein sequence already identified by Suzuki *et al.* (2000; DDBJ, accession number AB032726; Ensembl, ID ENSDARP00000026582, DDBJ). The latter was done using the ClustalW2 online program (EMBL-EBI, European Bioinformatics Institute).

#### **4.1.3 Digoxigenin-labeled probe synthesis**

Antisense and sense probes were generated in order to perform the *in situ* hybridization assay. An mRNA antisense probe is a labeled RNA-like sequence that is complementary to the sequence of a specific mRNA, in this case to *cugbp1* mRNA. Since antisense probe is complementary to *cugbp1* mRNA, the former can hybridize to the latter in the euthanized body of an organism, in this case to zebrafish embryos. The mRNA sense probe has the same sequence that *cugbp1* mRNA. So, it should not hybridize with the mRNA in question and it serves as a control.

Circular DNA purification from a D4 (*cugbp1* CS10R plasmid) bacterial stock culture was performed using the QIAprep Spin Miniprep Kit and a microcentrifuge (Qiagen). Plasmid digestion followed by incubation for 2 hours at 37°C was performed using the following amounts of reagents: 10µl plasmid DNA, 10µl Nebuffer 3 or Nebuffer 1, 2µl restriction enzyme Sall or KpnI (New England Biolabs) and 78µl H<sub>2</sub>O for a total volume of 100µl for antisense probe and sense probe, respectively. Purification of linearized DNA template was done using the PCR clean-up Kit Epoch Biolabs. Antisense and sense probes were synthesized following the DIG RNA Labeling Mix 10X conc. Protocol (Roche Applied Science; Annex 5) using T7 or SP6 RNA polymerase, respectively. Probes were labeled by adding to the synthesis mixture, in addition to the standard uridine triphosphate (UTP), a UTP conjugated with digoxigenin. Digoxigenin is a compound isolated and made by a limited group of plants and not found in animals. Hence, it will make any mRNA bound to the probe recognizably different from any other mRNA in the tissue being studied.

#### **4.1.4 *In situ* hybridization**

To suggest that *cugbp1* expression has a possible role in normal zebrafish early lens development, an mRNA expression assay was first performed. 1, 2, 3 and 4dpf embryo fixation, permeabilization, hybridization, anti-digoxigenin alkaline phosphatase (AP) labeling

and colorization were performed as described by Jowett and Lettice (2004; Annex 6). Fixation was realized to preserve the samples morphology and to avoid the loss of mRNA from the cells. The permeabilization treatment allows maximum exposure of target mRNAs to probe by facilitating probe diffusion in the cell and out when it is unbound. The hybridization step permits the binding of antisense probe to the target mRNA due to sequence complementarity. Labeling is done with an antibody against digoxigenin. The only places where the antibody should bind are where the antisense probe has bounded, thus where the target mRNA is. Moreover the antibody has been linked to the AP enzyme. At colorization, BCIP/NBT is used. BCIP/NBT reacts with AP generating a purple-blue precipitate where the antibody is located. The latter serves to indicate that the target mRNA is present where the insoluble purple/blue dye is at.

To observe in more detail the spatial and temporal *cugbp1* mRNA expression in the lens, transverse sections of the center of the eye from embryos submitted to *in situ* hybridization at 1, 2, 3 and 4dpf were analyzed. Cryosectioning was performed according to Uribe and Gross (2007; Annex 7). After sections were adhered to the slides, 50-55µl of DPX mounting medium were added directly to the slides. Afterwards a no. 1 thickness cover slip was placed on top. Mounting medium was left to harden overnight at room temperature. Imaging and pictures taken of cryosections were done using the Leica Microscope DM 2500. Figure 5.1.2a represents a transverse section of the zebrafish lens.

#### **4.2 *cugbp1* promoter activity in microinjected and transgenic zebrafish embryos**

To try to identify when and where inside the lens can Cugbp1 protein be present, a *cugbp1* potential enhancer-promoter (aka promoter) region was first sought. The latter since a promoter is a part of a gene where RNA polymerase first binds for subsequent DNA transcription. An enhancer is a part that tells where and when a promoter is used. Both are cis-DNA elements of a particular gene. Recognition of these sequences will help to observe the protein temporal and spatial pattern of expression driven by the identified *cugbp1* promoter when fused to a reporter gene (e.g., Enhanced Green Fluorescent Protein, EGFP).

#### 4.2.1 Search and cloning of a zebrafish *cugbp1* promoter region

To try to find a potential promoter region of the zebrafish *cugbp1* gene, the Evolutionary Conserved Region (ECR) Browser website was consulted. Special emphasis was given on conserved regions localized upstream of the start codon (ATG lies at exon4) of the zebrafish *cugbp1* gene, since promoter regions tend to be at this sites. A 1.2kb *cugbp1* potential promoter fragment was identified. This region was amplified from genomic zebrafish DNA and recognition sites for *KpnI* and *SpeI* restriction enzymes (Annex 8, purple shades) were created (for further subcloning see Section 4.2.3) by PCR using the following designed primers respectively:

5'-GTACAGGTACCGCTTTCTCTTCCTGC-3' and

5'-GTAGACACTAGTTTCTTCAGGCCTTC-3'

Afterwards, the 1.2kb PCR amplicon was cloned using the TA Cloning Strategy (Zhou and Gomez-Sanchez 2000) into linearized pGEM-T Easy Vector (3.015Kb). For this, 3'A-tailing of the PCR product was realized to create complementarity with the vectors single 3'-terminal thymidines (T-overhangs). Purification and 3'A-tailing of the potential promoter DNA fragment, ligation reaction and transformation were performed according to the pGEM-T and pGEM-T Easy Vector Systems Manual (Promega).

(4.2.1 Section was performed by Richard Nuckels, Research Associate).

#### 4.2.2 Location of the *cugbp1* promoter region in the zebrafish genome

To confirm that the potential promoter region previously cloned is part of the *cugbp1* zebrafish gene, an identification of its location was realized by using the *cugbp1* Ensemble genome sequence (ID ENSDARG00000005315). The latter sequence was submitted to *in silico* PCR with the primers mentioned above (4.2.1 Section). FastPCR 6.1 program was utilized. A *cugbp1* transcript sequence (ID ENSDART00000018448) was used to find the position of the promoter in relation to the ATG start codon and the transcription start site (1+).

### 4.2.3 Plasmids construction

An *in vitro* site-specific recombination approach (Hartley *et al.* 2000; Kwan *et al.* 2007) was used to create two expression constructs. An expression construct is basically a [promoter]-[coding sequence]-[3' tag or polyadenylation signal] construct in a Tol2 transposon backbone (Tol2 element function is explained in Section 4.2.4). In the present work, two constructs were generated: [*cugbp1* 1.2kb promoter]-[membrane or nuclear EGFP]-[SV40 polyA] to be introduced on an expression system (Zebrafish) and therefore to monitor the *cugbp1* promoter fragment activity *in vivo*. Site-specific recombinational cloning allows simultaneous cloning of multiple DNA fragments on one step and with a defined orientation.

The following steps were performed according to The MultiSite Gateway Three Fragment Vector Construction Kit (Invitrogen) and The Tol2kit (Kwan *et al.* 2007). The *cugbp1* promoter pGEM-T Easy Vector (from Section 4.2.1) was digested with KpnI and SpeI restriction enzymes and the 1.2kb *cugbp1* fragment was purified for posterior subcloning into p5E-MCS plasmid. The p5E-MCS vector contains the pBluescript multiple cloning site which includes a restriction site for KpnI and another for SpeI. A plasmid referred as p5E in the Tol2kit (Kwan *et al.* 2007) is a 5' entry clone where the DNA insert that is going to become part of the expression construct (and the multiple cloning site) is flanked by attL4 and attR1 sites for the posterior LR recombination reaction. Hence, the p5E-MCS construct was digested with KpnI and SpeI. The 1.2kb purified *cugbp1* promoter fragment and the digested p5E-MCS were submitted to a ligation reaction for subcloning of the 1.2kb *cugbp1* fragment into the p5E-MCS plasmid.

Two separate multisite gateway LR recombination reactions were performed to create two expression constructs that differ by their middle entry clones. Both reactions were performed with pDESTol2p2A (destination vector; with attR4, attR3 and Tol2 transposon ends), p5E-*cugbp1*-MCS (5' entry clone), nuclear-localized EGFP (pME-nlsEGFP) or membrane-localized EGFP (pME-EGFPCAAX) (middle entry clones; with attL1 and attL2) and SV40 late polyA signal sequence (p3E-polyA) (3' entry clone; with attR2 and attL3). Two expression plasmids were created with the LR recombination reaction: *cugbp1*:EGFPCAAX-polyA and *cugbp1*:nlsEGFP-polyA. In both constructs, the *cugbp1* promoter 5' element is

destined to drive expression of the nuclear or membrane- localized EGFP in zebrafish development.

(4.2.3 Section was performed by Research Associate Richard Nuckels).

#### **4.2.4 Transposase mRNA synthesis**

Both expression constructs previously generated (Section 4.2.3) possess two ~500bp sequences from each end of the Tol2 transposon gene, one upstream of the 5' element and the other one downstream of a polyA signal (Kwan *et al.* 2007). These Tol2 ends are necessary for transposition of the *cugbp1:EGFPCAAX-polyA* or the *cugbp1:nlsEGFP-polyA* fragments of the expression constructs with Tol2 transposase in the DNA of an expression system. Hence, for zebrafish transgenesis each expression plasmid has to be coinjected with *in vitro* transcribed transposase mRNA. The latter since this mRNA is capable of synthesizing a fully functional Tol2 transposase protein after being injected in 1-cell stage zebrafish embryos (Kawakami and Shima 1999; Kawakami 2007).

For Tol2 transposase mRNA synthesis, circular DNA purification from stock bacteria pCS2FA-transposase plasmid (Kwan *et al.* 2007) was performed using the QIAprep Spin Miniprep Kit and a microcentrifuge (Qiagen). Plasmid digestion followed by incubation for 2 hours at 37°C was performed using the following amounts of reagents: 10µl plasmid DNA, 10µl Nebuffer 3, 2µl restriction enzyme NotI (New England Biolabs) and 78µl H<sub>2</sub>O for a total volume of 100µl. Purification of linearized DNA template was done using the PCR clean-up Kit Epoch Biolabs. Capped mRNA synthesis from the DNA template was done with the mMESSAGING mMACHINE Kit from Applied Biosystems using SP6 RNA polymerase and lithium chloride precipitation for the recovery of the RNA.

#### **4.2.5 Injections**

For transgenesis, 25pg (pictograms) of either DNA expression construct and 25pg of transposase mRNA were injected into 1-cell stage embryos using a microinjector (Harvard Apparatus, Medical Systems Research Products). Injections were done directly to the cell and not the yolk for early transgene incorporation.

Injected embryos were examined under a fluorescence microscope (Leica Microscope MZ 16F) at different time points to assess for expression of the EGFP reporter gene under the control of the 1.2kb *cugbp1* promoter. EGFP<sup>+</sup> injected embryos (F0; founder fish) were grown up 3-4 months. F0 fish harboring the transgene were mated with wild type fish to generate transgenic stable lines (F1).

#### **4.2.6 Immunohistochemistry on transverse cryosections from embryonic zebrafish eyes**

To observe the pattern of expression driven by the *cugbp1* 1.2kb promoter fragment in the lens, an immunohistochemistry assay to detect EGFP was performed in transverse sections of the center of the eye from transgenic embryos at 1, 2, 3, 4 and 6dpf. Tissue fixation, cryosectioning and immunostaining assays were performed on F1 EGFP<sup>+</sup> embryos as described in Uribe and Gross (2007; Annex 7). The anti-GFP primary antibody (1:100; Santa Cruz Biotech) was used. Images were taken using a Zeiss LSM5 Pascal laser scanning confocal microscope.

#### **4.3 *cugbp1* down regulation by splice-altering morpholino injections**

In order to identify the function of Cugbp1 protein during zebrafish lens development, *cugbp1* pre-mRNA was targeted by injecting fertilized eggs with an antisense splice-altering morpholino (*cugbp1*-MO) to knock down protein expression (Morcos 2007). As a negative control, a second group of embryos of the same batch in every injection round were injected with a control mismatch morpholino (*cugbp1*-MM) which should not alter splicing events. Mismatch morpholino injections serve to guarantee that any phenotypic differences in *cugbp1*-MO injected embryos are not just due to the injection procedure, but indeed to the specific MO splice-altering activity.

##### **4.3.1 Splice-altering morpholino injections**

*cugbp1* antisense (*cugbp1*-MO) and *cugbp1* mismatch (*cugbp1*-MM; [5 mispair](#) compared to the MO) morpholinos (MOs) were purchased from Open Biosystems and Gene

Tools, respectively. Both MOs were injected with a concentration of 2.2ng/embryo at the 1-4 cell stage into wild type embryos. MOs sequences are the following:

*cugbp1*-MO 5'-AACATTTTCTCACCCCCTGGAAGAAT-3' and

*cugbp1*-MM 5'-AAGATTTTGTCACCCGCTGCAACAAT-3'

Injections were performed with the same equipment as mentioned before (Section 4.2.5). An uninjected control group of embryos of the same batch of every single injection round was also maintained to compare them with the *cugbp1*-MM embryos. If both uninjected and *cugbp1*-MM embryos presented any unusual phenotypes, it meant that the whole batch was defective and all uninjected, *cugbp1*-MM and *cugbp1*-MO treated embryos had to be discarded. Injections can be directed to the yolk of the embryo since an active process in which mRNAs at the yolk are transported to the overlying blastomeres takes place at early embryonic zebrafish development (Bill *et al.* 2009).

#### **4.3.2 Test of morpholino activity by reverse transcription PCR (RT-PCR).**

To confirm the splice-altering efficacy of the morpholino, RT-PCR was performed on both groups of injected zebrafish embryos (*cugbp1*-MO and *cugbp1*-MM). For RT-PCR, RNA isolation was performed according to The Trizol Reagent–Isolates RNA from Embryo Protocol (Invitrogen) from 1dpf injected embryos. Production of cDNA was done following the iScript cDNA Synthesis Kit (BIO-RAD). PCR was performed using Taq polymerase with the following conditions: 94°C for 2min; 39 cycles of 94°C for 30s / 55°C for 45s / 72°C for 1min. The following primers were utilized:

Forward primer 5'-ATGAATGGGTCTCTGGACCAC-3' and

Reverse primer 5'- CATTGTTTTTCTCACTGTCTGCAGG-3'

For further confirmation of the RT-PCR results and to show the nature of the *cugbp1* pre-mRNA transcript modification, the obtained bands in the agarose gel (RT-PCR results) were purified with the QIAquick Gel Extraction Kit (Qiagen). The separate clean DNA fragment samples were sent to sequence as mentioned before (Section 4.1.2). To identify the positions recognized and altered by the *cugbp1*-MO within this gene, the *cugbp1* transcript sequence (ID ENSDART00000018448) was utilized.

### **4.3.3 Observation of the phenotypes and behaviors of *cugbp1*-MO and *cugbp1*-MM injected embryos**

MO and MM injected embryos were visualized and monitored for phenotypic differences and pictures were taken with a microscope (Leica Microscope MZ 16F).

### **4.3.4 BrdU incorporation assay, immunohistochemistry on transverse cryosections from embryonic eyes of previously injected *cugbp1*-MO and *cugbp1*-MM embryos and statistical analysis**

An assay to visualize any differences in lens cells proliferation between *cugbp1*-MO and *cugbp1*-MM embryos was performed. BrdU (bromo-deoxyuridine) is an artificial thymine analogue that can be incorporated in the DNA of S-phase cells (Matsuoka *et al.* 1990) allowing visualization of dividing cells at specific time points. *cugbp1*-MO as well as *cugbp1*-MM injected embryos of 2 or 3dpf were bathed in 10mM 5-Bromo-2-deoxyuridine (BrdU Sigma) for 2 hours; specifically from 24 to 26 or 72 to 74hpf. Embryos were euthanized immediately after each exposure period of time. Fixation and cryosectioning were performed as described in Uribe and Gross (2007; Annex 7).

For immunohistochemistry, the area of interest in each slide with the samples was circled with hydrophobic PAP pen. Then, slides were rehydrated in PBTD (0.1% Tween-20, 1%DMSO in 1X PBS) at room temperature for 2-3min in Coplin Jar. Slides were removed from PBTD and any excess was drained. Cryosections were treated with 4M HCl for 10min at 37°C. 4M HCl was drained off and slides were washed 3 times in PBTD at room temperature in Coplin Jar. Slides were removed from PBTD, any excess was drained from slides and slides were placed in humid chamber. Immunohistochemistry was performed as described by Uribe and Gross (2007; Annex 7) from step 12 and afterwards. The anti-BrdU (1:250; Abcam, ab6326) antibody was used.

Statistical analyses were realized to find out if there were any significant differences in the total number of S-phase cells in the lens between conditions and at the specific time points mentioned above. 3 sections of the center of the eye from 9 eyes (n=27) from embryos exposed to each one of the four conditions (2dpf *cugbp1*-MO vs. 2dpf *cugbp1*-MM and 3dpf *cugbp1*-MO vs. 3dpf *cugbp1*-MM) were used. Total BrdU positive cells from each eye lens

section were counted. Statistical significance was determined using a two-parametric unpaired t-test (Graphpad Prism Program) with all the counts performed.

#### **4.3.5 Aquaporin0 (Aqp0) immunohistochemistry on transverse cryosections from embryonic eyes of previously injected *cugbp1*-MO and *cugbp1*-MM embryos**

To detect if *cugbp1* down regulation affects lens fiber early differentiation, an Aqp0 detection assay was performed on *cugbp1*-MM and *cugbp1*-MO embryos. 2, 3 and 4dpf *cugbp1*-MO and *cugbp1*-MM injected embryos were euthanized. Fixation, cryosectioning and immunohistochemistry were performed as Uribe and Gross (2007; Annex 7). The anti-aquaporin0 (1:500; Chemicon, ab3071) antibody was used to mark Aqp0 in the lens, which is a membrane-localized protein expressed early during differentiation of primary and secondary lens fibers (Varadaraj *et al.* 2007).

#### **4.3.6 F-actin staining on transverse cryosections from embryonic eyes of previously injected *cugbp1*-MO and *cugbp1*-MM embryos**

F-actin plays an important role in fiber cell elongation and migration (Rao and Maddala 2006). Moreover, it is involved in maintaining the hexagonal geometry of lens fibers (Nowak *et al.* 2009). Hence, F-actin staining was assessed in lens fibers during *cugbp1* down regulation to observe if *Cugbp1* protein has an important role in F-actin distribution and/ or arrangement at these lens cells. And thus, has a function in the development or in maintaining lens fibers shape.

First, 4dpf *cugbp1*-MO and *cugbp1*-MM injected embryos were euthanized. Fixation and cryosectioning were performed according to Uribe and Gross (2007; Annex 7). For F-actin staining, the area of interest in each slide was circled with hydrophobic PAP pen to form a well. Slides were rehydrated in PBTD at room temperature for 2-3min in Coplin Jar. Slides were removed from PBTD. Any excess of PBTD was removed and slides were placed in a humid chamber. Staining solution (Alexa-488 Phalloidin; 1:50; Molecular Probes) was added to the wells in the slides. Humid chamber was closed, a foil cover was added and they were incubated overnight at 4°C. Then, staining solution was eliminated by rinsing slides with

PBTD 3 times, 10min each time. Then, slides were treated as described in Uribe and Gross (2007; Annex 7) from step 21 and afterwards.

#### **4.3.7 Nuclei staining on transverse cryosections from embryonic eyes of previously injected *cugbp1*-MO and *cugbp1*-MM embryos**

An assay to detect nuclei in the lens was performed on MOs to determine if Cugbp1 is required for lens fiber maturation. This was done because organelle degradation, including nuclei is a late event during fibers differentiation (Weber and Menko 2006a).

4 and 5dpf injected MOs were euthanized. Fixation and cryosectioning were performed as described in Uribe and Gross (2007; Annex 7). For nuclei staining, the area of interest in each slide was circled with hydrophobic PAP pen to form a well in the slide. Slides were rehydrated in PBTD at room temperature for 2-3min in Coplin Jar. Afterwards, the PBTD was removed from the slides. Any excess of PBTD was eliminated and slides were placed in a humid chamber. Nuclei staining solution (SytoxGreen; 1:1000; Molecular probes) was added to the wells in the slides. The humid chamber was closed, a foil cover was added and the slides were incubated overnight at 4°C. Then, staining solution was eliminated by rinsing slides with PBTD 3 times, 10min each time. Subsequently, slides were treated as described in Uribe and Gross (2007; Annex 7) from step 21 and afterwards.

## **Chapter 5. Results**

To estimate what cell types are present at the places where *cugbp1* mRNA is expressed or at the regions where activity driven by the identified *cugbp1* promoter takes place, Greiling and Clark (2009) assay of early embryonic lens development in zebrafish was used as a fate map. The latter work mentioned above was used as the primary reference for cellular localizations at all-time points tested in the present paper. And also as a guide for lens mass normal overall shape and development. Hence, mentioning the reference would be omitted from the Results (Chapter 5).

### **5.1 RNA *in situ* hybridization with digoxigenin-labeled probe**

#### **5.1.1 *cugbp1* cDNA sequencing and protein sequence alignment**

The sequencing results from CS10R-*cugbp1* plasmid showed that the *cugbp1* cDNA has a length of 1494bp (Annex 3, Probe). The corresponding protein sequence has 497 amino acids (aa; Fig 5.1.1 A, PROBE; Annex 4). When this protein sequence was aligned with the 501aa zebrafish Cugbp1 sequence previously reported by Suzuki *et al.* (2000), the 497aa sequence seemed to be almost identical to the 501aa sequence. The only difference was that the sequence identified in this study lacked 4aa (Fig 5.1.1 A) which corresponded to 231-234aa of the Suzuki *et al.* (2000) protein sequence. This variation extends from 22103 to 22114bp (location: +22103 to +22114) downstream from the transcription initiation site (+1) of the DNA sequence from Suzuki *et al.* (2000) protein. More specifically, the DNA sequence variation present in Suzuki *et al.* (2000), but absent in the sequencing results of the present study was located from the 4-15bp (5'-3' direction) of exon10 of the formerly identified sequence. The DNA difference (12bp in tandem) that leads to the protein dissimilarity is shown in Figure 5.1.1 B (complete cDNA sequences are shown in Annex 3).

#### **5.1.2 *In situ* hybridization to detect mRNA expression**

At 1dpf, cells in the posterior-middle of the developing lens continue to enlarge and take a rounded shape forming a nuclear center. Around this core region primary lens fibers

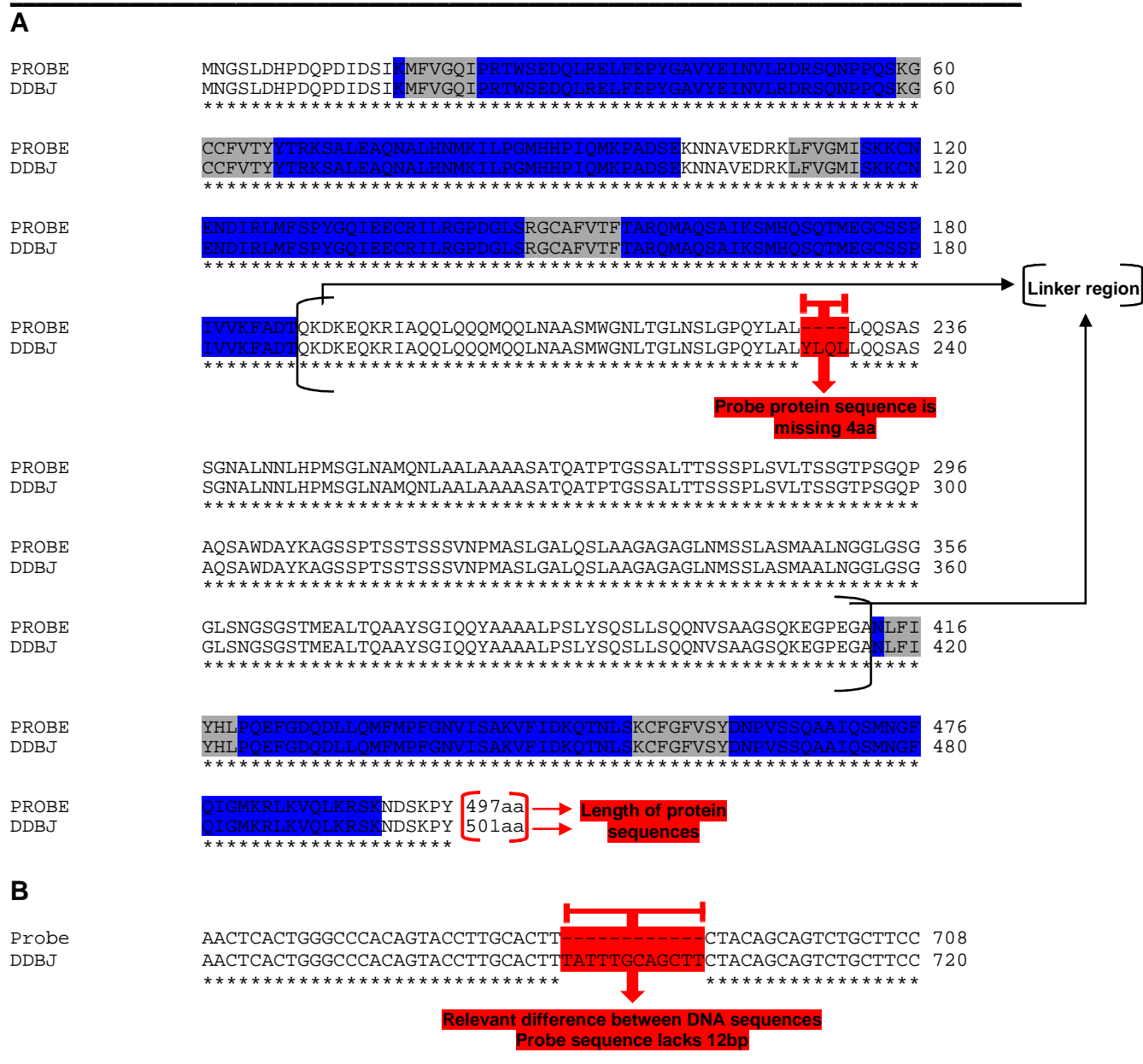


**Figure 5.1.1** Amino acid sequence alignment of *cugbp1* cDNA with previously reported *cugbp1* sequence DDBJ AB032726. **A:** PROBE is the protein sequence based on cDNA sequencing results from the previously cloned D4 *cugbp1* CS10R plasmid. DDBJ is the sequence previously reported by Suzuki *et al.* (2000). PROBE protein sequence is missing 4aa that are present at the linker region of DDBJ protein. Blue shades represent the RRM (RNA-recognition motifs). Gray shades represent the RNPs within the RRM. **B:** The nucleotide differences (12bp absent in Probe cDNA) that result in protein dissimilarities are shown. Complete cDNA sequences are shown in Annex 3.

elongate. Hence, layers of primary lens fibers surround the developing nucleus. In accordance with transverse sections (Fig 5.1.2a) of embryos submitted to *in situ* hybridization assay, these are the places where *cugbp1* mRNA expression appeared to be at 1dpf (Fig 5.1.2b A, B). Expression appeared more intense at the posterior-middle core region. The anterior region of the developing lens did not show *cugbp1* mRNA expression during this time point.

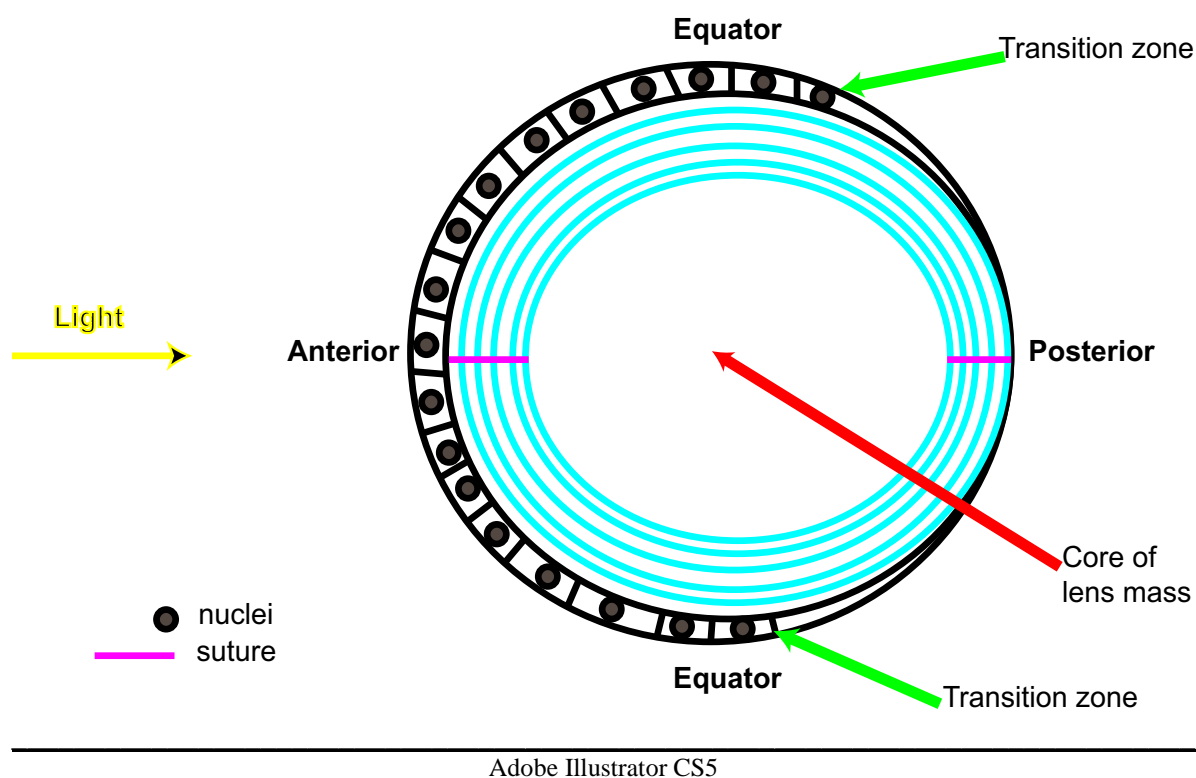
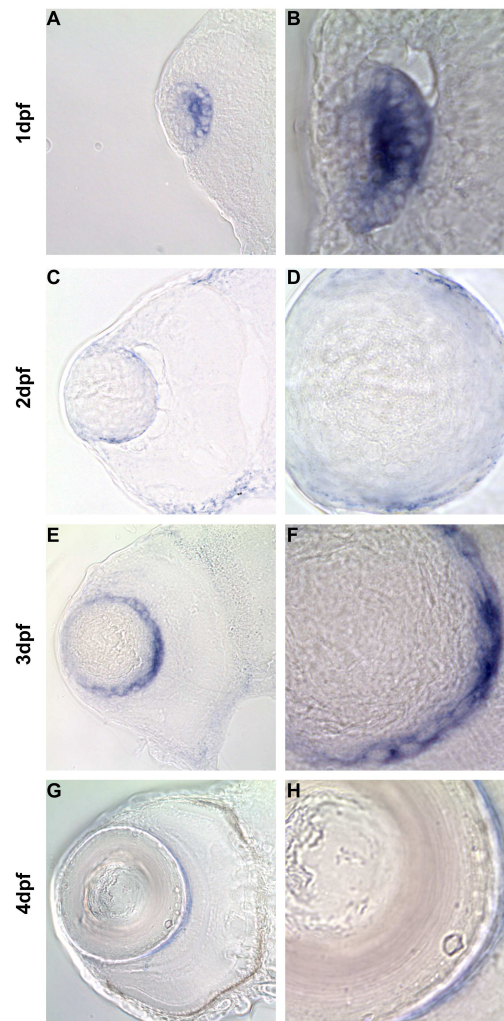


**Figure 5.1.2a** Diagram representing a transverse section of the zebrafish lens. All transverse sections presented in Figures 5.1.2b, 5.2.2a, 5.2.2b, 5.3.3, 5.3.4, 5.3.5, 5.3.6 are in the same orientation.

By 2dpf, *cugbp1* mRNA expression was observed at both transition regions of the lens (Fig 5.1.2b C, D); place where epithelial cells have withdrawn from the cell cycle and start to differentiate into secondary lens fibers. Expression at the middle part of the lens was no longer observed. At the anterior border of the lens, where cells remain as epithelium, there was no detectable expression.



Adobe Illustrator CS5

**Figure 5.1.2b** Transverse sections of zebrafish eyes show expression of *cugbp1* mRNA in the lens by *in situ* hybridization assay. **A, B:** At 1 day post fertilization (dpf) expression is shown at the posterior-middle, posterior-lateral and posterior regions of the lens. The former is constituted of cells that have a rounded shape forming a center. The last two areas are composed of primary lens fibers that surround the center. **C, D:** By 2dpf, expression was seen at both transition regions of the lens. **E, F:** 3dpf transverse sections showed expression at the posterior-middle and posterior borders of the lens, regions where secondary newly and still differentiating lens fibers are. **G, H:** Expression at the posterior border of the lens is still visible at 4dpf.

At 3dpf, expression of *cugbp1* mRNA appeared to be more intense at the posterior border of the lens (Fig 5.1.2b E, F). This region is where newly formed lens fibers are differentiating and the tips of this outer newly formed lens fibers from both differentiating zones meet at the posterior suture. A little bit less intense but still very obvious *cugbp1* mRNA expression was present at the posterior-lateral border regions which include both of the transition zones (TZs) of the lens (Fig 5.1.2b E, F). These TZs are located more posteriorly in zebrafish as compared to mammals.

*cugbp1* mRNA expression, at 4dpf, was still present at newly differentiating lens fibers at the posterior border of the lens (Fig 5.1.2b G, H). However this expression seemed to be less intense compared to the expression seen at 3dpf (Fig 5.1.2b E, F).

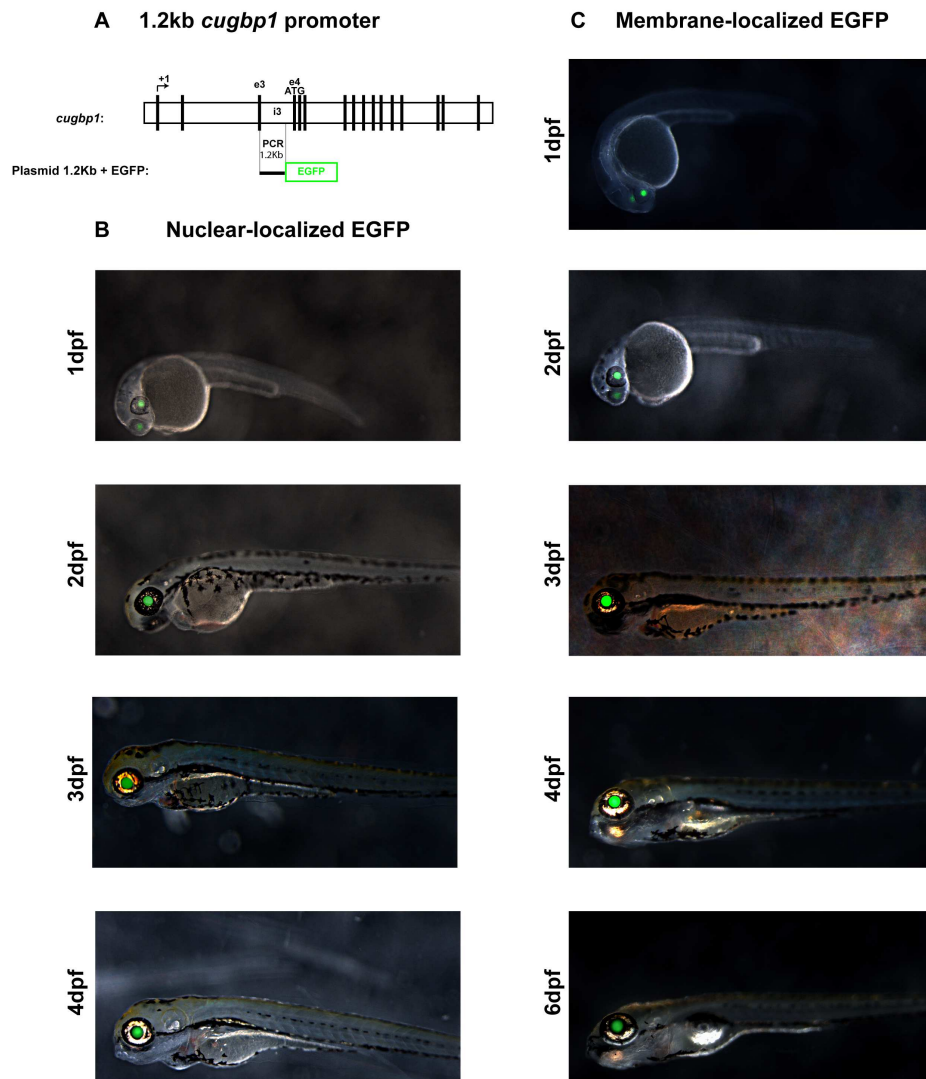
## **5.2 *cugbp1* promoter activity in microinjected and transgenic zebrafish embryos**

### **5.2.1 Identification of the location of the *cugbp1* promoter region in the zebrafish genome**

A 1.2kb *cugbp1* promoter fragment with high lens specificity was identified in zebrafish (Fig 5.2.1 A). This promoter is localized within the leader sequence (5'UTR) of the *cugbp1* gene and extends from 9 808 to 10 959bp (from +9 808 to +10959) downstream the transcription initiation site (+1). Its length is of 1152bp according to the Ensemble genome sequence (ID: ENSDARG00000005315). In the 5' to 3' direction, the identified promoter begins 85bp downstream of exon3 start site (including its last 39bp) and also contains the first 1113bp of intron3 (Annex 8). To avoid any confusion, it is important to clarify that the start codon (ATG) of the zebrafish *cugbp1* gene is located at exon4.

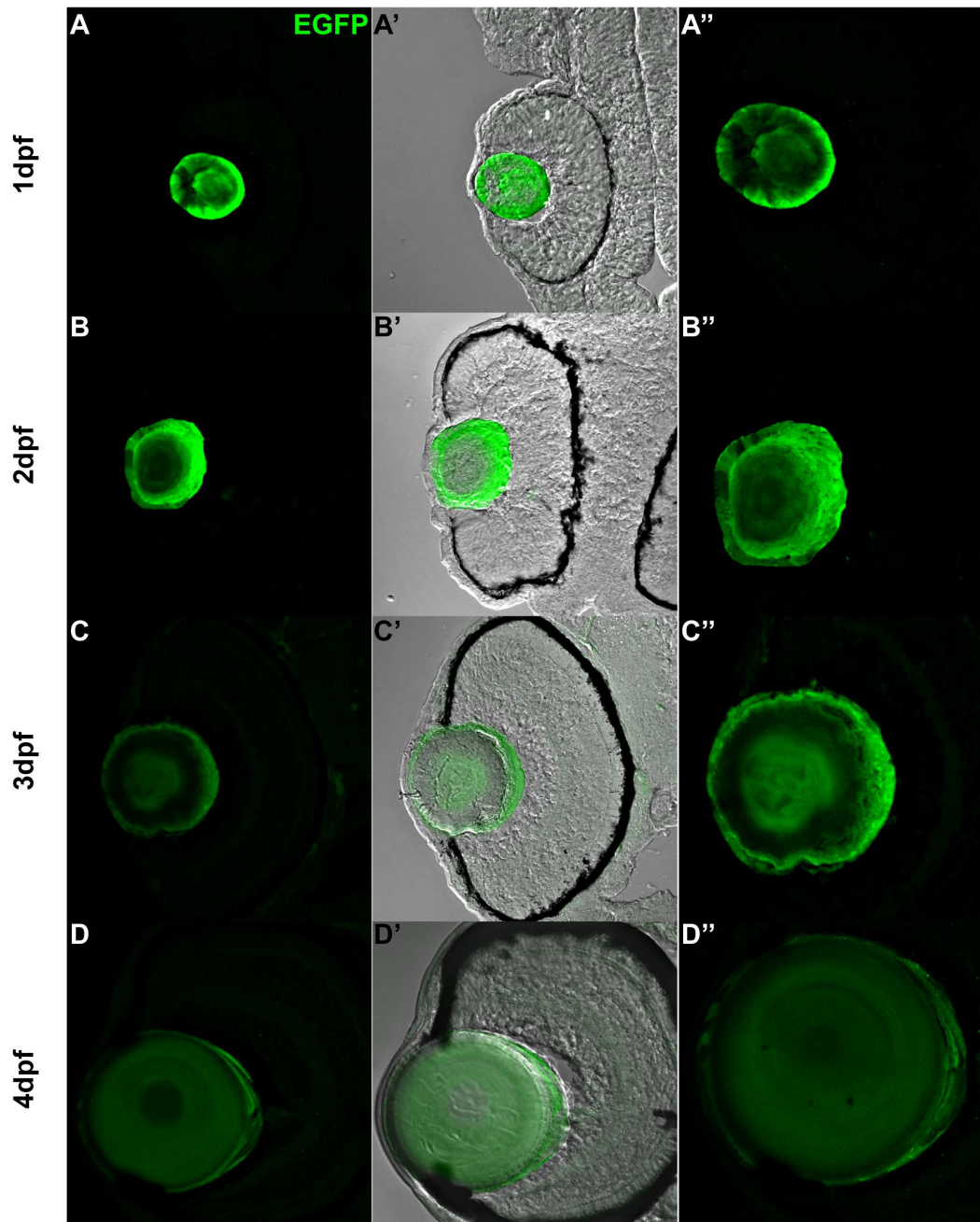
### **5.2.2 EGFP expression driven by a 1.2kb *cugbp1* promoter region**

High lens specificity was demonstrated by observing EGFP expression in the lens from 1dpf and onwards in embryos injected with either the nuclear (Fig 5.2.1 B) or membrane (Fig 5.2.1 C) localized EGFP constructs.



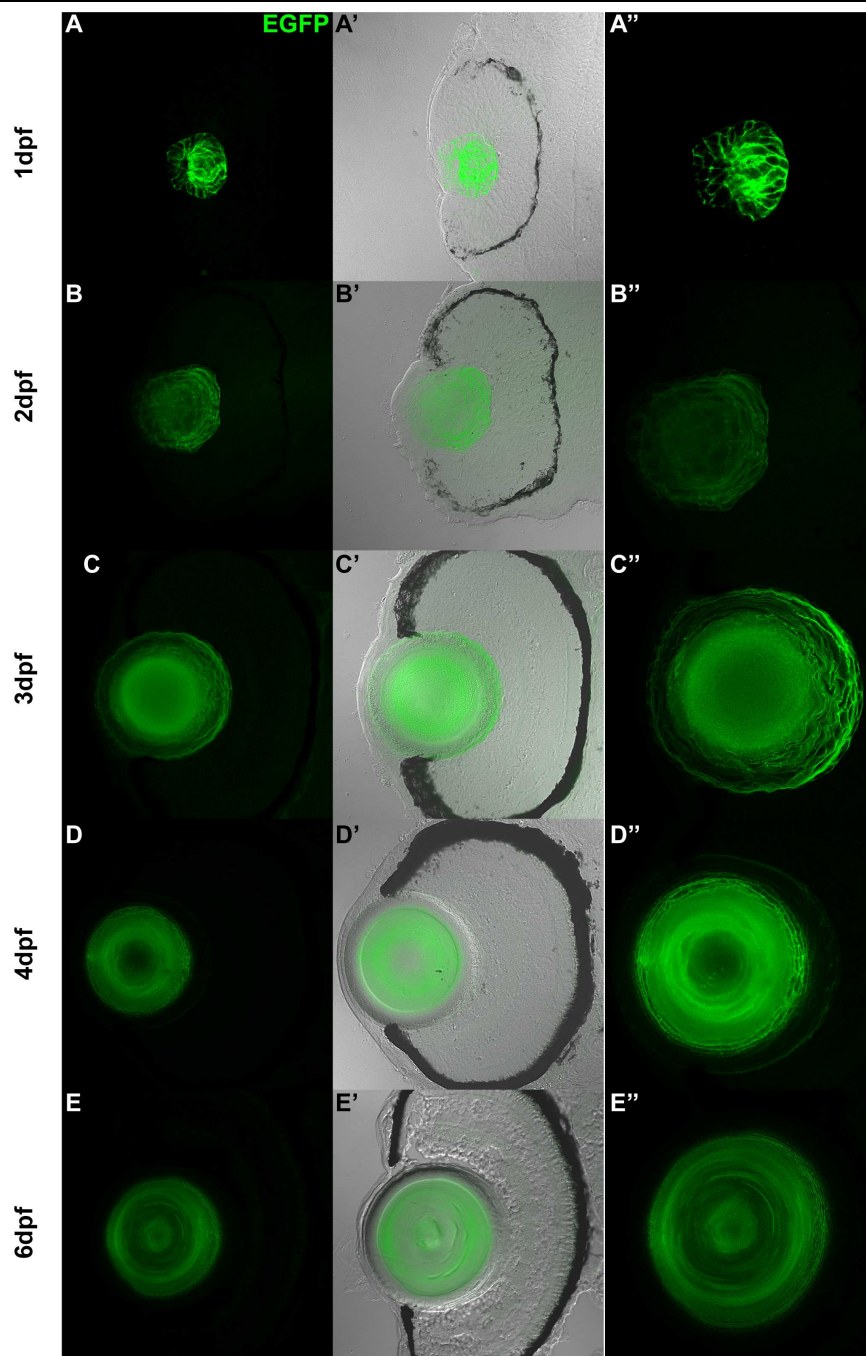
Adobe Illustrator CS5

**Figure 5.2.1 EGFP expression driven by a 1.2kb *cugbp1* promoter in F0 zebrafish embryos.** F0 embryos were microinjected at the one-cell stage with 25pg of transposase mRNA and 25pg of *cugbp1*:pME-nlsEGFP-polyA (nuclear-localized EGFP) or *cugbp1*:pME-EGFPCAAX-polyA (membrane-localized EGFP) DNA. **A:** Schematic diagram of plasmid constructs that contain a zebrafish 1.2kb *cugbp1* promoter fragment fused to the membrane-localized or nuclear localized EGFP. The *cugbp1* gene representation (not drawn to scale) shows the location of the 1.2kb fragment in the zebrafish genome. **B:** Zebrafish embryos at 1, 2, 3 and 4dpf showing nuclear-localized EGFP expression. **C:** Zebrafish embryos at 1, 2, 3, 4 and 6dpf showing membrane-localized EGFP expression. Both constructs reveal expression in the lens.



Adobe Illustrator CS5

**Figure 5.2.2a** Transverse sections at the eye region from zebrafish F1 stable transgenic line embryos carrying the 1.2kb *cugbp1*:pME-nlsEGFP-polyA transgene. The *cugbp1* promoter fragment possesses high lens specificity.



Adobe Illustrator CS5

**Figure 5.2.2b** Transverse sections at the eye region from zebrafish F1 stable transgenic line embryos carrying the 1.2kb *cugbp1*:pME-EGFPCAAX-polyA transgene. The *cugbp1* promoter fragment possesses high lens specificity.

Transverse sections of the center of the eye from transgenic embryos (F1) showed EGFP expression within the lens. Both the nuclear (Fig 5.2.2a) and membrane-localized (Fig 5.2.2b) EGFP expression driven by the 1.2kb *cugbp1* promoter was detected in a more general pattern inside the lens compared to the results obtained by the *in situ* hybridization assays (Fig 5.1.2b).

At 1, 2 and 3dpf, transverse sections of both transgenic lines showed strong expression at the posterior and posterior-middle regions of the lens (Fig 5.2.2a A-C; Fig 5.2.2b A-C) correlating with the results obtained in the *in situ* hybridization assay. Both nuclear or membrane localized transgenic embryos also displayed expression at the anterior region of the lens during these time points. At 4dpf, nuclear-localized EGFP embryos showed intense expression at the posterior border of the lens (Fig 5.2.2a D). High levels of EGFP seemed to be still present in the lens fibers at the middle-posterior and middle-anterior regions of the lens mass in the membrane localized EGFP transgenic embryos at 4dpf and 6dpf (Fig 5.2.2b D, E). At 4dpf, less intense expression of mem-EGFP was visualized at the posterior and lateral borders of the lens. However, at 6dpf mem-EGFP was not detected at these borders of the lens.

### **5.3 *cugbp1* down regulation by splice-altering morpholino injections in zebrafish embryos**

#### **5.3.1 Splice-altering morpholino activity tested by RT-PCR**

The *cugbp1*-MO binds to the splice junction of exon5/intron5 (Fig 5.3.1 A; Annex 9 A) to disrupt correct splicing of *cugbp1* pre-mRNA. RT-PCR results showed that *cugbp1*-MO injected embryos (“morphants”) possessed altered splicing by showing a 227bp band (Fig 5.3.1 B; Annex 9, A) in agarose gel. *cugbp1*-MM embryos (“controls”) exhibited a 310bp band (Fig 5.3.1 B; Annex 9, B) and no 227bp PCR product. Splice-altering activity was not 100% efficient since morphant samples also possessed the 310bp band. More specifically, the 310bp band corresponds to 178bp of exon4 downstream and beginning with the ATG start codon, exon5 (83bp) and exon6 (49bp; Fig 5.3.1 C; Annex 9). The latter represents unaltered splicing. The 227bp band corresponds to a removal of exon5 ( $310-83=227$ bp; Fig 5.3.1 C;

Annex 9). Exon5 exclusion at *cugbp1*-MO injected embryos was further confirmed after sequencing each purified band (Fig 5.3.1 D). Exon5 is located from +14 098 to +14 180bp.

### **5.3.2 Morphant vs. control embryos phenotype and behavior**

*cugbp1*-MO embryos exhibited less body movement when compared with controls. Most morphants were not able to get out of their chorions (normally realized at the 2-3dpf stage) by their own. By 2dpf, it was obvious that morphants exhibited a delayed phenotype by having less pigmentation (2dpf MO embryos had a pigmentation pattern as if they were 1dpf), being of smaller size and having bigger yolks due to its lower consumption compared with *cugbp1*-MM embryos. 4dpf *cugbp1*-MO embryos exhibited smaller bodies, enlarged hearts, had smaller eyes (microphthalmia) and possessed an evident cataract phenotype when compared with *cugbp1*-MM embryos (Fig 5.3.1 E). Morphants were very still in contrast with *cugbp1*-MM embryos which swam and were in constant movement as uninjected littermates.

### **5.3.3 Cell proliferation analysis by BrdU incorporation assay in lens cells after *cugbp1* down regulation**

At 24 to 26hpf (Fig 5.3.3 A; Annex 10), *cugbp1*-MM lens contained an average total number of  $8.037 \pm 0.5188$  BrdU+ cells, and *cugbp1*-MO possessed a  $7.963 \pm 0.4117$  value ( $P=0.9114$ ). At 72 to 74hpf (Fig 5.3.3 B; Annex 10), *cugbp1*-MM lens had a par of  $9.222 \pm 0.6047$  BrdU+ total cells and *cugbp1*-MO possessed a mean of  $8.111 \pm 0.3711$  BrdU+ cells ( $P=0.1234$ ). There were no statistical differences in the total number of BrdU+ cells between *cugbp1*-MO vs. *cugbp1*-MM embryos at both time periods analyzed (Fig 5.3.3 C). Hence, morphants epithelial lens cells retain their ability to proliferate at the same rate as epithelial cells of control embryos do, despite *cugbp1* down regulation.

### **5.3.4 Expression of lens fiber membrane protein Aquaporin0 as a marker of early fiber differentiation after *cugbp1* down regulation**

At all-time points tested (2, 3 and 4dpf) detectable levels of Aqp0 protein were present in *cugbp1*-MM as well as in *cugbp1*-MO embryos lenses (Fig 5.3.4 A-F). Demarcation of lens fiber membranes by Aqp0 immunology assay showed a considerable difference in size and

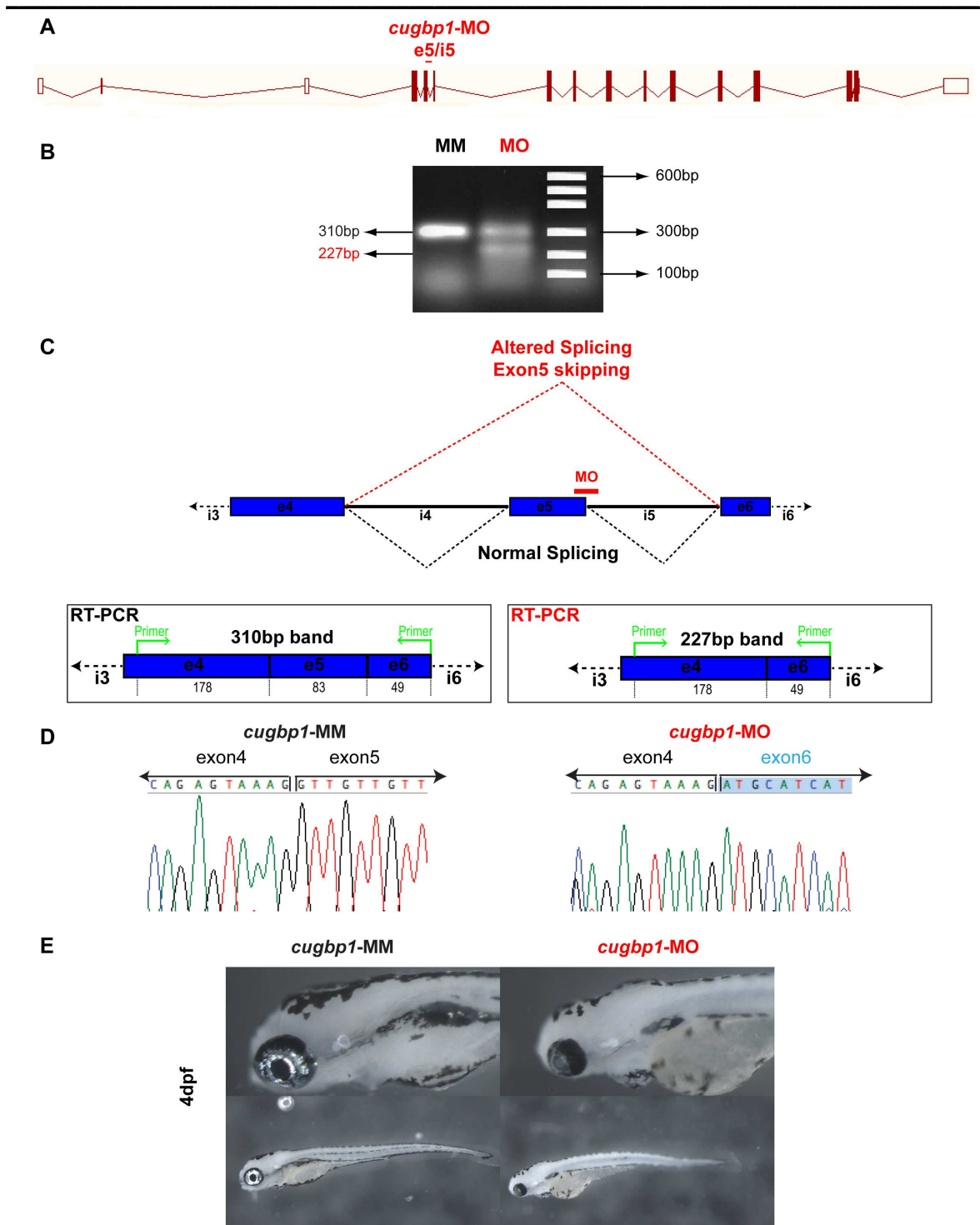
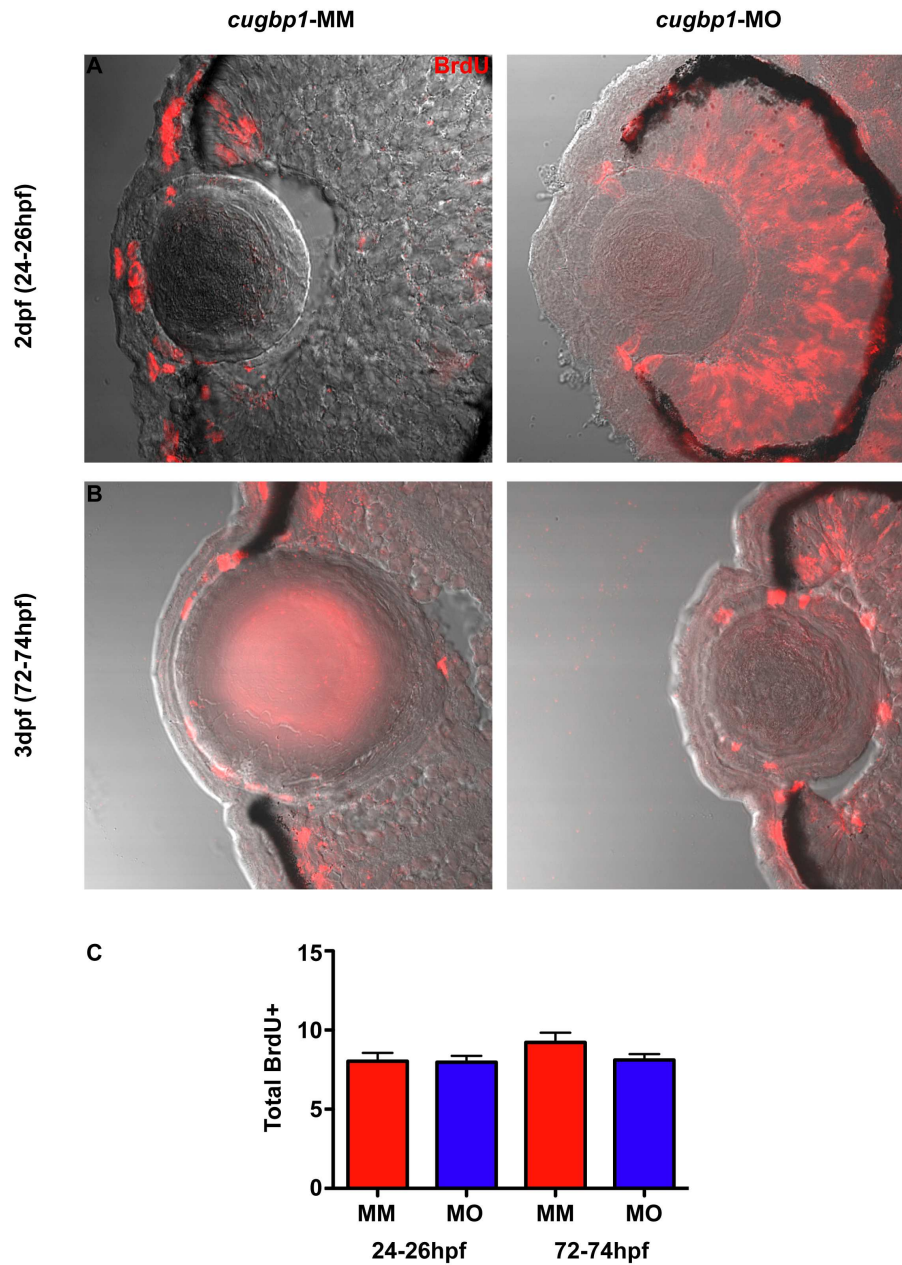


**Figure 5.3.1 Knock down of *cugbp1* function in zebrafish embryonic development by splice-altering morpholino results in a cataract phenotype and other features that resemble DM1 disease.** **A:** *Ensembl* diagram (ENSDARP00000026582) of *cugbp1* gene showing the region where the splice-altering morpholino binds to *cugbp1* pre-mRNA (exon5/intron5). **B:** RT-PCR results from *cugbp1*-MO and *cugbp1*-MM embryos show splice-altering activity in *cugbp1*-MO samples evidenced by a 227bp band (DNA ladder was superimposed on agarose gel photo). **C:** Schematic representation (not drawn to scale) of altered splicing vs. normal splicing and its corresponding RT-PCR results. The 310bp band corresponds to 178bp of exon4, 83bp of exon5 and 49bp of exon6. The 227bp band is present due to a removal of 83bp from exon5 **D:** Automatic sequencing results of each purified band exhibit removal of exon5 from the 227bp band detected only on the *cugbp1*-MO RT-PCR products. **E:** Lateral view of 4dpf *cugbp1*-MO and *cugbp1*-MM embryos. Whereas *cugbp1*-MM embryos displayed normal early development, *cugbp1*-MO embryos showed a defective phenotype which included opacification of the lens.

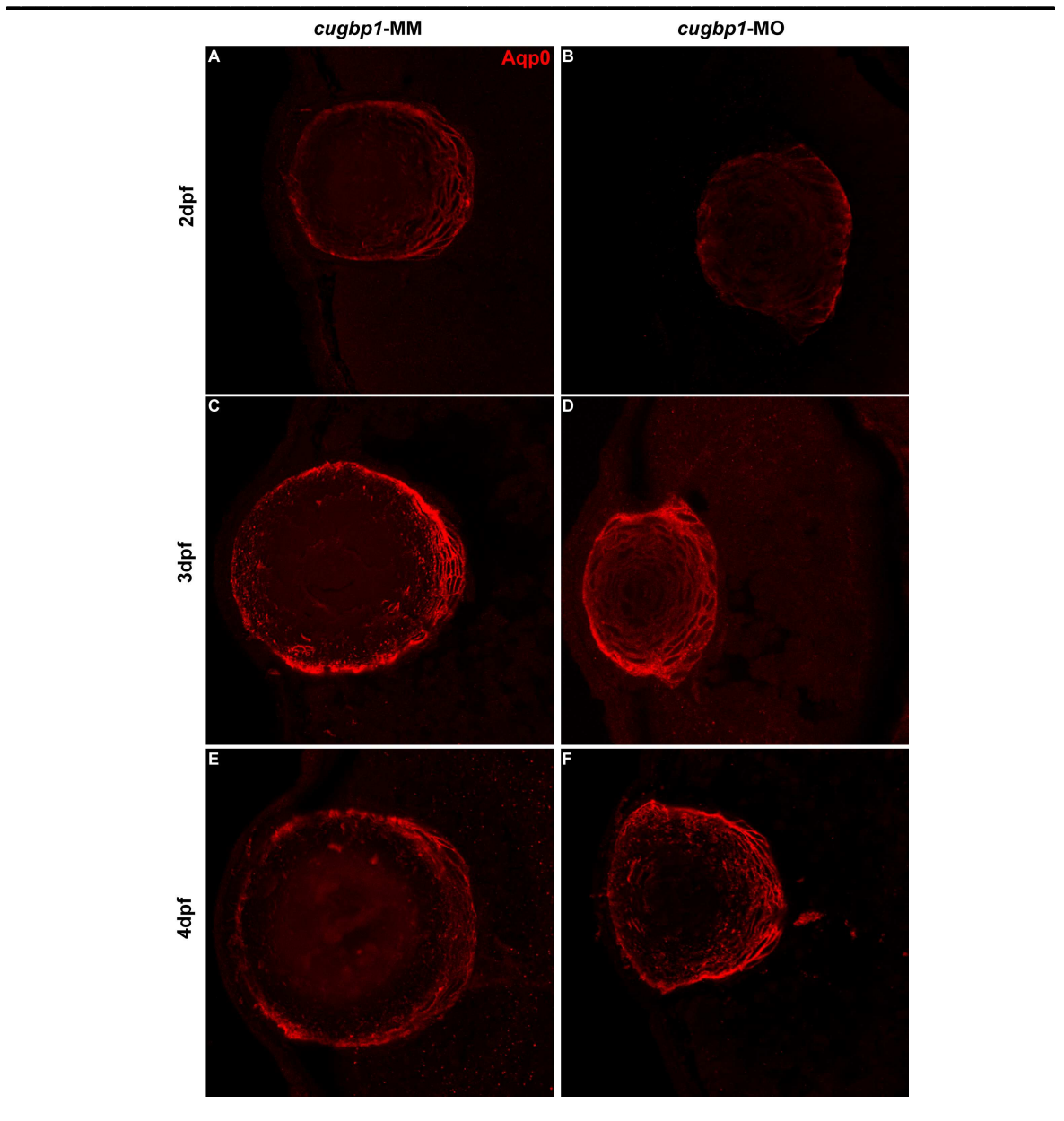
shape of the lens fiber mass of *cugbp1*-MM vs. *cugbp1*-MO embryos. At 2dpf, MM lenses seemed spherical along the equator and lentoid along the anterior to posterior region (Fig 5.3.4 A). Whereas, 2dpf MO lenses appeared to have an oval shape with an equatorial diameter that seemed longer than the anterior to posterior diameter and a squeezed-like phenotype at both equatorial regions of the lens (Fig 5.3.4 B). By 3dpf, MM lens mass seemed to have a spherical form in all dimensions (Fig 5.3.4 C). But, 3dpf MO lens mass appeared to retain the oval shape with the squeezed-like phenotype at the equatorial regions (Fig 5.3.4 D). The 4dpf MM injected embryos exhibited a lens mass form that looked as a larger and still spherical version of the 3dpf lenses (Fig 5.3.4 E). However, 4dpf MO lenses still retain the squeezed phenotype at both equatorial zones (Fig 5.3.4 F). Mismatch morpholino injected embryos possessed a lens overall shape that appeared to be as expected in normal development during all periods of time analyzed. Nevertheless, this was not the case for embryos submitted to *cugbp1* down regulation as early as the 1-4 cell stage.

Moreover, 2 and 3dpf *cugbp1*-MO embryos showed obvious Aqp0 protein presence in the lens nucleus, place where primary fibers reside. Aqp0 expression was also observed in the secondary fibers immediately surrounding the lens primary fibers (Fig 5.3.4 B, D). However, in *cugbp1*-MM embryos, Aqp0 expression in the center of the lens could not be detected (Fig 5.3.4 A, C). At the outer-most lens fibers, Aqp0 protein was observed in morphants (MO) as well as in controls (MM) in all times tested.



Adobe Illustrator CS5

**Figure 5.3.3** BrdU incorporation assay at 24-26 or 72-74hpf showed that there were no differences in the total number of proliferative cells in the lens between *cugbp1*-MO and *cugbp1*-MM embryos. **A:** 2dpf control embryos and morphants show proliferative cells in the lens. **B:** 3dpf control embryos and morphants show proliferative cells in the lens **C:** Chart showing the number of BrdU<sup>+</sup> cells in each condition (n = 27; p < 0.05).



Adobe Illustrator CS5

**Figure 5.3.4** Lens fibers express differentiation marker Aqp0 in *cugbp1-MO* embryos. **A,C,E**: 2, 3 and 4 dpf lens sections from control embryos, respectively. **B,D,F**: 2, 3, and 4 dpf lens sections from morphants. All conditions tested showed Aqp0 expression. In addition, *cugbp1-MO* embryos have smaller lenses and abnormal lens shape.

### 5.3.5 F-actin organization in the lens after knocking down *cugbp1* expression

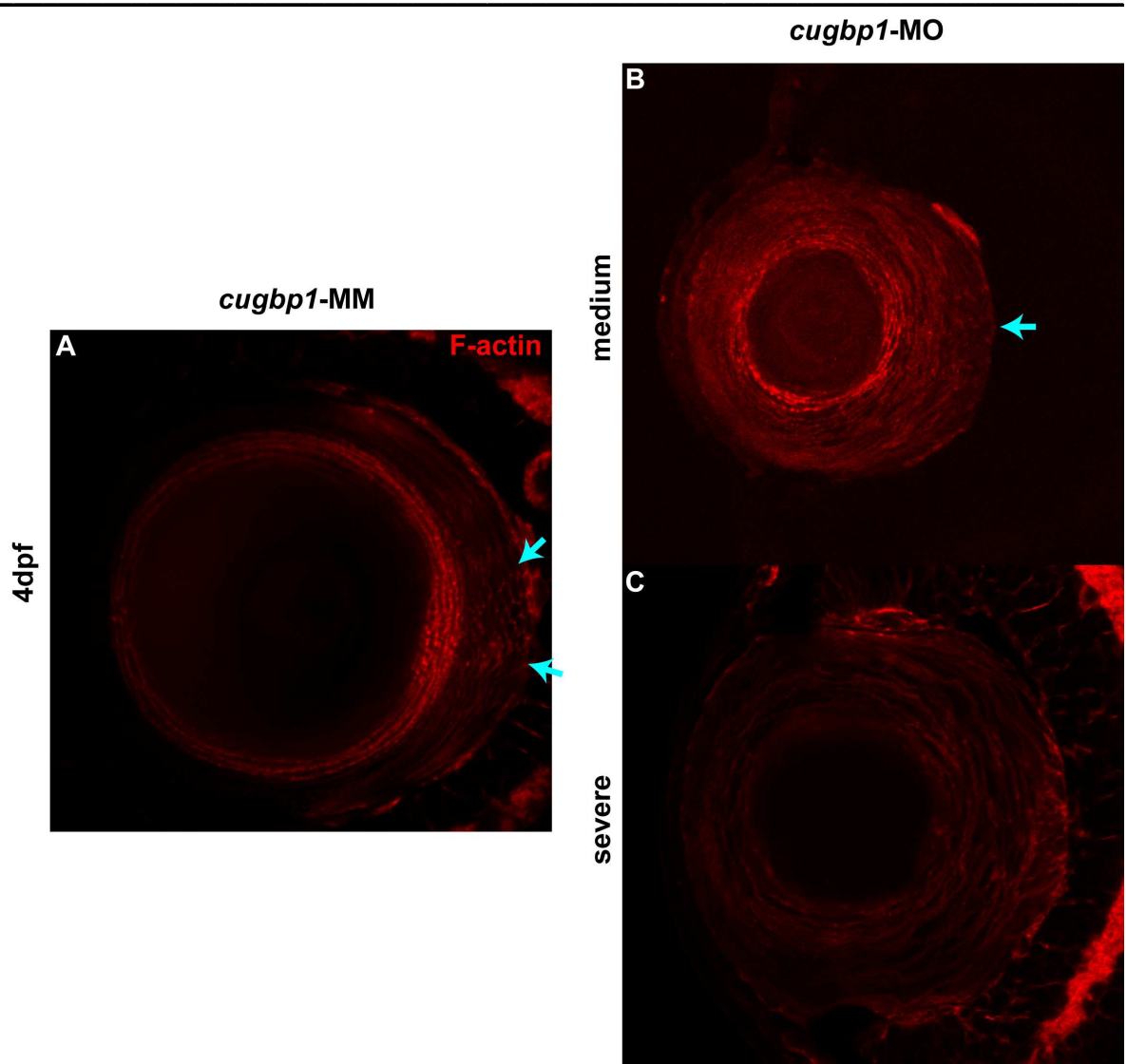
Since Aqp0 protein detection assay demonstrated that the initiation of fiber cell differentiation happened, but lens overall form is affected due to down regulation of *cugbp1* expression, an F-actin marker was used to longer examine lens fiber morphology. Lens fibers from 4dpf *cugbp1*-MM embryos displayed normal F-actin organization. This was shown as a ring-like structure with concentric thin rings or layers surrounding the center of the lens (Fig 5.3.5 A). This ring-like F-actin staining pattern was present at the region of the lens where newly formed secondary lens fibers are being constantly added and subsequently displaced inward for younger fiber cells to be at the periphery. No F-actin staining was visible at the lens nucleus, probably because this region has very compacted primary and surrounding secondary lens fibers. An evident posterior lens suture (Fig 5.3.5 A, cyan arrows) was observed in *cugbp1*-MM embryos, but an anterior lens suture was still not apparent.

In contrast, 4dpf *cugbp1*-MO embryos seem to have a diverse defective phenotype. A medium flawed phenotype (Fig 5.3.5 B) showed smaller lenses as observed before (Fig 5.3.4 F). The innermost region of the lens was not stained, although this area was not as big as the stained-free region observed in MM embryos. F-actin arrangement showed that lens fibers appear as concentric rings of outer fibers surrounding the rings of inner fibers. A posterior-like suture is evident (Fig 5.3.5 B, cyan arrow), but it does not have the same appearance of the one seen in controls (Fig 5-3.5 A). A severe phenotype (Fig 5.3.5 C) did not show F-actin concentric rings from fibers, rather a disorganized pattern (wave-like) of actin filaments was present. There was no evidence of a posterior suture in this severe phenotype (Fig 5.3.5 C).

### 5.3.6 Lens fiber nuclei degradation in *cugbp1*-MM vs. *cugbp1*-MO embryos

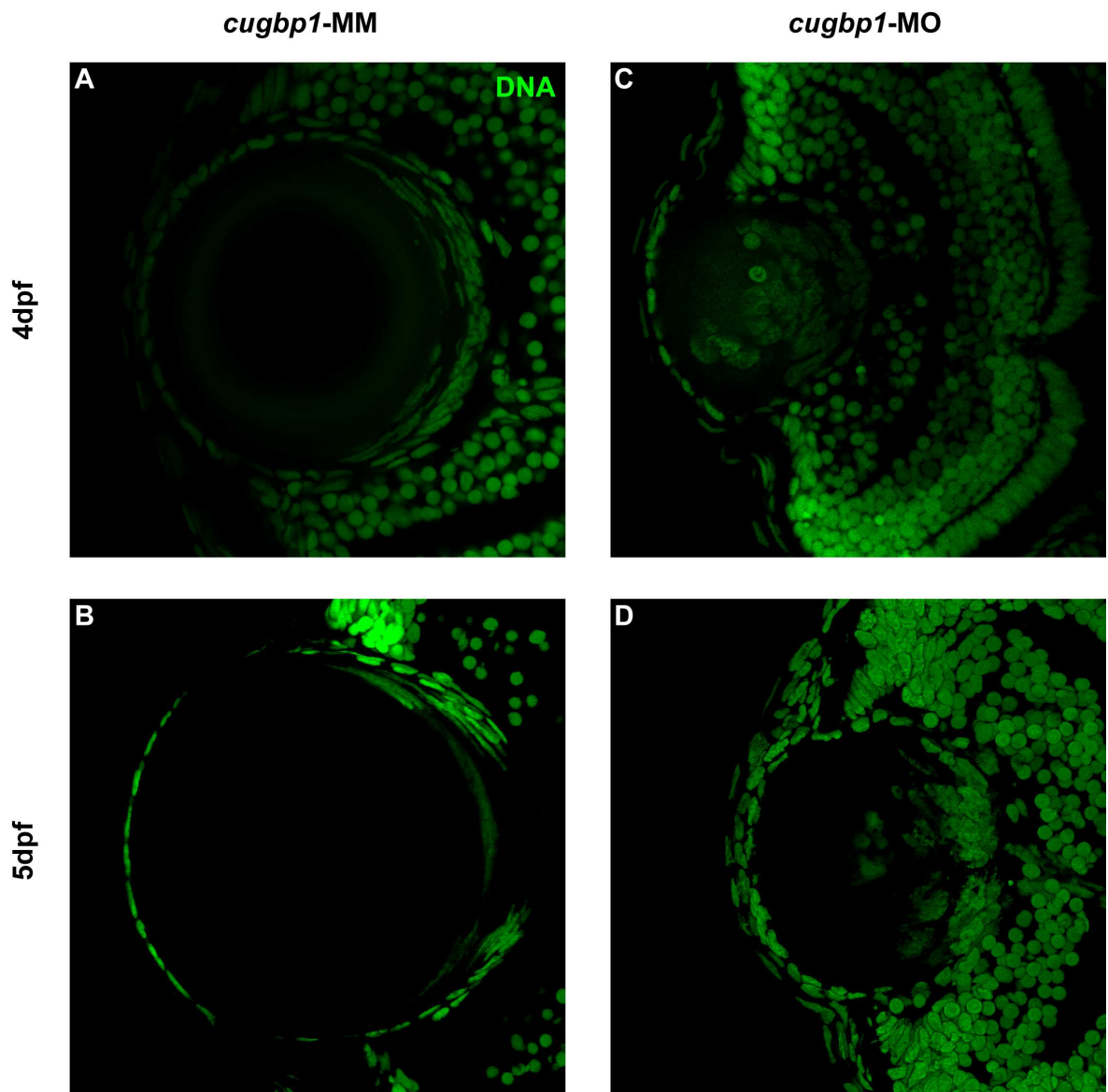
4 and 5dpf *cugbp1*-MM embryos (Fig 5.3.6 A, B) had rounded shape lens morphology and lens fiber nuclei appeared to be localized at the lateral-posterior (including the TZ) and very posterior borders of the fiber lens mass. No lens fiber nuclei were detected at the anterior, posterior-middle or the core of the lens mass at both periods of time.

Differently, 4 and 5dpf *cugbp1*-MO embryos (Fig 5.3.6 C, D) further exhibited a cataract phenotype, due to retained nuclei obstructing the light path. Morphant lenses were



Adobe Illustrator CS5

**Figure 5.3.5 F-actin organization in the lens mass shows differences between *cugbp1*-MO and *cugbp1*-MM embryos. A:** 4dpf *cugbp1*-MM embryos lenses exhibit a ring-like structure where concentric rings of outer fibers are surrounding the rings of inner fibers. No staining is visible at the lens nucleus. A posterior lens suture is evident (cyan arrows). **B, C:** 4dpf *cugbp1*-MO embryos exhibit a diverse defective phenotype. **B:** A medium flawed phenotype shows a smaller lens with a concentric ring-like structure. A posterior-like suture is visible (cyan arrow), but it does not look like the suture observed in A. **C:** Severe lens morphology exhibits a completely disorganized cortical microfilament organization at the lens fibers and no posterior lens suture at all.



---

Adobe Illustrator CS5

**Figure 5.3.6** Nuclei staining (Sytox Green) exhibits a flawed lens fiber late differentiation after knocking down *cugbp1* expression. **A,B:** 4dpf and 5dpf *cugbp1*-MM embryos lens. At both time points embryos exhibit round shape lenses with lens fiber nuclei only at the posterior and lateral-posterior borders of the lens mass. **C,D:** 4dpf and 5dpf *cugbp1*-MO embryos lens. At both periods of time embryos exhibit a cataract phenotype with smaller, not rounded-shape lenses and fibers that still retain their nuclei in the center and the posterior-middle regions of the lens mass.

smaller than control lenses and their overall shape was not spherical, as evidenced before (Fig 5.3.4; Fig 5.3.5). These abnormal lenses had a squeezed-like phenotype still evident at 5dpf. During both time points, nuclei were still visible in the central and posterior-middle regions of the lens mass demonstrating flawed fiber late differentiation at these regions of the lens.

Moreover, lens fiber nuclei signals at the posterior and posterior-lateral fibers observed in transverse sections from controls looked elongated and they seemed to become thinner before disappearing in an outer to inner direction. Elongated nuclei positions appeared as concentric rings and/or dashed lines at the posterior and posterior-lateral borders (Fig 5.3.6 A, B). On the other hand, 4dpf *cugbp1*-MO lenses (Fig 5.3.6 C) had spherical nuclei in the central region where primary lens fibers reside. Ovoid-like shape or irregular-shaped nuclei were also present at the center and middle-posterior regions of the lens, but in both cases they did not look as elongated as in control lenses. 5dpf morphant lenses (Fig 5.3.6 D) also exhibited nuclei that were not as elongated as in control lenses. They exhibited ovoid-like or irregularly shaped nuclei; however the center of the lens had fewer nuclei signals compared to 4dpf morphant lenses (Fig 5.3.6 C).

## **Chapter 6. Discussion and Conclusions**

### **6.1 *cugbp1* expression on zebrafish early lens development**

#### **6.1.1 *cugbp1* cDNA sequencing and protein sequence alignment**

The 497aa protein sequence identified in the present study contained the same three RNA-recognition motifs (RRMs; Fig 5.1.1 A, blue shade) with their corresponding RNP2 (hexamer) and RNP1 (octamer) motifs (Fig 5.1.1 A, gray shade) as the previously reported *Cugbp1* protein of 501aa from zebrafish (Suzuki *et al.* 2000). Two RRMs are at the N-terminal region and a third one in the C-terminal site. The linker region corresponds to the whole sequence between the second and third RRMs (Barreau *et al.* 2006). The only difference between the 497aa and 501aa sequences (lack of four in tandem amino acids) appeared to be within this linker region (Fig 5.1.1 A). The sequence conservation of this linker region between the members of the CELF protein family (including CUGBP1) is much lower in comparison with the RRMs. In fact, there is no significant conservation of sequence identity for this region between some CELF proteins (Barreau *et al.* 2006). BLAST searches have revealed that these linker regions are unique divergent domains in each CELF protein. No known predicted secondary structures have been identified within this domain (Ladd *et al.* 2001).

#### **6.1.2 *cugbp1* mRNA expression and promoter activity**

Zebrafish *cugbp1* mRNA specific and strong expression in the lens was previously identified as early as 24hpf and embryo sectioning proved it was abundant in lens fiber cells (Suzuki *et al.* 2000) supporting the results of the present study (Fig 5.1.2b A, B). At 24hpf, the current study revealed that expression of *cugbp1* mRNA was more intense at the posterior-middle region of the lens, place where rounded cells form a nuclear organizing center (Greiling and Clark 2009). All the cells in this nuclear center are considered part of the lens primary fiber cell mass (Greiling *et al.* 2010). There was also mRNA expression at the lateral-posterior and posterior borders, regions of the lens where still elongating lens fibers are surrounding the nuclear center (Greiling and Clark 2009), but this expression was less strong than the expression seen at the posterior-middle region of the lens.

At 24hpf, there was no detectable mRNA expression at the anterior and anterior-middle regions and borders of the lens; areas where the cells within it are destined to organize into a single layer of lens epithelium (Soules and Link 2005; Greiling and Clark 2009; Greiling *et al.* 2010). In contrast, Suzuki *et al.* (2000) exhibited strong expression at the anterior-middle region of the lens at the same time point. This difference might have happened because it is common that different zebrafish embryos develop at slightly different rates and this happens even within a single clutch (Kimmel *et al.* 1995). Hence, the anterior-middle region from embryo lenses, in the present results, might have been composed of still disorganized and undifferentiated cells that have not yet migrated to the anterior and anterior-lateral borders of the lens to constitute the lens epithelium. Differently, in Suzuki *et al.* (2000) 24hpf embryo lenses, the cells destined to become epithelium may have already migrated to the anterior and anterior middle borders of the lens epithelium. Then, the anterior-middle region might have been already comprised of differentiating lens fibers as how this region is supposed to be formed of at slightly later moments in development (Greiling and Clark 2009) in comparison with the present data. In fact, in Suzuki *et al.* (2000) results, the 24hpf lens section looks slightly more developed and bigger than the lens seen in the present results.

The detection of mRNA expression at specific patterns allows the visualization of the expression of a determined gene at the transcriptional level. But if the gene encodes a protein product, it is important to detect the protein location as some proteins are made at one type of cell, and then migrate to other tissues where they perform their function. Moreover, the mRNA of a specific protein can be degraded and no longer synthesized at a certain time point; whereas the protein can remain in the cells where it was previously produced to perform its function(s) (Alberts *et al.* 2008). Due to technical difficulties it was not possible to detect Cugbp1 protein expression by performing an immunohistochemistry assay on lens transverse sections, specifically with anti-CUGBP1 (sc-21076, Santa Cruz Biotech) antibody.

Hence, two zebrafish lines were created with a transgene composed of membrane or nuclear localized EGFP (as a reporter gene) driven by a 1.2kb *cugbp1* potential promoter fragment. The purpose of this was to estimate the pattern of Cugbp1 protein expression in wild type zebrafish embryos due to the activity of the specific promoter fragment on the expression

of EGFP in transgenic embryos. Whole mount embryos showed that the promoter fragment had high lens specificity in both transgenic lines (Fig 5.2.1 B, C).

At 24hpf and onwards, EGFP showed to be strongly expressed at the lens (Fig 5.2.1). In addition, it is important to mention that even though all embryos that expressed EGFP showed strong signals at the lens, some few F0 embryos also exhibited EGFP expression at the head and/or at diverse middle and posterior parts of their bodies. These posterior or middle regions constitute the places where the somites are. These expression patterns were seen sporadically, in small regions and not in all somites nor at the whole head at the same time.

Hashimoto *et al.* (2006) have previously reported Cugbp1 protein expression on whole mount zebrafish embryos by immunohistochemistry and Western Blot assays; hence supporting the latter results of the present work. A broader Cugbp1 protein expression pattern in their whole mount embryos was observed compared to the embryos from both transgenic lines in this study. Hashimoto *et al.* (2006), reported protein expression distributed all over the embryo (but not the yolk) from the 1-cell stage to 28hpf, including the head and somites. Indeed, by 28hpf their results showed expression throughout the whole embryo and stronger signals were seen in the lens and somites. These two regions of higher levels of expression correlate with EGFP expression in the transgenic embryos developed in these work. Since every transient (F0) and stable (F1) transgenic embryo showed EGFP in the lens, it can be concluded that the promoter identified has high lens specificity. The differences observed might be because the 1.2kb *cugbp1* promoter fragment lacks the sequence portion or portions that contribute to the expression in the whole embryo at early stages of developmental activity. The broad expression promoter and/or enhancer sequence(s) may also be present as separate units and not in tandem from the 1.2kb fragment. But, the promoter identified might also contain a small portion of the sequence(s) that direct expression in somites and in the head; this would explain why the EGFP is detected not very often and in small different regions of the head and somites in a few transient transgenics.

Transverse sections from 24hpf transgenic embryos (Fig 5.2.2a A; Fig 5.2.2b A) showed a similar pattern of expression as the *in situ* hybridization results (Fig 5.1.2b A, B). Intense expression was seen at the nuclear center of the lens mass in both transgenic lines and less concentrated EGFP in the surrounding primary lens fibers as in mRNA expression assay.

The anterior-middle regions of the lens showed more expression of EGFP than the mRNA expression results. This might have been because of the same reasons mentioned above that explained the differences between the *in situ* data from the present study and the Suzuki *et al.* (2000) results. The anterior-middle region in the lens from the transgenic embryos might have differentiating lens fibers. Whereas, the anterior-middle region at 24hpf lenses from the mRNA expression assay are probably comprised of undifferentiated cells that will migrate and give rise to lens epithelial cells.

By 2dpf, *cugbp1* mRNA seemed to be localized only at both bow regions of the lens (Fig 5.1.2b C, D), zones that are located more posteriorly in comparison to the transition regions in mammalian lenses (Soules and Link 2005). So, it seemed that mRNA is being synthesized at cells that are in a conversion moment in which they are in their first moments of differentiating from epithelial cells to secondary lens fibers. Since both transgenic lines demonstrated intense EGFP expression at these same transition positions of the lens at 2dpf (Fig 5.2.2a B; Fig 5.2.2b B), translation of *cugbp1* most probably happens quickly and early in differentiation as soon as *cugbp1* mature mRNA is synthesized. It is possible that Cugbp1 might be needed for the proper differentiation of lens fibers by playing a post-transcriptional regulatory role. The latter since Cugbp1 is well known as an mRNA binding protein that regulates gene expression at the post-transcriptional level (Barreau *et al.* 2006) and dramatic changes in gene expression happen early in fibrogenesis (Weber and Menko 2006a). In addition, Cugbp1 protein may contribute to the correct morphology of lens fibers, at least at very early lens development, as cell shape changes happen early during differentiation (Weber and Menko 2006a; Varadaraj *et al.* 2007). Hence, playing a role in lens overall shape and function as fiber cells proper formation and migration are key determinants of the lens structure as a whole (Rao and Maddala 2006).

2dpf transgenic fish also showed strong EGFP expression at the most posterior region of the lens. In this region, newly synthesized fibers had elongated and form contacts with their counterparts from the opposite side of the lens (Rao and Maddala 2006; Greiling and Clark 2009). This EGFP might have been translated when the fibers were starting to change in morphology at the transition regions of the lens because no mRNA was seen at the most posterior border of the lens at 2dpf. Most probably, during this time point, most of the *cugbp1*

mRNA had already been translated or degraded before it could reach a posterior-most location as the fibers elongated.

At 3dpf, *cugbp1* transcript expression was present at both transition zones of the lens (Fig 5.1.2b E, F) as in 2dpf. Hence, at 3dpf, *cugbp1* mRNA is also present where future fiber cells are in their transitional moment from epithelial to lens fibers. In addition, the strongest mRNA expression was present at the most posterior border of the lens. This intense mRNA expression, at 3dpf might be from mRNA that was previously synthesized when the cells that contain it were in earlier stages of differentiation and still at one of the bow regions. At least some of that very-posterior located mRNA might still be quickly translated, since the translation machinery is still functional in cortical differentiating fibers (Li *et al.* 2001). Otherwise, that mRNA will probably become degraded because as lens fibers mature they lose all their compartments and their machinery to perform translation (Bassnet 2009). However, the possibility that the mRNA located at the posterior-most lens fibers could have been synthesized when the fibers were already located at that region cannot be discarded as these fiber cells are not completely differentiated and still contain nuclei. Indeed, cortical lens fibers are transcriptionally active until quite late in differentiation. Once nuclear degradation is complete, the capacity of transcription is lost (Bassnett 2009).

4dpf *in situ* hybridization assay (Fig 5.1.2b G, H) evidenced *cugbp1* mRNA expression at the posterior border of the lens, region where there are newly formed already elongated and still differentiating secondary lens fibers (Greiling and Clark 2009). As mentioned in 3dpf, this mRNA might have been synthesized when those cells were at the bow regions of the lens at an earlier time point. And at least a part of it is possibly going to be translated before these fibers lose their capacity to do so.

EGFP expression from 1-3dpf (Fig 5.2.2a A-C; Fig 5.2.2b A-C) showed an interesting pattern where strong promoter activity seems to be happening in the regions where cells are going to become and/or are already turning into lens fibers. Whereas, the 4-6dpf (Fig 5.2.2a D; Fig 5.2.2b D, E) pattern looks like most EGFP is at the cells that synthesized it at earlier moments of development and when they were still capable of translating mRNA. 3dpf EGFP is strongly present at the bow regions of lenses and also at the posterior border and the middle-posterior zone of the lens. But at 4dpf, membrane-localized EGFP showed that it is more

intensively located at more inner fibers of the lens. This EGFP might have been synthesized when the fibers were at a more outer position, probably at the posterior-lateral and posterior borders of the lens as they were on their differentiation process. Less strong expression at outer fibers might have been due to a progressive decrease in the *cugbp1* promoter activity at posterior moments in development. At 6dpf, membrane-localized EGFP is present at inner fibers, but is no longer seen at any border region of the lens, including the bow zone and posterior area of the lens. It seems that EGFP expression is located at the fibers that synthesized this protein at earlier moments of development, but there is no more EGFP synthesis in the younger fibers (outer) or the cells in the transition differentiating state.

The transgenic promoter fused to EGFP approach gave valuable results. Nevertheless, it is important to bear in mind that there might be differences in the moments of expression, retention and/or degradation between Cugbp1 zebrafish protein and EGFP. For example, EGFP presence in inner fibers that are devoid of organelles may just reflect where Cugbp1 used to be at earlier moments of development and/or when these cells were at other and/or outer positions within the lens mass. The latter could happen because there is not a pathway that eliminates EGFP from lens cells as zebrafish do not express EGFP under normal conditions. Hence, EGFP presence in inner fibers might not mean that Cugbp1 actually remains in these differentiated cells.

Differences may have also occurred because the promoter fragment might be missing other units that could act as repressors or/and enhancers at certain specific moments or places during development. There was also EGFP seen at the anterior border of lenses, where epithelial cells reside and no *cugbp1* mRNA expression was detected. This might have happened because there may be a basal level of expression at the epithelial cells as it has been mentioned that *cugbp1* is expressed ubiquitously at the zebrafish embryo (Hashimoto *et al.* 2004; Hashimoto *et al.* 2006). In normal conditions, Cugbp1 protein might be present at 1dpf in the lens epithelium due to synthesis from mRNA transcribed before 1dpf. Or maybe the promoter fragment used is missing a repressor region that in normal circumstances suppresses *cugbp1* expression at 1dpf and/or later moments of development in lens epithelial cells. But, since the promoter fragment might lack at least a part of that repressor region, there is detectable EGFP in the anterior border of the lens.

The pattern of *cugbp1* mRNA expression and the *cugbp1* promoter fragment activity seemed to indicate that, at early development, *cugbp1* is expressed at the lens in cells that are in their differentiation process to become the mass of the lens (cells in the nuclear central core and surrounding lens fibers). Afterwards, *cugbp1* is expressed at the first cells that are becoming secondary lens fibers (fibers in the bow region). But at posterior moments (~5-6dpf) of development it seems that *cugbp1* is no longer being expressed at new differentiating fibers. If the latter is true, Cugbp1 might no longer be needed for proper morphogenesis of newly synthesized secondary lens fibers at further development. Another protein may switch places with Cugbp1 to continue performing modified regulatory functions. Actually, a postnatal switch has been reported between CUGBP1 and MBNL1 during striated muscle development. CUGBP1 is expressed at early embryonic development. Then, as development proceeds CUGBP1 is down regulated and MBNL1 is concomitantly up regulated in these tissues. This shift reprograms embryonic (by CUGBP1) to postnatal/adult (by MBNL1) alternative splicing patterns of other proteins expressed in skeletal and heart tissues (Kalsotra *et al.* 2008; Cooper *et al.* 2009; Schoser and Timchenko 2010). In fact, it has been observed that adult MBNL1 knock out mice develop cataracts (Kanadia *et al.* 2003).

However, further expression studies should be performed to corroborate if Cugbp1 protein is no longer expressed in the lens as development proceeds (~5dpf and onwards) Moreover, protein detection experiments with an appropriate anti-*cugbp1* antibody for zebrafish could elucidate the region(s) inside the fiber cells where Cugbp1 is located.

EGFP expression at transgenic fish was monitored until 9dpf and whole mount fish still showed EGFP expression. Although this expression was real, it might not reflect the real promoter activity or Cugbp1 spatial and temporal locations. The latter could be because, as mentioned before, EGFP might remain in lens cells as there is not a pathway that eliminates this protein from zebrafish cells. In conclusion, *cugbp1* mRNA and promoter activity have been observed in the lens of zebrafish embryos. So, *cugbp1* should have a role in lens early development.

Additionally, other distinctions in expression could occur because it is not possible to control where the transgene is inserted within the zebrafish genome using this approach. So, the transgenes may be inserted in regions with nearby DNA sequences (enhancers, repressors,

etc.) that could contribute to dissimilar patterns of expression as compared with the wild type location of the zebrafish *cugbp1* gene. This could account for differences in expression between EGFP and *cugbp1* mRNA and also between different transient transgenics and their descendants. However, since EGFP expression at the lens was observed at every transient and stable transgenic embryo; this shows that *cugbp1* promoter truly drives expression in the lens. And this expression is not just a consequence of where the transgene was inserted.

## **6.2 *cugbp1* down regulation by splice-altering morpholino injections in zebrafish embryos**

It is important to clarify that even though knocking down *cugbp1* expression by morpholino injections was performed at 1-4 cell stage embryos, there might have been uninterrupted *cugbp1* expression at early embryonic development. The latter because it has been shown that Cugbp1 is a maternal factor and *cugbp1* mRNA as well as protein expression have been found at unfertilized eggs, 1 cell stage embryos and afterwards (Hashimoto *et al.* 2004; Hashimoto *et al.* 2006; Suzuki *et al.* 2000). Since we utilized a splice-altering morpholino, it targets expression at the level of pre-mRNA. Therefore, any *cugbp1* mature mRNA and Cugbp1 protein already present at the moment of injections or before was expected to function normally.

### **6.2.1 Splice-altering morpholino activity tested by RT-PCR**

RT-PCR and sequencing results confirmed that the *cugbp1* morpholino altered correct splicing by removing exon5 from *cugbp1* mature mRNA (Fig 5.3.1). In normal *cugbp1* translation, the amino acid number 60 (Fig 6.2.1 A) corresponds to Glycine (G) and it is encoded by the last nucleotide (G) of exon4 and the first (G) and second (T) nucleotides of exon5. Since exon5 was removed from *cugbp1* mature mRNA of MO injected embryos, a frameshift was generated. The first frameshift occurred in the amino acid number 60 (D, Aspartic acid; Fig 6.2.1 B) because it was encoded by a nucleotide triplet composed by the last nucleotide from exon4 (G) and the first (A) and second (T) nucleotides of exon6, instead of exon5. The sequence downstream from this first site (GGT→GAT) was frameshifted as well.



**Figure 6.2.1 Splice-altering *cugbp1* morpholino activity generates a frameshift and a premature stop codon by removing exon5.** **A:** Normal *cugbp1* translation (Annex3 has the complete translated sequence). Amino acid 60 corresponds to glycine (first amino acid shaded in yellow). **B:** *cugbp1*-MO caused a frameshift (yellow shade) as the MO disrupted exon5 junction between exons4 and 6 during *cugbp1* mRNA splicing. In addition, a premature stop codon in-frame is generated at amino acid 72 (GCA→TGA=STOP). **C:** The frameshift begins at the first C-terminal RRM of Cugbp1 protein. Figure 5.1.1 indicates the three RRMs. Blue shades represent the RRMs (RNA-recognition motifs). Gray shades represent the RNPs within the RRMs. Cross out represents the frameshift downstream sequence.

In fact, a premature stop codon in-frame (TGA) was produced at position 72 in the frameshifted mature mRNA sequence (Fig 6.2.1 B). Early termination codons trigger nonsense-mediated decay (NMD) of transcripts after passing through a ribosome as a mechanism to monitor defective mature mRNAs. NMD degrades mRNAs by deadenylation-independent decapping and, subsequent 5' to 3' decay of the transcript body by exonuclease activity. Another pathway involves accelerated deadenylation followed by 3' to 5' decay of the mRNA body by exonuclease activity (Isken and Maquat 2007). So, at least part of the defective mature mRNA variant generated by the *cugbp1*-MO is probably eliminated by nonsense mediated decay, and hence Cugbp1 protein synthesis is down regulated.

Any protein synthesized from the flawed *cugbp1* mature mRNA should generate a truncated protein since the excision of exon5 should produce a frameshift downstream sequence by altering the amino acids encoded by and downstream of exon5. In fact, the first amino acid that is changed due to the morpholino activity is part of the RNP1 from the first RNA-recognition motif of Cugbp1 protein (Fig 6.2.1 C, G→D). The premature stop codon is generated twelve amino acids downstream from the first frameshifted amino acid. It is also located in the first RRM where there is an L-alanine in wild type zebrafish Cugbp1 protein (Fig 6.2.1 C, A→STOP). This means that any MO-dependent truncated Cugbp1 protein should be composed of only 71aa. It does not have the most important fractions of the protein-coding regions, as a part of the amino acids that generate the first RRM and the complete second and third RRMs should be eliminated. RRMs are the functional motifs of RNA-binding proteins, including Cugbp1; hence are required for regulation of post-transcriptional expression of specific gene targets (Maris *et al.* 2005; Barreau *et al.* 2006). Therefore, any

truncated Cugbp1 protein generated by the morpholino activity of the present study should not be functional.

In addition it is important to mention that splice-altering activity using morpholinos is not 100% efficient (Heasman 2002; Morcos 2007). This was shown at the RT-PCR assay where *cugbp1*-MO samples also possessed the 310bp band, in addition to the 227bp band (Fig 5.3.1 B). So, there is always going to be a reduced, but still functional amount of protein.

### **6.2.2 Morphant (MO) vs. control (MM) embryos phenotype and behavior**

As anticipated, knocking down Cugbp1 protein expression resulted in a defective phenotype (Fig 5.3.1 E) confirming that the correct expression of this protein is fundamental for proper early embryonic zebrafish development. It was interesting to observe that the flawed characteristics observed in *cugbp1*-MO injected zebrafish embryos correlate with symptoms observed in Myotonic dystrophy 1 (DM1), especially in the congenital form (CDM) of this disease. Similarities occurred even though CUGBP1 protein levels are elevated in all forms of DM1 (Schoser and Timchenko 2010). In contrast, Cugbp1 protein expression was decreased in the present study during zebrafish morphants early development. The latter suggests that CUGBP1 protein levels have to be tightly regulated for normal early development in vertebrates.

In DM1, increased CUGBP1 protein half-life and steady state levels are responsible for part of the DM1 defective features. It has been shown that in DM1 cells nuclei these increased levels occur due to binding of CUGBP1 to soluble mutant *DMPK* mRNA and hyperphosphorylation of CUGBP1 by protein kinase C (PKC) which is activated by expanded *DMPK*-CUG RNAs. PKC-dependent hyperphosphorylation of nuclear CUGBP1 has been shown in COS M6 cells expressing *DMPK*-CUG960 RNA, DM1 cell cultures, DM1 tissues and in heart-specific *DMPK*-CUG960 inducible DM1 mice model. Likewise, hyperphosphorylation of CUGBP1 was demonstrated in normal heart tissues from mice at embryonic days 16 and 17 (E16, E17) and normal newborn heart and skeletal muscle tissues from mice, but not in normal adult heart or skeletal mice tissues (Kuyumcu-Martinez *et al.* 2007). This is concomitant to the proposed pattern of expression of Cugbp1 protein in the lens. As a possibility, Cugbp1 might have a role at lens fiber differentiation at early embryonic

development but later on (beginning at ~4-5dpf) *Cugbp1* is no longer needed in the fibers differentiation process. As mentioned before, another post-transcriptional regulatory protein might replace *Cugbp1* as lens development proceeds. However, *Cugbp1* activity as lenses grow throughout life cannot be discarded until further investigation and also as CUGBP1 strong expression in mice has been observed in various adult tissues (Ladd *et al.* 2001). In addition, if *Cugbp1* protein expressed in lens early development is hyperphosphorylated also remains to be studied.

As morphant embryos were examined, it was noteworthy that at 1-4dpf they seemed very still and most of them had to be taken out of their chorions with tweezers. Otherwise they would not have come out by their own. In CDM, it has been reported that human fetal movements are reduced in pregnancies. Immobility and delayed motor development are also one of the first postnatal symptoms (Schoser and Timchenko 2010).

*cugbp1*-MO embryos also exhibited a delay in development and smaller size compared with controls. Although, this traits have been previously associated with a non-specific effect of morpholino injections (Uribe and Gross 2010) this does not seem to be the case because control injected embryos (*cugbp1*-MM) did not show these traits. Indeed, it is common for CDM children to be born as premature infants (Schoser and Timchenko 2010). Forsberg *et al.* (1990) have observed that patients (ages 11-27 years old) with CDM are thinner than normal (body mass index <20kg/m<sup>2</sup>). Likewise a recent report showed that a transgenic mice line, in which *Cugbp1* gene was inactivated, displayed growth retardation already apparent at the embryonic stage and it was not compensated in postnatal life. *Cugbp1* null mice never reached the size and average weight of their control littermates (Kress *et al.* 2007). In addition, transgenic mice overexpressing CUGBP1 in skeletal muscle during early embryonic development were also underdeveloped, growth-retarded and had less weight than controls (Timchenko *et al.* 2004).

Skeletal muscle (responsible for conscious movement) develops from somites (Heather *et al.* 2000) and *Cugbp1* is normally expressed in somites during early development as demonstrated in some of the transgenic zebrafish embryos of the present study and previously reported in mice (Kress *et al.* 2007), zebrafish embryos (Hashimoto *et al.* 2006), *Xenopus* (Gautier-Courteille *et al.* 2004) and in the muscle sheet of *Caenorhabditis elegans* (Milne and

Hodgkin 1999). Moreover, it has been shown that CUGBP1 regulates the expression of several genes important for muscle development at a transcriptional and/or a translational level (Timchenko *et al.* 2001; Timchenko *et al.* 2004; Charlet-B *et al.* 2002; Kalsotra *et al.* 2008).

As an example, it has been demonstrated that CUGBP1 is required in myogenesis by enhancing fibroblast conversion into myoblast as well as in myoblast differentiation into myotubes. It has been reported that CUGBP1 can enhance myogenesis by ~50% via direct translational regulation of MEF2A (a DNA-binding transcription factor). Moreover, CUGBP1 protein is required for the increase of MEF2A and p21 protein levels in differentiating myoblasts. Then, MEF2A induces myosin for proper fusion of myotubes and myotubes give rise to skeletal muscle (Timchenko *et al.* 2004). So, flawed traits and a motionless behavior seen in zebrafish *cugbp1* morphants are probably, at least in part because of an impaired embryonic development of skeletal muscle. Fibroblast conversion into myoblasts might happen at a lower rate in morphants because there is not enough *Cugbp1* to enhance *Mef2a*. This could be one of the reasons why MO-injected embryos appear delayed and smaller. They possibly have lower levels of myosin. If this is true, then their myoblasts might not align properly and in turn they would not fuse correctly for myotube synthesis; hence leading to impaired skeletal muscle tissues and immobility of *cugbp1*-MO injected embryos.

Additionally, in DM1 disease CUGBP1 levels are higher in proliferating myoblasts and lower in differentiating cells compared to normal cells. So, since the latter leads to lower levels of MEF2A in differentiating myoblasts; these cells have lower levels of myosin and myoblasts do not fuse correctly. Muscular dystrophy and delay of muscle development are attributed to the above mentioned impaired *CUGBP1* translational activity in DM1 illness (Timchenko *et al.* 2004). So, less body movement and a delayed appearance in *cugbp1*-MO injected embryos as well as immaturity of skeletal muscle (Sarnat and Silbert 1976; Silver *et al.* 1984; Furling *et al.* 2001; Timchenko *et al.* 2004), fetal and postnatal immobility and natal premature appearance in CDM are due to (at least in part) CUGBP1 protein abnormal levels that lead to CUGBP1 disrupted post-transcriptional activity.

Another feature shared by *cugbp1* knock down zebrafish embryos and DM1 disease is the presence of an enlarged and weakened heart. Dilated cardiomyopathy and arrhythmias are common features in DM1 disease. Sudden cardiac death is not uncommon, even in young

patients (Schoser and Timchenko 2010). Also, a heart-specific *Dmpk*-CUG960 inducible DM1 mice model exhibited dilated cardiomyopathy and elevated CUGBP1 steady state levels (Kuyumcu-Martinez *et al.* 2007). Moreover, to test the hypothesis that *CUGBP1* up regulation also contributes to the cardiac phenotype in DM1; Koshelev *et al.* (2010) created a tetracycline-inducible and heart-specific *Cugbp1* mice line. These transgenic mice displayed enlarged hearts as a sign of cardiomyopathy when compared with controls. Histology analysis revealed that these transgenic mice reproduce DM1 features in heart tissues like widespread degeneration and necrosis (Koshelev *et al.* 2010). So, enlarged hearts in *cugbp1*-MO embryos are due to *Cugbp1* disrupted levels.

A wide range of different studies have suggested that at least several of the DM1 symptoms are caused by increased steady state levels of CUGBP1 protein and/or a reduction of MBNL1 protein (Schoser and Timchenko 2010). MBNL1 protein decrease in DM1 is caused due to its sequestration by insoluble mutant long *DMPK*-CUG repeats (Cardani *et al.* 2006). MBNL1 and CUGBP1 proteins regulate alternative splicing in an antagonistic manner during normal heart and skeletal muscle development (Kalsotra *et al.* 2008; Cooper *et al.* 2009; Schoser and Timchenko 2010).

In normal heart development, for instance, it has been shown that CUGBP1 protein is expressed at low levels in adults compared with embryonic high levels in hearts. In mice heart, CUGBP1 protein levels begin to decrease by postnatal day 6 (PN6). In contrast, MBNL1 protein levels in mice hearts start increasing at PN5. This postnatal switch of CUGBP1 and MBNL1 protein expression controls fetal to postnatal/adult transitions for a subset of alternative splicing events. There are also alternative splicing events that are under the control of CUGBP1 and not MBNL1 and vice versa. Since in DM1 human tissues and animal models, CUGBP1 protein levels are increased and MBNL1 protein levels are decreased this leads to an aberrant expression of CUGBP1-dependent embryonic alternative splicing variants in postnatal/adult tissues (Kalsotra *et al.* 2008). In fact, Ho *et al.* (2005) observed that overexpression of CUGBP1 in neonatal transgenic mice reproduces alternative splicing alterations observed in DM1.

Hence, abnormal enlarged hearts observed in *cugbp1*-MO injected embryos are most probably caused by a reduction in the expression of embryonic splicing variants that are

Cugbp1 targets and are essential for proper early embryonic development of the heart. Other post-transcriptional regulation processes performed by Cugbp1 should also be altered in MO cardiac tissues that contribute to an abnormal embryonic development of heart. It would be interesting to observe if histopathological features observed in DM1 tissues and DM1 models that present abnormally enlarged hearts are reproduced in *cugbp1*-MO injected zebrafish embryos hearts.

Morpholino induced down regulation of *cugbp1* in zebrafish embryos could also lead to failure or reduction of expression of embryonic protein isoforms in other tissues that are dependent on CUGBP1 regulation. The latter since CUGBP1 protein has been reported to be ubiquitously expressed at early embryonic development in zebrafish (Hashimoto *et al.* 2006) and other vertebrate species (Gautier-Courteille *et al.* 2004; Kress *et al.* 2007). An abnormal induction of embryonic splicing variants by up regulation of CUGBP1 expression in postnatal/adult tissues has also been shown in skeletal muscle (Ward *et al.* 2010). Therefore, Cugbp1 protein is important for proper skeletal muscle and probably overall embryonic development and consequently for a healthy phenotype. The latter since *cugbp1*-MO injected embryos possessed smaller bodies with a delayed appearance. In addition, inactivation of *CUGBP1* ortholog in *Caenorhabditis elegans* caused embryonic lethality (Milne and Hodgkin 1999), and in mice it causes a significant augmentation of neonatal deaths (Kress *et al.* 2007).

In fact, it has been demonstrated that a *Mbnl1* knock out mice line that disrupts MBNL1 isoforms associated with expanded (CUG)<sub>n</sub> and (CCUG)<sub>n</sub> RNAs is sufficient to cause physical features, like myotonia and RNA splicing defects that resemble those seen in adult DM1. Nevertheless, there were no defects at early embryonic/postnatal transgenic mice development that resembled those observed at newborn or neonatal CDM patients or CDM animal models (Kanadia *et al.* 2003). CDM patients display severe underdeveloped muscles (Timchenko *et al.* 2004) and older studies revealed higher mortality rates (17-41%) due to respiratory muscle weakness and complications of prematurity. Nevertheless, with the improvement of neonatal care survival rates have increased (Longman 2006).

In contrast, *Mbnl1* knock out mice did not show any visibly or higher rates of lethality in embryos and/or early newborns compared to controls (Kanadia *et al.* 2003). However, an 8-10 fold elevation of CUGBP1 in skeletal muscle of transgenic mice leads to *in utero* or after

birth death and a severely underdeveloped phenotype (Timchenko *et al.* 2004). Transgenic mice overexpressing CUGBP1 (4-6 fold), specifically in heart and skeletal muscle, were also stillbirth (Ho *et al.* 2005). The latter suggests that overexpression of CUGBP1 in embryos might have a severe effect on early embryonic development. Whereas MBNL1 inhibition may not have a critical impact in embryonic development and its primary function and effect on DM1 might occur until later stages in development. This correlates with the observation that transgenic mice overexpressing CUGBP1 protein so far are the only mice models reproducing symptoms of CDM (Timchenko *et al.* 2004; Schoser and Timchenko 2010). In the present study, morphants also resemble some of CDM first symptoms, but instead of increased steady state *Cugbp1* protein levels at embryonic development, they had a decrease of *Cugbp1* protein at analogous time points. Hence, normal *Cugbp1* protein levels are required for normal embryonic and early postnatal/larval development in vertebrates.

In addition, CDM patients do not suffer from myotonia during their first ten years of life even though they display a severe muscular phenotype (Longman 2006; Schoser and Timchenko 2010; Vanier 1960). MBNL1 knock out mice manifest myotonia beginning at around 6 weeks of age. Since myotonia is not present in CDM this correlates with the previous observation that MBNL1 protein sequestration in DM1 might not have a severe effect in embryonic development. Rather, it seems to have a negative effect in later stages of life (postnatal to adult) in DM1 animal models (that suppress expression or sequester MBNL1 protein) and DM1 patients. This is also concomitant with the observations that MBNL1 protein is needed for a subset of postnatal/adult alternative splicing changes during skeletal muscle (Lin *et al.* 2006) and heart (Kalsotra *et al.* 2008) development. Whereas normal CUGBP1 down regulation occurs at this postnatal switch and its up regulation happens before, during an embryonic/early postnatal splicing pattern (Kuyumcu-Martínez *et al.* 2007; Kalsotra *et al.* 2008) This is why, at least in part, a reversion to the embryonic/early postnatal splicing pattern is observed in DM1 adult tissues and mouse models when CUGBP1 is overexpressed (Ranum and Cooper 2006).

Morpholino injected zebrafish larvae also exhibited a cataract phenotype (Fig 5.3.1 E) and this was evident as early as 3dpf. In addition, Kress *et al.* (2007) *Cugbp1* null mice line also displayed a defective lens phenotype. In these mice, cataracts are easy to observe at

adulthood (~6months; Paillard, unpublished). However, no results have been published describing the appearance or age of onset of this lens defective phenotype in this mice line. In addition, cataracts are a very common feature observed in DM1 patients. An obvious cataract phenotype has not been described in any patient younger than at least 10 years old (Rhodes, unpublished). However, Ekström (2009) has reported that bilateral (both eyes) subtle haze or condensation in the posterior lens pole was found in 39% of 49 individuals with congenital (n=30) and childhood-onset (n=19) myotonic dystrophy 1 (females: n=20, 7.3-21.4 years; males: n=29, 1.6-21.9 years). These abnormalities are suggestive of early stages of cataract development. But these abnormalities are not yet registered as true cataracts, probably because no opacifications (white appearance, instead of a uniform black look) are evident at first sight.

In the present study, *cugbp1* mRNA expression was observed in the posterior-middle and very posterior regions of the developing solid cluster of cells that constitutes the lens at 24hpf, in zebrafish (Fig 5.1.2b A, B). At this area few rounded cells constitute the core of the lens nucleus, and primary lens fibers are elongating and surrounding the core of the lens (Greiling and Clark 2009). However, in mammalian lens development instead of a solid mass of cells; a hollow fluid-filled vesicle forms from head ectoderm. Then, cells in the anterior hemisphere give rise to the lens epithelium. Cells at the posterior hemisphere elongate in a posterior to anterior direction and a parallel-like manner and differentiate to fill the lens vesicle cavity as primary lens fibers. In addition, *cugbp1* mRNA expression is also evident in secondary lens fibers that are elongating around the primary lens fibers at zebrafish embryonic and early larvae development.

Since Kress *et al.* (2007) *Cugbp1* null mice develop cataracts (Paillard, unpublished), it is very probable that CUGBP1 protein function in the lens is conserved between zebrafish and mammals. It is likely that *Cugbp1* has a role at the elongating primary fibers that fill the vesicle in mammals and, at least, in the first secondary lens fibers that start elongating around the lens center (region with primary fibers) during embryonic development. However, the dissimilarities observed in the formation of the lens center between mammals and zebrafish may account for the differences in time of onset of a cataract phenotype due to altered CUGBP1 levels. In zebrafish, the function of *cugbp1* in the appropriate formation of the central area of the lens may be more important for the organization and positioning of

surrounding fibers and overall lens form in early development. So, *cugbp1* knock down contributes to lens opacities early in life (3-4dpf). In contrast, in mammals the negative effect caused by an aberrant lens core development could be more important in the long term, resulting in obvious lens opacities until later in life.

In addition, secondary lens fibers elongate in a different pattern in zebrafish as compared to mammals giving rise to obvious differences in lens sutures formation. In zebrafish, all fiber cells are meridians and taper at the ends as they extend from pole to pole and meet with opposing fibers to produce a suture at each pole. However, in mammals all fibers in the same layer do not elongate in the same manner. The fiber cells contacting the middles of each branch in the Y-shaped sutures in mice lenses possess S-shaped curvatures. Indeed, sporadic instead of uniform perturbations in lens fibers packing in *Tmod1* null mice lenses have been potentially attributed to these differences in fiber cells morphology; even though *Tmod1* is a structural protein in the membrane skeleton of lens fibers regardless of their shape or location (Nowak *et al.* 2009). This evidences that in mice lenses (and probably other mammals) a disruption in the expression of a lens fiber protein does not affect all fibers equally due to differences in their shape, even if they are in the same layer.

*Cugbp1* function in primary and the first secondary lens fibers may be critical for the overall shape of lenses in zebrafish as the present results show that *cugbp1*-MOs do not have an overall spherical shape by 4dpf (Fig 5.3.4 E, F ) in comparison with normal lenses (Greiling and Clark 2009). However, in mice a lack of CUGBP1 in lens early development may not affect in the same way all cells in a single layer resulting in a less severe phenotype. Nevertheless, as lenses grow throughout life, the defects in early development produced by a lack of CUGBP1 activity may become more apparent in maintaining the lens overall shape, and transparency.

DM1 cataracts are probably a result of both a MBNL1 sequestration and CUGBP1 increased steady state levels. The latter since the present results have evidenced that *Cugbp1* levels and, hence activity are critical for lens development. Moreover, *Mbnl1* null adult mice possess a cataract phenotype (Kanadia *et al.* 2003). It would be interesting to study *mbnl1* mRNA and protein expression specifically in the lens to observe if a switch-like expression pattern between *Cugbp1* and *Mbnl1* is observed in lens development as described before in

skeletal and heart tissues (Lin *et al.* 2006; Kalsotra *et al.* 2008). A change in alternative splicing variants may take place at embryonic to larval/postnatal development in differentiating lens fibers.

Moreover, *cugbp1* expression during lens early development in zebrafish correlates with DMPK protein detection in mice and chicken at embryonic lens development with a specific antibody. In the present work, *cugbp1* expression is detected in differentiating lens fibers. Likewise, DMPK protein, in the lens, was detected specifically at fiber cells and not at the epithelium (Harmon 2008). This overlapping gene expression pattern at the lens during early development between *cugbp1* and *Dmpk* indicates that in DM1, DMPK mutant mRNAs with expanded CUG repeats are probably expressed at embryonic differentiating fiber cells that also express CUGBP1. Hence, in DM1, lens fibers probably possess CUGBP1 increased steady state levels due to mutant DMPK mRNA expression during early lens development. So, CUGBP1 disrupted activity may affect embryonic lens fibers differentiation in DM1, even though a cataract obvious phenotype is not apparent at early development. In *cugbp1*-MO embryos, *Cugbp1* activity is also disturbed at lens embryonic development leading also to flawed lens fibers differentiation.

In addition, zebrafish embryos and larvae where *Cugbp1* protein was down regulated also exhibited smaller eyes. As mentioned before, *Cugbp1* protein has been shown to be expressed ubiquitously at early embryonic development in zebrafish (Hashimoto *et al.* 2006) and other vertebrates (Gautier-Courteille *et al.* 2004; Kress *et al.* 2007). Hence, it may play a function in the development of other regions of the eye. In addition, microphthalmia, short axial length (distance between the anterior and posterior poles of the eye) and other eye problems have been reported in DM1 patients. However, ophthalmological flawed features in DM1 need further investigation (Ekström 2009).

### **6.2.3 Cell proliferation and differentiation analysis in the lens of *cugbp1* knock down zebrafish embryos**

According to the expression results from this study, at 2 and 3dpf *cugbp1* seemed to be expressed at the transition zone of the lens (Fig 5.1.2b C-F), place where epithelial cells stop

being proliferative by exiting the cell cycle and start differentiating to become lens fibers (Soules and Link 2005; Griep 2006; Dahm *et al.* 2007; Greiling and Clark 2009).

CUGBP1 has been implicated as a key regulator in myogenesis, especially during the transition from myoblasts to the differentiation of myotubes. CUGBP1 activity is regulated by phosphorylation at specific amino acids by different kinases depending on the cell stage. In proliferating myoblasts, CUGBP1 is phosphorylated by Akt kinase in the position 28 (Ser28). Ph-S28-CUGBP1 has high affinity towards cyclin D1 mRNA increasing its translation. Since D1 is a strong promoter of cell proliferation ph-S28-CUGBP1 increases cell proliferation in myoblasts. Unlike cyclins D1 and D2 that promote cell proliferation, cyclin D3 supports cell growth arrest and differentiation. At differentiating myoblasts (to become myotubes) cyclin D3 levels are increased and Cyclin D3/cdk4 phosphorylates CUGBP1 at Ser302. Ph-S302-CUGBP1 binds strongly to cdk inhibitor p21 mRNA increasing its translation; thus promoting cell cycle arrest which is required for cell differentiation (Salisbury *et al.* 2008; Schoser and Timchenko 2010).

As mentioned before CUGBP1 has a critical function in myoblasts proliferation and is also involved in inducing myoblasts differentiation to myotubes by promoting p21 translation (Salisbury *et al.* 2008). So, a cell proliferation assay in *cugbp1*-MO and MM embryos was performed to observe if Cugbp1 protein has a similar role in lens epithelial cell cycle arrest to induce fiber cell differentiation, specifically at the transition zone of the lens. However, BrdU incorporation assay did not show any differences between morphant and control lenses at 2dpf nor at 3dpf (Fig 5.3.3). Morphants did not exhibit any significant difference in the total number of proliferating cells. So, it is not likely that epithelial cells that should be differentiating to become lens fibers remain proliferative at the transition zones due to failure to translate enough levels of p21. In addition, proliferation was observed at the lateral epithelium of morphant lenses. So, it is not probable that cells in this region fail to translate appropriate levels of cyclin D1.

Since *cugbp1*-MO embryos display smaller lenses, it is possible that a count of the percentage of BrdU+ cells (instead of the total number) between *cugbp1*-MO vs. *cugbp1*-MM embryos would show that morphant lenses have a higher percentage in BrdU+ cells, but this might be because morphant fiber cells fail to degrade their nuclei as shown in Fig 5.3.6 and

discussed below. So, there might be BrdU positive signals in lens fibers from morphant lenses while their BrdU positive counterparts in control lenses are not present when counting. This would be due to DNA degradation as a normal process in control lens fiber cells differentiation (Counis *et al.* 1998; Bassnet 2009).

Then, the ability of *cugbp1*-MO embryos to start their differentiation process from lens epithelial cells to lens fibers was tested, by analyzing the expression of Aquaporin0 (Aqp0) as a lens fiber marker (Fig 5.3.4). Varadaraj *et al.* (2007) have shown that AQP0 is a plasma membrane protein expressed in newly formed and still differentiating mice primary and secondary lens fibers, but not in lens epithelial cells. Immunohistochemistry results demonstrated that morphants as well as control embryos expressed Aqp0 in their lens evidencing that *Cugbp1* is not required for the initiation of fiber cell differentiation. In addition, these results demonstrated that *Cugbp1* protein is not needed for Aqp0 protein synthesis pathway.

Furthermore, it was interesting to observe that Aqp0 could be detected at the center and most inner part of the lens in morphant embryos at 2 and 3dpf. In contrast, this was not possible in controls. This could have happened because morphant lens fibers fail to arrange in a compact manner at the same rate as in controls. So, anti-Aqp0 antibody can reach the innermost primary fiber cells at the center of the lens. In contrast, control embryos displayed an organized arrangement in which fiber cells elongate to form a new layer covering the previous formed fiber layers in a compact manner (Varadaraj *et al.* 2007; Greiling and Clark 2009; Chepelinsky 2009) otherwise controls would have displayed an abnormal lens phenotype.

The visualization of Aqp0 expression allowed the observation of lens fiber membranes since Aqp0 constitutes more than 50% of the membrane protein in lens fibers (Varadaraj *et al.* 2007). The latter permitted the examination of the lens mass shape arrangements during early development in *cugbp1* knock down embryos. Indeed, morphant embryos have a defective lens mass shape that does not correlate with the shape seen in control and other wild type zebrafish lenses (Greiling and Clark 2009). The latter could be due to an impaired lens fiber morphogenesis. If lens fibers fail to elongate properly and/or do not have the right overall thickness and/or form then they are not going to compact in a correct manner. This would lead

to an impaired overall structure of the lens mass as how it was observed in *cugbp1*-MO embryos.

This defective lens mass shape, the faulty lens fiber arrangement phenotype and *cugbp1* expression pattern might suggest that Cugbp1 protein is required for proper lens mass overall architecture by having an effect at least in lens fibers organization. Morphants lens mass seems to have a defective structure and not compact fibers in the lens nucleus during early zebrafish development. In addition, epithelial to fiber cell fate does not seem to be compromised.

#### **6.2.4 F-actin organization in the lens of *cugbp1*-MO zebrafish embryos**

Aqp0 immunodetection experiment revealed that knocking down *cugbp1* expression did not alter the epithelial to fiber cell differentiation pathway. Rather, lens mass overall structure and lens fibers compaction seems to be affected. Then, an F-actin staining assay on the lens was performed (Fig 5.3.5) to further observe if a possible flawed fiber cell shape was identified.

It is known that the actin cytoskeleton has an essential role in lens fiber cell elongation and differentiation. Epithelial cell morphology changes are accompanied with membrane cytoskeleton remodeling and actin filament reassembly. Lens epithelial cell differentiation is coincident with the disassembly of actin stress fibers and the reorganization of F-actin as cortical actin during fibrogenesis (Rao and Maddala 2006; Lee *et al.* 2000; Weber and Menko 2006a).

The F-actin concentric staining appearance seemed to coincide with an enrichment of cortical F-actin (membrane bound) along the length (lateral surfaces) of normal lens fibers (Weber and Menko 2006a). Such pattern was apparent at MM lenses. The medium flawed phenotype also exhibited an organized concentric F-actin pattern in lens fibers. Nevertheless, lenses were smaller and had less compact lens fibers. The latter was evidenced by F-actin staining in inner concentric fiber membranes compared to control lenses.

A severe phenotype showed a highly disorganized F-actin pattern. However, F-actin still appeared to be present along lens fibers as in controls and medium flawed phenotype lenses. Depolymerization of F-actin has been associated with disordered lens fiber cell

packing (Nowak *et al.* 2009) and blebbing of the plasma membrane (Weber and Menko 2006a). In the severe phenotype, an abnormal wave/blebbing-like morphology (but still concentric) instead of an appearance of concentric rings was obvious, but F-actin still appears to be enriched in lens fibers cortical cytoskeleton.

The fact that there were two flawed phenotypes: one less severe that appeared to have an organized F-actin pattern and another with a wave-like F-actin overall arrangement might indicate that F-actin disorganization is not a direct effect of *cugbp1* down regulation. Rather, it is probably a consequence of another important disrupted pathway that is crucial for lens fiber proper morphogenesis. In addition, Cugbp1 protein does not seem to be important for the maintenance of cortical F-actin in lens cortical fibers.

Additionally, it is important to remember that the zebrafish lens TZ is located posterior to the equator. So, the anterior elongation of secondary fibers is greater than the posterior elongation in respect to the TZ and this difference makes the appearance of the posterior suture to happen before the anterior suture (Greiling and Clark 2009). This is most probably the reason why an evident posterior lens suture was observed in 4dpf *cugbp1*-MM embryos, while the anterior suture was still not apparent after F-actin staining (Fig 5.3.5 A).

### **6.2.5 Nuclei degradation in *cugbp1*-MM embryos vs. *cugbp1*-MO embryos**

It has been demonstrated that lens fibers terminal differentiation includes losing their organelles including their nucleus (Appleby and Modak 1977; Counis *et al.* 1998; Bassnett 2009). SytoxGreen staining was performed in morphant lenses to test if Cugbp1 might be involved in DNA degradation as a normal part of lens fiber differentiation.

Nuclei staining results on morphant lenses further evidenced an impaired lens fiber phenotype due to Cugbp1 down regulation (Fig 5.3.6). 4 and 5dpf morphants still retain nuclei in their inner-most fibers; moment at which normal primary fiber cell maturation and organelle break-down in the core of the lens should have already occurred. This DNA presence scatters incident light and does not allow appropriate focusing on the retina resulting in a cataract phenotype (Greiling and Clark 2008; Bassnett 2009).

In contrast, control embryos exhibited DNA only in the posterior-lateral and posterior borders of the lens. Both regions correlate with the places at which newly secondary lens

fibers are still differentiating, so it is expected to still observe nuclei in these positions (Bassnett 2009).

It was evident that at 5dpf *cugbp1*-MO embryos had less amounts of DNA in their lens body compared with morphants at 4dpf. This probably happened because at 5dpf the morpholino had already dissipated too much, so its effectiveness is being reduced. However, it could also have happened just due to delayed nuclei disintegration.

De María and Arruti (2004) have observed that lens fibers nuclei undergo characteristic morphological changes according to the lens fibers differentiation stage. First, nuclei are large, round shape and with uncondensed chromatin. Lens from morphants seem to retain their nuclei appearance in this stage even at the core region of the lens. Then, as lens fibers normally mature, they elongate and nuclei also becomes elongated (De María and Arruti 2004). Control lenses exhibit this nuclei shape in differentiating cortical fibers. The elongation of nuclei is a process that seems to correlate with the development of an elongated form in lens fibers. If nuclei do not start elongating and becoming thinner; then fibers are going to have a big round structure that is not going to let them elongate properly. And this would lead to a disorganized packaging of the fibers and less compact fibers correlating with the lens defective phenotype from this study.

Finally, as the nuclei disintegrate it is viewed as small rounded bodies (De María and Arruti 2004). This conformation is not apparent in the control (MM) neither the morphant lenses, most likely because in this last conformation the rounded bodies are too small. They probably form as a separation of the elongated shaped nuclei and the small rounded parts are so close that at the magnification utilized the separations are not visible and just look as a curved thin line.

It can be speculated that the observation that morphant lenses had not compacted lens fibers at the center of the lens (evidenced by Aqp0 expression detection; Fig 5.3.4) could be due to a lack of organelle degradation, at least in part. If nuclei and/or other organelles are not eliminated from lens fibers then, it is reasonable to think that fibers are not going to be able to elongate and stretch properly to become long and relatively thin cells which are organized as concentric layers. This could also explain the general flawed lens mass shape observed in

morphants, if fibers do not arrange in a highly compacted way then the lens mass is not going to be able to have a spherical form.

An abnormal persistence of nuclei in the center of the lens mass was evident. And this happened due to *cugbp1* knock down. Nevertheless, most mutations that lead to cataracts affect organelle breakdown to some extent. It is possible that a certain mutation can impact the organelle disintegration process directly. However, organelle breakdown involves a complex series of interdependent steps. So, any mutation that affects lens homeostasis can indirectly affect organelle breakdown (Bassnett 2009).

In general, it was interesting to observe that knocking down *cugbp1* expression in morpholino injected zebrafish embryos led to defective features that resemble those observed in DM1 patients. And that this happened even though *cugbp1* is up regulated in this disease. Hence, CUGBP1 protein levels have to be tightly regulated for proper development and overall morphology in vertebrates.

Cugbp1 is a very versatile protein present in both nucleus and cytoplasm and known to regulate the expression of other proteins by binding to pre and mature mRNAs (Philips *et al.* 1998; Vlasova *et al.* 2008; Kalsotra *et al.* 2008; Rattenbacher *et al.* 2010). So it seems obvious that the next step to try to unravel the molecular mechanism/s regulated by this protein in the lens will be aimed to identify the targets of *cugbp1* in this region of the eye.

## **Chapter 7. Recommendations and Future Directions**

### **7.1 Identification of Cugbp1 RNA targets at the developing zebrafish lens**

Since this study has demonstrated that Cugbp1 has a role in lens early formation, the next step should be directed to identify what molecules are bound and thus regulated by Cugbp1 protein during zebrafish early lens development. In order to do so, the creation of a transgenic line with an expression construct that drives Cugbp1 protein expression specifically at the lens during early development and where this transgenic protein can easily be isolated with its bound targets seems a viable approach.

First, an expression construct should be synthesized. This study showed that the 1.2kb *cugbp1* promoter element identified has high lens specificity during the time points monitored. Hence, this DNA sequence could be used as a 5' element in the creation of a new expression construct using Tol2kit technology (Kwan *et al.* 2007). A full-length zebrafish *cugbp1* cDNA sequence should be used as a middle element. Thermo Fisher Scientific has a vector with a complete *cugbp1* cDNA insert (Vector pME18S-FL3; Clone ID 5776879). This cDNA should include the cap sequence, translation initiation site and all the exons for proper *in vivo* translation. Clone 5776879 could be aligned with Suzuki *et al.* (2000; Ensembl, ID ENSDARP00000026582) complete *cugbp1* cDNA sequence and the sequence of the cDNA used to make probe (for *in situ* hybridization assay; 5.1.1 Section; Annex 3; Fig 5.1.1). This alignment is important to identify if there are any significant differences between sequences that could alter the function of the synthesized protein in the lens.

A C-terminal fusion protein tag can be added to *cugbp1* transgenic protein for easier isolation of the RNA-protein complex. The Tol2kit has a 3' entry clone with a c-myc-tag and a SV40 late polyA signal (p3E-MTpA, Kwan *et al.* 2007). The stop codon of the middle element (*cugbp1* cDNA) has to be removed for the tag to be in-frame with the protein sequence. Then, when the transgenic protein is expressed, it will possess the c-myc polypeptide sequence in its C-terminal region. This will allow immune precipitation of transgenic Cugbp1 by using a c-myc-tag antibody. The myc-tag is a polypeptide with 11aa (Terpe 2003). Since it is a small peptide, it is unlikely that it will interfere with the biochemical properties of Cugbp1 transgenic protein.

In the multisite gateway LR recombination reaction, the use of destination vector pDestTol2CG2 will be helpful to visualize animals that have incorporated the expression construct. The latter since this destination vector includes an extra *cmlc*:EGFP-pA expression cassette as a marker for transgenesis. In this cassette, the *cmlc* 3' element corresponds to a promoter from the cardiac myosin light chain gene. This promoter is used to drive cytoplasmic EGFP expression specifically in the developing heart (Kwan *et al.* 2007).

Then, a transgenic line can be created with the injection of transposase mRNA and the created plasmid. The new DNA that should be incorporated in the zebrafish genome has the expression construct *cugbp1*:Cugbp1:MTpA and the transgenesis marker construct. Injections have to be performed into one cell-stage zebrafish embryos as described in 4.2.5 Section. The embryos that have incorporated the foreign DNA are identified by observing EGFP expression in their developing hearts. F0 embryos can be grown up to develop a transgenic line for further investigation.

Alternatively, a transgenic line could be created with a different construct from the one mentioned above. A bicistronic construct in which Cugbp1 protein with the myc-tag is encoded by the first cistron and GFP is encoded by a second cistron on the same mRNA can be created. This can be done when expression of the second cistron is driven by an IRES (internal ribosome entry site). An IRES is a sequence that induces translation initiation without 5' cap recognition (Hellen and Sarnow 2001). This construct would have the 1.2kb *cugbp1* promoter. The major advantage that this construct would have, over the one previously mentioned, is that the temporal and spatial expression of both proteins Cugbp1 and GFP would be directed by the same promoter. Thus, every cell that expresses GFP would also express Cugbp1. This is useful because it marks with fluorescence the cells that are expressing the gene of interest (*cugbp1*), in addition to just being a general transgenesis marker. Plasmid pCMV6-AC-IRES-GFP (No. PS100027) from ORIGENE has myc-tag, IRES and GFP sequences in tandem and downstream from a multiple cloning site (MCS). *cugbp1* cDNA sequence could be cloned into this MCS and this new plasmid could be used to develop a new DNA cassette with expression of Cugbp1 and GFP driven by the 1.2kb *cugbp1* promoter at the same time. Monitoring the regions where Cugbp1-myc is present is needed since the 1.2kb promoter exhibited activity in other parts of the zebrafish embryo body. Although this activity

was rare, this cellular expression marker is useful to discard embryos (or their body parts) that express Cugbp1 in other regions besides the lens.

The next step of this assay is to coimmunoprecipitate (Co-IP) transgenic Cugbp1 with its RNA targets. To identify the early role of Cugbp1 in lens development, it will be preferable to use 1dpf and 2dpf embryos, since at these days *cugbp1* expression was more intense in the lens (Fig 5.1.2b). There are several commercially available Kits to Co-IP transgenic proteins with a c-myc epitope tag. The ProFound™ c-Myc Tag IP/Co-IP Kit (Thermo Scientific Pierce) is one of them. In this kit, the sample lysate interacts with a high affinity anti-c-Myc antibody-coupled agarose resin in a spin column allowing coimmunoprecipitation of c-Myc-tagged proteins. After the spin column is washed to eliminate cellular components that did not IP, the c-myc-tagged protein and its bound targets are eluted from the column. The mRNAs that are bound with the transgenic protein can then be separated by phenol/chloroform extraction and isopropanol precipitation.

Afterwards, RNAs can be amplified by Reverse Transcriptase PCR. Then, the samples may be amino-allyl labeled with a fluorescent dye. This latter technique consists in incorporating a nucleotide analog that has a chemically reactive group to which a fluorescent dye can be attached. This can be done while performing PCR. Then, the analog group can be linked to an N-hydroxysuccinimidyl ester group attached to a dye. The labeled samples can then be probed to a cDNA microarray and the data obtained (positive signals) analyzed (Shepard *et al.* 2003). In this case, a zebrafish cDNA microarray should be used (Lo *et al.* 2003). These last mentioned steps are usually performed with a collaboration of a Bioinformatics laboratory.

Usually a bioinformatics laboratory sends a list with the targets identified. Then, first candidates are selected for posterior studies. These studies can include expression assays and MO knock downs to observe if a defective phenotype overlaps with the one observed with the morpholino against *cugbp1*. The aim is to identify proteins that are post-transcriptionally regulated by Cugbp1 protein at the developing zebrafish lens.

## 7.2 Reversal of *cugbp1* morpholino phenotype by RNA rescue

A common strategy to further test morpholino specificity is to reverse its effects by an assay referred as RNA rescue (Bill *et al.* 2009). The *cugbp1*-MO injected in this study is a splice-altering morpholino that targets pre-mRNA by binding to the splice junction of exon5/intron5. Hence, the MO does not recognize mature mRNA because the latter does not possess the intron5 sequence. So, the complete cDNA sequence of *cugbp1* gene (Clone ID 5776879; Thermo Fisher Scientific) can be used to produce mature mRNA that is capable of being translated in zebrafish embryos. At this type of assay, mature mRNAs are normally generated *in vitro* and they can be produced by the same general mechanism as transposase mRNA was synthesized in 4.2.4 Section.

Then, an assay in which *cugbp1* mRNA and *cugbp1*-MO are injected at the same time at the yolk of 1-4 cell-stage embryos should be done. In this test, the protein synthesized from the injected mRNA is intended to reverse the effects of the MO. This principal is the purpose of a RNA rescue experiment. First, the MO with the concentration previously established (2.2ng/embryo; 4.3.1 Section) is injected with different concentrations of mRNA to identify the appropriate concentration of mRNA that can eliminate the flawed phenotype of the MO, but is not toxic to the embryo.

Then, embryos of the same batch should be divided into several groups (Bill *et al.* 2009). As a control, one group of embryos is injected with the targeting MO and with a control mRNA. This control mRNA can be GFP-encoding, so its expression can be verified under a fluorescence microscope (Leica Microscope MZ 16F). These embryos should have the same defects as *cugbp1*-MO injected embryos (5.3.2 Section). Another group is the one injected with *cugbp1*-MO and the appropriate concentration of *cugbp1* mRNA that exhibits the rescued phenotype. In addition, groups injected only with the *cugbp1* mRNA, the GFP mRNA or just the MO should be maintained.

In particular, embryos injected with different concentrations of just the *cugbp1* mRNA should be carefully monitored. Since it has been previously discussed (6.2.2 Section), that overexpression of CUGBP1 in transgenic mice and DM1 models and tissues produces

defective features, some of which are similar to the ones observed in *cugbp1*-MO injected embryos.

### 7.3 Other experiments

*cugbp1*-MO embryos seem to mimic characteristics observed in DM1 disease and transgenic mice overexpressing CUGBP1 in heart and skeletal muscles. Therefore, it will be interesting to realize histological analyses in *cugbp1*-MO heart and skeletal muscle tissues. A comparison of the histopathological abnormalities seen in DM1 tissues, DM1 mice models and transgenic mice induced to overexpress CUGBP1 should be addressed.

In addition, a characterization of the differences in lens sections from *cugbp1*-MO and *cugbp1*-MM embryos should be performed by using light microscopy. Transmission electron microscopy imaging can be realized, especially on the regions of the lens that exhibit any abnormalities seen during light microscopy observations.

It will also be interesting to study if CUGBP1 expressed in early lens development is hyperphosphorylated. The latter since Kuyumcu-Martinez *et al.* (2007) have shown that CUGBP1 is hyperphosphorylated at early development in mice heart and skeletal muscle, but not at the adult stage. These studies would be easier to perform in mice embryos because zebrafish lenses in early development are too small. Lens tissue could be separated from mice embryos during E12.0-12.5 since at this time lapse primary lens fibers are elongating. 2D-gel electrophoresis and Western Blot could be used to observe the isoelectric point of CUGBP1. Alkaline phosphatase treatment (CIAP) would be done to identify if an acidic shift is observed due to phosphorylation. These techniques can be performed essentially as described by Kuyumcu-Martinez *et al.* (2007). This assay could also be tried out in zebrafish *Cugbp1*-myc transgenic protein from 7.1 Section.

## References

- Agre, P., Bonhivers, M. and Borgnia, M. 1998. The aquaporins, blueprints for cellular plumbing systems. *The Journal of Biological Chemistry*. 273(24):14659-14662.
- Alberts, B., Johnson, A., Lewis, J. Raff, M. Roberts, K. and Walter, P. 2008. *Molecular Biology of the Cell*. 5<sup>th</sup> ed. Garland Science, Taylor and Francis Group.
- Al-Ghoul, K., Kirk, T., Kuszak, A., Zoltoski, R., Shiels, A. and Kuszak, J. 2003. Lens structure in MIP-deficient mice. *The Anatomical Record Part A, Discoveries in molecular, cellular and evolutionary biology*. 273:714-730.
- Alwazzan, M., Newman, E., Hamshere, M. and Brook, D. 1999. Myotonic dystrophy is associated with a reduced level of RNA from the DMWD allele adjacent to the expanded repeat. *Human Molecular Genetics*. 8(8):1491-1497.
- Appleby, D. and Modak, S. 1977. DNA degradation in terminally differentiating lens fiber cells from chick embryos. *Cell Biology*. 74(12):5579-5583.
- Barreau, C., Paillard, L., Méreau, A. and Osborne, H. 2006. Mammalian CELF/Bruno-like RNA-binding proteins: molecular characteristics and biological functions. *Biochimie*. 88:515-525.
- Bassnett, S. 2009. On the mechanism of organelle degradation in the vertebrate lens. *Experimental Eye Research*. 88:133-139.
- Bassnett, S. and Beebe, D. 1992. Coincident loss of mitochondria and nuclei during lens fiber cell differentiation. *Developmental Dynamics*. 194:85-93.
- Bassnett, S. and Mataic, D. 1997. Chromatin degradation in differentiating fiber cells of the eye lens. *The Journal of Cell Biology*. 137(1):37-49.
- Berul, C., Maguire, C., Aronovitz, M., Greenwood, J. Miller, C., Gehrman, J., Housman, D., Mendelsohn, M. and Reddy, S. 1999. DMPK dosage alterations result in atrioventricular conduction abnormalities in mouse myotonic dystrophy model. *The Journal of Clinical Investigation*. 103(4):R1-R7.

- Bill, B., Petzold, A., Clark, K., Schimmenti, L. and Ekker, S. 2009. A primer for morpholino use in zebrafish. *Zebrafish*. 6(1):69-77.
- Buj-Bello, A., Furling, D., Tronchere, H., Laporte, J., Lerouge, T., Butler-Browne and Mandel, J. 2002. Muscle-specific alternative splicing of myotubularin-related 1 gene is impaired in DM1 muscle cells. *Human Molecular Genetics*. 11(19):2297-2307.
- Cardani, R., Mancinelli, E., Rotondo, G., Sansone, V. and Meola, G. 2006. Muscleblind-like protein 1 nuclear sequestration is a molecular pathology marker of DM1 and DM2. *European Journal of Histochemistry*. 50:177-182.
- Charlet-B, N., Savkur, R., Singh, G., Philips, A., Grice, E. and Cooper, T. 2002. Loss of the muscle-specific chloride channel in type 1 myotonic dystrophy due to misregulated alternative splicing. *Molecular Cell*. 10:45-53.
- Chepelinsky, A. 2009. Structural Function of MIP/Aquaporin 0 in the Eye Lens; Genetic Defects Lead to Congenital Inherited Cataracts. *Handbook of Experimental Pharmacology*. 190(4):265-297.
- Cho, D. and Tapscott, S. 2007. Myotonic dystrophy: emerging mechanisms for DM1 and DM2. *Biochimica et Biophysica Acta- Molecular Basis of Disease*. 1772(2):195-204.
- Chow, R. and Lang, R. 2001. Early eye development in vertebrates. *Annual Review of Cell and Developmental Biology*. 17:255-296.
- Chrzanowska-Wodnicka, M. and Burridge, K. 1996. Rho-stimulated contractility drives the formation of stress fibers and focal adhesions. *The Journal of Cell Biology*. 133(6):1403-1415.
- Cooper, G. 2000. *The Cell a Molecular Approach*. 2<sup>nd</sup> ed. Sunderland, MA, Sinauer Associates.
- Cooper, T. and Ordahl, C. 1985. A single cardiac troponin T gene generates embryonic and adult isoforms via developmentally regulated alternative splicing. *The Journal of Biological Chemistry*. 260(20):11140-11148.
- Cooper, T., Wan, L. and Dreyfuss, G. 2009. RNA and disease. *Cell*. 136:777-793.
- Corey, D, and Abrams, J. 2001. Morpholino antisense oligonucleotides: tools for investigating vertebrate development. *Genome Biology*. 2(5):105.1-105.3.

- Counis, M., Chaudun, E., Arruti, C., Oliver, L., Sanwal, M., Courtois, Y. and Torriglia, A. 1998. Analysis of nuclear degradation during lens cell differentiation. *Cell Death and Differentiation*. 5:251-261.
- Dahm, R., Schonhaler, H., Soehn, A., van Marle, J. and Vrensen, G. 2007. Development and adult morphology of the eye lens in the zebrafish. *Experimental Eye Research*. 85:74-89.
- Danysh, B. and Duncan, M. 2009. The lens capsule. *Experimental Eye Research*. 88(2):151-164.
- De María, A and Arruti, C. 2004. DNase I and fragmented chromatin during nuclear degradation in adult bovine lens fibers. *Molecular Vision*. 10:74-82.
- Dunne, P., Ma, L., Casey, D. and Epstein, H. 1996. Myotonic protein kinase expression in human and bovine lenses. *Biochemical and Biophysical research communications*. 225(1):281-288.
- Easter, S. and Nicola, G. 1996. The development of vision in the Zebrafish (*Danio rerio*). *Developmental Biology*. 180:646-663.
- Easter, S. and Nicola, G. 1997. The development of eye movement in the zebrafish (*Danio rerio*). *Developmental Psychobiology*. 31(4):267-276.
- Ekker, S. 2000. Morphants: a new systematic vertebrate functional genomics approach. *Yeast*. 17:302-306.
- Ekström, A. 2009. Congenital and childhood myotonic dystrophy type 1: the impact on central nervous system, visual and motor function. M.D. Thesis. Gothenburg, Sweden, University of Gothenburg.
- Eshaghian, J., March, W., Goossens, W. and Rafferty, N. 1978. Ultrastructure of cataract in myotonic dystrophy. *Investigative Ophthalmology and Visual Science*. 17(3):289-293.
- Fadool, J. and Dowling, J. 2008. Zebrafish: A model System for the Study of Eye Genetics. *Prog Retin Eye Res. Investigative Ophthalmology and Visual Science*. 27(1): 89-110.

- Fardaei, M., Rogers, M., Thorpe, H., Larkin, K., Hamshere, M., Harper, P. and Brook, D. 2002. Three proteins , MBNL, MBLL and MBXL, co-localize in vivo with nuclear foci of expanded-repeat transcripts in DM1 and DM2 cells. *Human Molecular Genetics*. 11(7):805-814.
- Filatov, V., Katrukha, A., Bulargina, T. and Gusev, N. 1999. Troponin: structure, properties, and mechanism of functioning. *Biochemistry (Moscow)*. 64(9):969-985.
- Fischer, R., Lee, A. and Fowler. 2000. Tropomodulin and tropomyosin mediate lens cell actin cytoskeleton reorganization in vitro. *Investigative Ophthalmology and Visual Science*. 41(1):166-174.
- Forsberg, H., Olofsson, B., Eriksson, A, and Andersson, S. 1990. Cardiac involvement in congenital myotonic dystrophy. *British Heart Journal*. 63:119-121.
- Froger, A., Clemens, D., Kalman, K., Németh-Cahalan, K., Schilling, T. and Hall, J. 2010. Two distinct aquaporin Os required for development and transparency of the zebrafish lens. *Investigative Ophthalmology and Visual Science*. 51(12):6582-6592.
- Furling, D., Lemieux, D., Taneja, K and Puymirat, J. 2001. Decreased levels of myotonic dystrophy protein kinase (DMPK) and delayed differentiation in human myotonic dystrophy. *Neuromuscular Disorders*. 11(8):728-735.
- Gautier-Courteille, C., Le Clainche, C., Barreau, C., Audic, Y., Graindorge, A., Maniey, D., Osborne, B. and Paillard, L. 2004. EDEN-BP-dependent post-transcriptional regulation of gene expression in *Xenopus* somatic segmentation. *Development*. 131(24):6107-6117.
- Glass, A. and Dahm, R. 2004. The zebrafish as a model organism for eye development. *Ophthalmic Research*. 36(1):4-24.
- Graindorge, A., Le Tonqueze, O., Thuret, R., Pollet, N. Osborne, H. and Audic, Y. 2008. Identification of CUG-BP1/EDEN-BP target mRNAs in *Xenopus tropicalis*. *Nucleic Acids Research*. 36(6):1861-1870.
- Graw, J. 1999. Cataracts mutations and lens development. *Progress in Retinal and Eye Research*. 18(2):235-267.

- Greiling, T., Aose, M. and Clark, J. 2010. Cell fate and differentiation of the developing ocular lens. *Investigative Ophthalmology and Visual Science*. 51(3):1540-1546.
- Greiling, T. and Clark, J. 2008. The transparent lens and cornea in the mouse and zebrafish eye. *Seminars in Cell and Developmental Biology*. 19(2):94-99.
- Greiling, T. and Clark, J. 2009. Early lens development in the zebrafish: a three-dimensional time-lapse analysis. *Developmental Dynamics*. 238:2254-2265.
- Griep, A. 2006. Cell cycle regulation in the developing lens. *Seminars in Cell and Developmental Biology*. 17(6):686-697.
- Gross, J. and Perkins, B. 2007. Zebrafish mutants as models for congenital ocular disorders in humans. *Molecular Reproduction and Development*. 75: 547–555.
- Harmon, E., Harmon, M., Larsen, T., Paulson, A. and Perryman, B. 2008. Myotonic dystrophy protein kinase is expressed in embryonic myocytes and is required for myotube formation. *Developmental Dynamics*. 237:2353-2366.
- Hashimoto, Y., Maegawa, S., Nagai, T., Yamaha, E. Suzuki, H., Yasuda, K. and Inoue, K. 2004. Localized maternal factors are required for zebrafish germ cell formation. *Developmental Biology*. 268:152-161.
- Hashimoto, Y., Suzuki, H., Kageyama, Y., Yasuda, K. and Inoue, K. 2006. Bruno-like protein is localized to zebrafish germ plasm during the early cleavage stages. *Gene Expression Patterns*. 6:201-205.
- Heasman, J. 2002. Morpholino Oligos: making sense of antisense? *Developmental Biology*. 243:209-214.
- Hellen, C and Sarnow, P. 2001. Internal ribosomal entry sites in eukaryotic mRNA molecules. *Gene and Development*. 15:1593-1612.
- Ho, T., Bundman, D., Armstrong, D. and Cooper. 2005. Transgenic mice expressing CUG-BP1 reproduce splicing mis-regulation observed in myotonic dystrophy. *Human Molecular Genetics*. 14(11):1539-1547.

- Ho, T., Charlet-B, N., Poulos, M., Singh, G., Swanson, M. and Cooper, T. 2004. Muscleblind proteins regulate alternative splicing. *The European Molecular Biology Organization Journal*. 23:3103-3112.
- Huang, H., Wahlin, K., McNally, M., Irving, N. and Adler, R. 2008. Developmental regulation of muscleblind-like (MBNL) gene expression in the chicken embryo retina. *Developmental dynamics*. 237:286-298.
- Isken, O. and Maquat, L. 2007. Quality control of eukaryotic mRNA: safeguarding cells from abnormal mRNA function. *Genes and Development*. 21(15):1833-1856.
- Jansen, G., Bachner, D., Coerwinkel, M., Wormskamp, N., Hameister, H. and Wieringa, B. 1995. Structural organization and developmental expression pattern of the mouse WD-repeat gene immediately upstream of the myotonic-dystrophy locus. *Human Molecular Genetics*. 4:843-852.
- Jiang, H., Mankodi, A., Swanson, M., Moxley, R. and Thornton, C. 2004. Myotonic dystrophy type 1 is associated with nuclear foci of mutant RNA, sequestration of muscleblind proteins and deregulated alternative splicing in neurons. *Human Molecular Genetics*. 13(24):3079-3088.
- Jin, S., Shimizu, M., Balasubramanyam, A. and Epstein, H. 2000. Myotonic dystrophy protein kinase (DMPK) induces actin cytoskeleton reorganization and apoptotic-like blebbing in lens cells. *Cell Motility and the Cytoskeleton*. 45:133-148.
- Jowett, T. and Lettice, L. 1994. Whole-mount in situ hybridization on zebrafish embryos using a mixture of digoxigenin- and fluorescein-labelled probes. *Trends in Genetics*. 10(3):73-74.
- Junghans, R. 2009. Dystrophia myotonica: why focus on foci? *European Journal of Human Genetics*. 17:543-553.
- Kaliman, P. and Llagostera, E. 2008. Myotonic dystrophy protein kinase (DMPK) and its role in the pathogenesis of myotonic dystrophy 1. *Cellular Signalling*. 20:1935-1941.

- Kalsotra, A., Xiao, X., Ward, A., Castle, J., Johnson, J., Burge, C. and Cooper, T. 2008. A postnatal switch of CELF and MBNL proteins reprograms alternative splicing in the developing heart. *Developmental Biology*. 105(51):20333-20338.
- Kanadia, R., Johnstone, K., Mankodi, A., Lungu, C., Thornton, C., Esson, D., Timmers, A., Hauswirth, W. and Swanson, M. 2003. A muscleblind knockout model for myotonic dystrophy. *Science*. 302:1978-1980.
- Kane, D. and Kimmel, C. 1993. The zebrafish midblastula transition. *Development* 119:447-456.
- Kawakami, K. and Shima, A. 1999. Identification of the Tol2 transposase of the medaka fish *Oryzias latipes* that catalyzes excision of a nonautonomous Tol2 element in zebrafish *Danio rerio*. *Gene*. 240:239-244.
- Kawakami, K. 2007. Tol2: a versatile gene transfer vector in vertebrates. *Genome Biology*. 8(Suppl 1):S7.
- Kimmel, C., Ballard, W., Kimmel, S., Ullmann, B. and Schilling, T. 1995. Stages of embryonic development of the Zebrafish. *Developmental Dynamics*. 203:253-310.
- Klesert, T., Cho, D., Clark, J., Maylie, J., Adelman, J., Snider, L., Yuen, E., Soriano, P. and Tapscott, S. 2000. Mice deficient in Six5 develop cataracts: implications for myotonic dystrophy. *Nature Genetics*. 25:105-109.
- Klesert, T., Otten, A., Bird, T. and Tapscott, S. 1997. Trinucleotide repeat expansion at the myotonic dystrophy locus reduces expression of DMAHP. *Nature Genetics*. 16:402-406.
- Koshelev, M., Sarma, S., Price, R., Wehrens, X. and Cooper, T. 2010. Heart-specific overexpression of CUGBP1 reproduces functional and molecular abnormalities of myotonic dystrophy type 1. *Human Molecular Genetics*. 19(6):1066-1075.
- Kress, C., Gautier-Courteille, C., Osborne, H., Babinet, C. and Paillard, L. 2007. Inactivation of CUGBP1/CELF1 causes growth, viability and spermatogenesis defects in mice. *Molecular and Cellular Biology*. 27(3):1146-1157.

- Kuszak, J. and Costello, M. 2006. Embryology and anatomy of human lenses, at Tasman, W. and Jaeger, E. Duane's Ophthalmology, (Vol. 1, Chapter 71A), Lippincott Williams and Wilkins.
- Kuszak, J., Zoltoski, R. and Tiedemann, C. 2004. Development of lens sutures. *International Journal of Developmental Biology*. 48:889-902.
- Kuyumcu-Martínez, N. Wang, G. and Cooper, T. 2007. Increased steady state levels of CUGBP1 in Myotonic Dystrophy 1 are due to PKC-mediated hyperphosphorylation. *Molecular Cell*. 28(1):68-78.
- Kwan, K., Fujimoto, E., Grabher, C., Mangum, B., Hardy, M., Campbell, D., Parant, J., Yost, J. Kanki, J. and Chien, C. 2007. The Tol2kit: a multisite gateway-based construction kit for Tol2 transposon transgenesis constructs. *Developmental Dynamics*. 236(11):3088-3099.
- Ladd, A., Charlet-B, N. and Cooper, T. 2001. The CELF family of RNA binding proteins is implicated in cell-specific and developmental regulated alternative splicing. *Molecular and Cellular Biology* 21(4):1285-1296.
- Lee, A., Fischer, R. and Fowler, V. 2000. Stabilization and remodeling of the membrane skeleton during lens fiber cell differentiation and maturation. *Developmental Dynamics* 217:257-270.
- Leyenaar, J., Camfield, P. and Camfield, C. 2005. A schematic approach to hypotonia in infancy. *Paediatrics and Child Health*. 10(7):397-400.
- Li, D., Xiang, H. Fass, U, and Zhang, X. 2001. Analysis of expression patterns of protein phosphatase-1 and phosphatase-2A in rat and bovine lenses. *Investigative Ophthalmology and Visual Science*. 42(11):2603-2609.
- Lin, X., Miller, J., Mankodi, A., Kanadia, R., Yuan, Y, Moxley, R., Swanson, M. and Thornton, C. 2006. Failure of MBNL1-dependent post-natal splicing transitions in myotonic dystrophy. *Human Molecular Genetics* 15(13):2087-2097.
- Lo, J., Lee, S., Xu, M., Liu, F., Ruan, H., Eun, A., He, Y., Ma, W., Wang, W., Wen, Z. and Peng, J. 2003. 15,000 unique zebrafish EST clusters and their future use in microarray for profiling gene expression patterns during embryogenesis. *Genome Research*. 13:455-466.

- Longman, C. 2006. Myotonic dystrophy. Royal College of Physicians of Edinburgh. 36:51-55.
- Maris, C., Dominguez, C. and Allain, F. 2005. The RNA recognition motif, a plastic RNA-binding platform to regulate post-transcriptional gene expression. *The FEBS Journal*. 272:2118-2131.
- Mathias, R., White, T. and Gong, X. 2010. Lens gap junctions in growth, differentiation and homeostasis. *Physiological Reviews* 90:179-206.
- Matsuoka, K., Nomura, K., and Hoshino, T. (1990). Mutagenic effects of brief exposure to bromodeoxyuridine on mouse FM3A cells. *Cell Tissue Kinetics*. 23:495-503.
- Meyer, A. and Schartl, M. 1999. Gene and genome duplications in vertebrates: the one-to-four (-to-eight in fish) rule and the evolution of novel gene functions. *Current Opinion in Cell Biology* 11:699-704.
- Mills, J., Stone, N., Erhardt, J. and Pittman, R. 1998. Apoptotic membrane blebbing is regulated by myosin light chain phosphorylation. *The Journal of Cell Biology*. 140(3):627-636.
- Milne, C. and Hodgkin, J. 1999. ETR-1, a homologue of a protein linked to myotonic dystrophy, is essential for muscle development in *Caenorhabditis elegans*. *Current Biology*. 9(21):1243-1246.
- Morcos, P. 2007. Achieving targeted and quantifiable alteration of mRNA splicing with morpholino oligos. *Biochemical and Biophysical Research Communications*. 358(2007):521-527.
- Nowak, R., Fischer, R., Zoltoski, R., Kuszak, J. and Fowler, V. 2009. Tropomodulin1 is required for membrane skeleton organization and hexagonal geometry of fiber cells in the mouse lens. *Journal of Cellular Biology*. 186(6):915-928.
- Orengo, J., Chambon, P., Metzger, D., Mosier, D. and Snipes, J. 2008. Expanded CTG repeats within the DMPK 3' UTR causes severe skeletal muscle wasting in an inducible mouse model for myotonic dystrophy. *Proceedings of the National Academy of Sciences*. 105(7):2646-2651.
- Otten, A. and Tapscott, S. 1995. Triplet repeat expansion in myotonic dystrophy alters the adjacent chromatin structure. *Proceedings of the National Academy of Sciences of the United States of America*. 92:5465-5469.

- Paillard, L. 2011. Inactivation of *Cugbp1* in mice and cataracts (e-mail). Rennes, FR. Université de Rennes. (luc.paillard@univ-rennes1.fr).
- Paillard, L., Omilli, F., Legagneux, V., Bassez, T., Maniey, D. and Osborne, H. 1998. EDEN and EDEN-BP, a cis element and an associated factor that mediate sequence-specific mRNA deadenylation in *Xenopus* embryos. *The European Molecular Biology Journal* 17(1):278-287.
- Pelegri, F. 2003. Maternal Factors in Zebrafish Development. *Developmental Dynamics*. 228:535-554.
- Philips, A., Timchenko, L., Cooper, T. 1998. Disruption of splicing regulated by a CUG-binding protein in myotonic dystrophy. *Science* 280:737-741.
- Postlethwait, J., Amores, A., Cresko, W., Singer, A., Yan, Y. 2004. Subfunction partitioning, the teleost radiation and the annotation of the human genome. *Trends in Genetics* 20:481-490.
- Ranum, L. and Cooper, T. 2006. RNA-mediated neuromuscular disorders. *The Annual Review of Neuroscience*. 29:59-77.
- Ranum, L and Day, J. 2004. Myotonic Dystrophy: RNA pathogenesis comes into focus. *The American Society of Human Genetics*. 74:793-804.
- Rao, P. and Maddala, R. 2006. The role of the lens actin cytoskeleton in fiber cell elongation and differentiation. *Seminars in cell and Developmental Biology*. 17:698-711.
- Rattenbacher, B., Beisang, D., Wiesner, D. Jeschke, J., von Hohenberg, M., Louis Vlasova, I. and Bohjanen, P. 2010. Analysis of CUGBP1 targets identifies GU-repeat sequences that mediate rapid mRNA decay. *Molecular and Cellular Biology* 30(16):3970-3980.
- Reza, H. and Yasuda, K. 2004. Lens differentiation and crystallin regulation: a chick model. *International Journal of Developmental Biology*. 48:805-817.
- Rhodes, J. 2011. Myotonic dystrophy 1 (DM1) and cataracts (e-mail). Norwich, UK. University of East Anglia. (j.Rhodes@uea.ac.uk).
- Ridley, A. and Hall, A. 1992. The small GTP-binding protein rho regulates the assembly of focal adhesions and actin stress fibers in response to growth factors. *Cell*. 70:389-399.

- Salisbury, E., Sakai, K., Schoser, B., Huichalaf, C., Schneider-Gold, C., Nguyen, H., Wang, G., Albrecht, J. and Timchenko, L. 2008. Ectopic expression of cyclin D3 corrects differentiation of DM1 myoblasts through activation of RNA CUG-binding protein, CUGBP1. *Experimental Cell Research*. 314:2266-2278.
- Sarnat, H. and Silbert, S. 1976. Maturation arrest of fetal muscle in neonatal myotonic dystrophy. A pathologic study of four cases. *Archives of Neurology*. 33(7):466-474.
- Schara, U. and Schoser, B. 2006. Myotonic dystrophies type 1 and 2: a summary on current aspects. *Seminars in Pediatric Neurology*. 13:71-79.
- Schmitt, E. and Dowling, J. 1994. Early eye morphogenesis in the zebrafish, *Brachydanio rerio*. *The Journal of Comparative Neurology*, 344: 532–542.
- Schoser, B. and Timchenko, L. 2010. Myotonic dystrophies 1 and 2: complex diseases with complex mechanisms. *Current Genomics*. 11:77-90.
- Shepard, K., Gerber, A., Jambhekar, A., Takizawa, P., Brown, P., Herschlag, D., DeRisi, J. and Vale, R. 2003 Widespread cytoplasmic mRNA transport in yeast: identification of 22 bud-localized transcripts using DNA microarray analysis. *Proceedings of the National Academy of Sciences*. 100(20):11429-11434.
- Silver, M., Vilos, G., Silver, M., Shaheed, W. and Turner, K. 1984. Morphologic and morphometric analyses of muscle in the neonatal myotonic dystrophy syndrome. *Human Pathology*. 15(12):1171-1182.
- Soules, K. and Link, B. 2005. Morphogenesis of the anterior segment in the zebrafish eye. *BMC Developmental Biology*. 5:12.
- Stickney, H., Barresi, M. and Devoto, S. Somite development in zebrafish. 2000. *Developmental Dynamics*. 219:287-303.
- Suzuki, H., Maegawa, S., Nishibu, T., Sugiyama, T., Yasuda, K. and Inoue, K. 2000. Vegetal localization of the maternal mRNA encoding an EDEN-BP/Bruno-like protein in zebrafish. *Mechanisms of development*. 93:205-209.

- Taneja, K., McCurrach, M., Schalling, M., Housman, D. and Singer, R. 1995. Foci of trinucleotide repeat transcripts in nuclei of myotonic dystrophy cells and tissues. *The Journal of Cell Biology*. 128(6):995-1002.
- Teplova, M., Song, J., Gaw, H., Teplov, A. and Patel, D. 2010. Structural insights into RNA recognition by the alternative-splicing regulator CUG-Binding Protein 1. *Structure*. 18:1364-1377.
- Terpe, K. 2003. Overview of tag protein fusions: from molecular and biochemical fundamentals to commercial systems. *Applied Microbiology and Biotechnology*. 60:523-533.
- Timchenko, L., Miller, J. Timchenko, N. DeVore, D., Datar, K., Lin, L., Roberts, R., Caskey, T. and Swanson, M. 1996. Identification of a (CUG)<sub>n</sub> triplet repeat RNA-binding protein and its expression in myotonic dystrophy. *Nucleic Acids Research*. 24(22):4407-4414.
- Timchenko, N., Iakova, P., Cai, Z., Smith, J. and Timchenko, L. 2001. Molecular basis for impaired muscle differentiation in myotonic dystrophy. *Molecular and Cellular Biology*. 21(20):6927-6938.
- Timchenko, N., Patel, R., Iakova, P., Cai, Z., Quan, L. Timchenko, L. 2004. Overexpression of CUG triplet repeat-binding protein, CUGBP1, in mice inhibits myogenesis. *The Journal of Biological Chemistry*. 279(13):13129-13139.
- Timchenko, L., Timchenko, N., Caskey, C. and Roberts, R. 1993. Novel proteins with binding specificity for DNA CTG repeats and RNA CUG repeats: implications for Myotonic dystrophy. *Human Molecular Genetics*. 5(1):115-121.
- Tingaud-Sequeira, A., Calusinska, M., Finn, R., Chauvigné, F. Lozano, J. and Cerdà, J. 2010. The zebrafish genome encodes the largest vertebrate repertoire of functional aquaporins with dual paralogy and substrate specificities similar to mammals. *BMC Evolutionary Biology*. 10:38.
- Tsang, S. and Gouras, P. 2006. Molecular physiology and pathology of the retina, at Tasman, W. and Jaeger, E. *Duane's Ophthalmology*, (Vol. 3, Chapter 2), Lippincott Williams and Wilkins.

- Tsuda, K., Kuwasako, K., Takahashi, M., Someya, T., Inoue, M., Terada, T, Kobayashi, N., Shirouzu, M., Kigawa, T., Tanaka, A., Sugano, S. Gunter, P., Muto, Y. and Yokoyama, S. 2009. Structural basis for the sequence-specific RNA-recognition mechanism of human CUG-BP1 RRM3. *Nucleic Acid Research*. 37(15):5151-5166.
- Turner, C. and Hilton-Jones, D. 2010. The myotonic dystrophies: diagnosis and management. *Journal of Neurology, Neurosurgery and Psychiatry*. 81:358-367.
- Uribe, R. and Gross, J. 2007. Immunohistochemistry on cryosections from embryonic and adult zebrafish eyes. *Cold Spring Harbor Protocols*. doi:10.1101/pdb.prot4779.
- Vanier, T. 1960. Dystrophia myotonica in childhood. *British Medical Journal*. 2:1284-1288.
- Varadaraj, K., Kumari S. & Mathias, R. 2007. Functional expression of aquaporins in embryonic, postnatal, and adult mouse lenses *Developmental Dynamics*. 236:1319-1328.
- Vlasova, I., Tahoe, N., Fan, D., Larrson, O. Rattenbacher, B., StemJohn, J., Vasdewani, J., Karypis, G. Reilly, C., Bitterman, P. and Bohjanen, P. 2008. Conserved GU-rich elements mediate mRNA decay by binding to CUG-binding protein 1. *Molecular Cell*. 29:263-270.
- Wang, G., Kearney, D., De Biasi, M. Taffet, G. and Cooper, T. 2007. Elevation of RNA-binding protein CUGBP1 is an early event in an inducible heart-specific mouse model of myotonic dystrophy. *The Journal of Clinical Investigation*. 117(10):2802-2811.
- Ward, A., Rimer, M., Killian, J., Dowling, J., and Cooper, T. 2010. CUGBP1 overexpression in mouse skeletal muscle reproduces features of myotonic dystrophy type 1. *Human Molecular Genetics*. 19(18):3614-3622.
- Weber, G. and Menko, S. 2006a. Actin filament organization regulates the induction of lens cell differentiation and survival. *Developmental Biology*. 295:714-729.
- Weber, G. and Menko, S. 2006b. Phosphatidylinositol 3-Kinase is necessary for lens fiber cell differentiation and survival. *Investigative Ophthalmology and Visual Science*. 47(10):4490-4499.

- Winchester, C., Ferrier, R., Sermoni, A., Clark, B. and Johnson, K. 1999. Characterization of the expression of DMPK and SIX5 in the human eye and implications for pathogenesis in myotonic dystrophy. *Human Molecular Genetics*. 8(3):481-492.
- WHO (World Health Organization) 2011. Visual impairment and blindness. Fact Sheet N° 282 (online). Consulted 3 Oct. 2011. <http://www.who.int/mediacentre/factsheets/fs282/en/index.html>.
- Wormstone, M. and Wride, M. 2011. The ocular lens: a classic model for development, physiology and disease. *Philosophical Transactions of The Royal Society*. 366:1190-1192.
- Wride, M. and Sanders, M. 1998. Nuclear degeneration in the developing lens and its regulations by TNF $\alpha$ . *Experimental Eye Research*. 66:371-383.
- Zhang, L., Lee, J., Wilusz, J. and Wilusz, C. 2008. The RNA-binding CUGBP1 regulates stability of tumor necrosis factor mRNA in muscle cells. *The Journal of Biological Chemistry*. 283(33):22457-22463.
- Zhou, M. and Gomez-Sanchez, C. 2000. Universal TA cloning. *Current Issues in Molecular Biology*. 2(1):1-7.

**Annexes**

**Annex 1. Signed accreditation**

**THE ROLE OF CUGBP1 IN THE DEVELOPMENT OF ZEBRAFISH  
LENS**

**Accreditation**

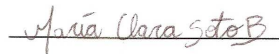
**Report of final graduation work presented to the School of Biology**

**Costa Rica Institute of Technology**

**In partial fulfillment of the requirements for the Degree of**

**Bachelor of Biotechnology Engineering**

**Tribunal Members**



**M.Sc. María Clara Soto-Bernardini  
Professor Costa Rica Institute of Technology**

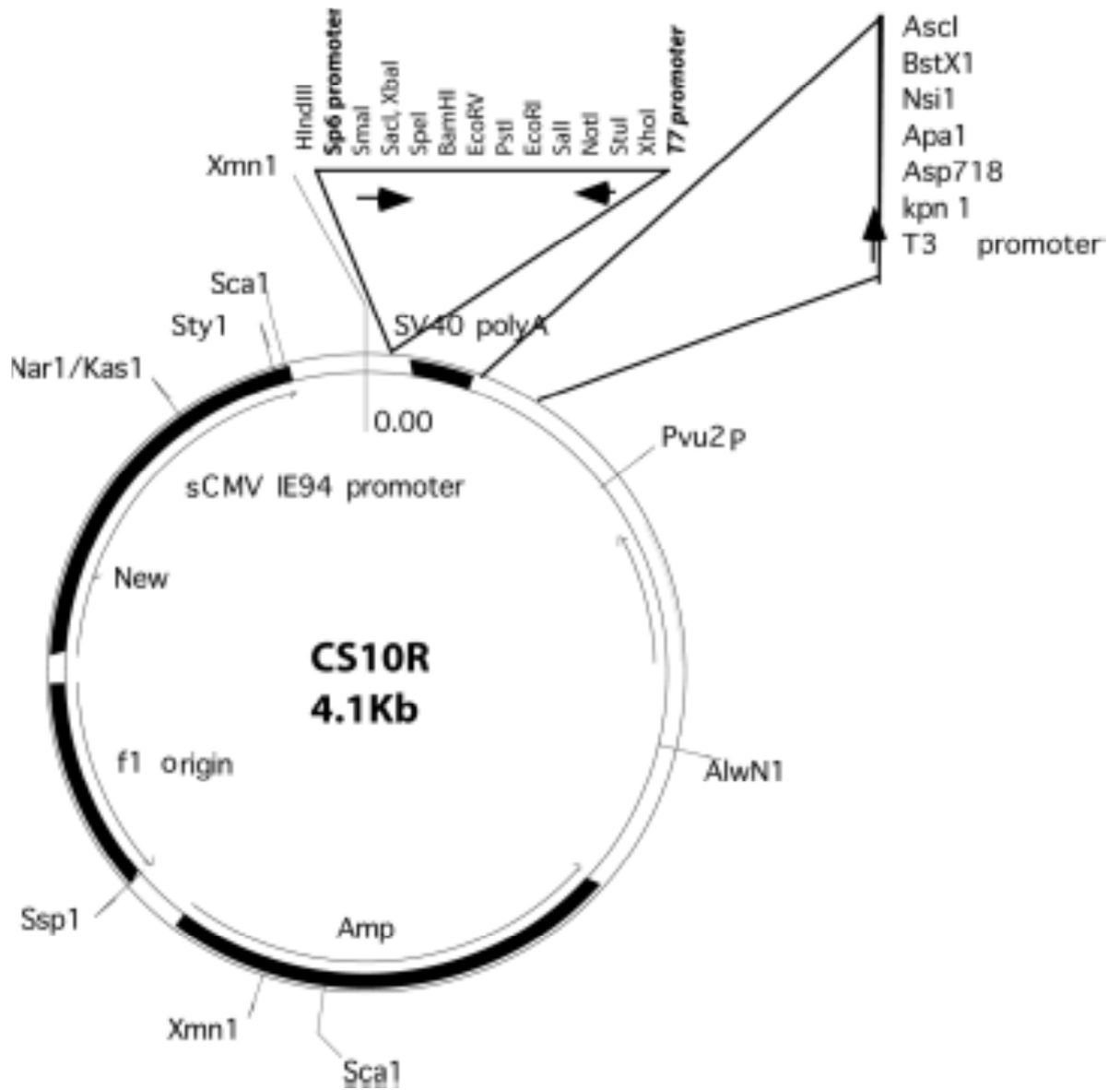


**Ph.D. Jeffrey Gross  
Professor University of Texas at Austin**



**M.Sc. Olga Rivas-Solano  
Lector**

Annex 2. CS10R plasmid



\*CS10R plasmid figure was provided by Dr. Chanjae Lee, Postdoc.

### Annex 3. Sequence alignment of *cugbp1* cDNA used for probe synthesis

		<b>Start codon</b>	
Probe	ATGAATGGGTCTCTGGACACCCAGACCAGCCCGACATTGATTCTATAAAGATGTTTGTG		60
DDBJ	ATGAATGGGTCTCTGGACACCCAGACCAGCCCGACATTGATTCTATAAAGATGTTTGTG		60
	*****		
Probe	GGTCAGATCCCTCGGACGTGGTCAGAGGATCAGCTGCGTGAGCTGTTTGAGCCCTATGGT		120
DDBJ	GGTCAGATCCCTCGGACGTGGTCAGAGGATCAGCTGCGTGAGCTGTTTGAGCCCTATGGT		120
	*****		
Probe	GCAGTTTATGAAATCAATGTTCTTCGTGACAGGAGTCAAAACCCCCACAGAGTAAAGGT		180
DDBJ	GCAGTTTATGAAATCAATGTTCTTCGTGACAGGAGTCAAAACCCCCACAGAGTAAAGGT		180
	*****		
Probe	TGTTGTTTTGTCACATATTACACCCGTAAGTCTGCATTAGAAGCACAAAATGCCCTTAC		240
DDBJ	TGTTGTTTTGTCACATATTACACCCGTAAGTCTGCATTAGAAGCACAAAATGCCCTTAC		240
	*****		
Probe	AACATGAAGATTCTTCCAGGGATGCATCATCCCATACAAATGAAACCTGCAGACAGTGAG		300
DDBJ	AACATGAAGATTCTTCCAGGGATGCATCATCCCATACAAATGAAACCTGCAGACAGTGAG		300
	*****		
Probe	AAAAACAATGCGGTAGAAGATAGAAAGCTGTTTGTGGAATGATTTCAAAGAAGTGCAAT		360
DDBJ	AAAAACAATGCGGTAGAAGATAGAAAGCTGTTTGTGGAATGATTTCAAAGAAGTGCAAT		360
	*****		
Probe	GAGAACGACATCAGACTCATGTTTTCTCCATATGGTCAAATCGAGGAGTGCCGCATATTG		420
DDBJ	GAGAACGACATCAGACTCATGTTTTCTCCATATGGTCAAATCGAGGAGTGCCGCATATTG		420
	*****		
Probe	AGAGGTCCAGACGGACTAAGCCGTGGCTGTCCTTCGTACATTCACAGCGAGACAGATG		480
DDBJ	AGAGGTCCAGACGGACTAAGCCGTGGCTGTCCTTCGTACATTCACAGCGAGACAGATG		480
	*****		
Probe	GCCCAGTCTGCCATCAAATCCATGCACCAGTCACAGACTATGGAGGGCTGTTCTTCTCCC		540
DDBJ	GCCCAGTCTGCCATCAAATCCATGCACCAGTCACAGACTATGGAGGGCTGTTCTTCTCCC		540
	*****		
Probe	ATCGTGGTGAAGTTTGCAGACACACAGAAGGATAAAGAACAGAAACGCATCGCCAGCAG		600
DDBJ	ATCGTGGTGAAGTTTGCAGACACACAGAAGGATAAAGAACAGAAACGCATCGCCAGCAG		600
	*****		
Probe	CTGCAGCAACAGATGCAACAGCTCAATGCTGCCTCCATGTGGGAAACCTTACAGGGCTG		660
DDBJ	CTGCAGCAACAGATGCAACAGCTCAATGCTGCCTCCATGTGGGAAACCTTACAGGGCTG		660
	*****		
Probe	AACTCACTGGGCCACAGTACCTTGCACCTT-----CTACAGCAGTCTGCTTCC		708
DDBJ	AACTCACTGGGCCACAGTACCTTGCACCTT <b>FATTTCAGCTT</b> CTACAGCAGTCTGCTTCC		720
	*****		
			
		<b>Relevant difference between sequences</b>	
		<b>Probe sequence lacks 12bp</b>	
Probe	TCTGAAATGCGCTCAACAATCTCCATCCAATGTCAGGTCTGAATGCCATGCAAAATCTG		768
DDBJ	TCTGAAATGCGCTCAACAATCTCCATCCAATGTCAGGTCTGAATGCCATGCAAAATCTG		780
	*****		
Probe	GCTGCATTAGCAGCAGCAGCGAGTGTACACAGGCCACACCTACAGGTAGCAGTGCAGCTG		828
DDBJ	GCTGCATTAGCAGCAGCAGCGAGTGTACACAGGCCACACCTACAGGTAGCAGTGCAGCTG		840
	*****		
Probe	ACCACCTCAGCTCCCCTCTCAGCGTCTCACCAGCTCAGGTACGCCCTCCGGACAGCCT		888
DDBJ	ACCACCTCAGCTCCCCTCTCAGCGTCTCACCAGCTCAGGTACGCCCTCCGGACAGCCT		900
	*****		

Probe	GCTCAATCTGCCTGGGATGCCTACAAGGCAGGTTCCCTCTCCACCTCCAGTACTAGTTCT	948
DDBJ	GCTCAATCTGCCTGGGATGCCTACAAGGCAGGTTCCCTCTCCACCTCCAGTACTAGTTCT	960
	*****	
Probe	TCTGTGAACCCCATGGCATCTTTAGGTGCTCTTCAGTCTCTTGCTGCGGGCGCTGGAGCA	1008
DDBJ	TCTGTGAACCCCATGGCATCTTTAGGTGCTCTTCAGTCTCTTGCTGCGGGCGCTGGAGCA	1020
	*****	
Probe	GGTCTCAACATGAGTTCCTTAGCAAGCATGGCTGCTCTAAATGGTGGTCTGGGCAGCGGA	1068
DDBJ	GGTCTCAACATGAGTTCCTTAGCAAGCATGGCTGCTCTAAATGGTGGTCTGGGCAGCGGA	1080
	*****	
Probe	GGTCTCTCCAACGGCTCTGGAAGCACTATGGAGGCTCTGACTCAGGCGGCCTATTCTGGG	1128
DDBJ	GGTCTCTCCAACGGCTCTGGAAGCACTATGGAGGCTCTGACTCAGGCGGCCTATTCTGGG	1140
	*****	
Probe	ATCCAGCAGTATGCAGCTGCCGCTCTGCCAAGCCTCTACAGTCAGAGTTTACTGTCCCAG	1188
DDBJ	ATCCAGCAGTATGCAGCTGCCGCTCTGCCAAGCCTCTACAGTCAGAGTTTACTGTCCCAG	1200
	*****	
Probe	CAGAACGTTAGCGTCTGTCGAGCCAAAAAGAAGGCCCTGAAGGAGCAAACCTGTTTCATC	1248
DDBJ	CAGAACGTTAGCGTCTGTCGAGCCAAAAAGAAGGCCCTGAAGGAGCAAACCTGTTTCATC	1260
	*****	
Probe	TACCATCTGCCACAGGAGTTTGGTGATCAGGATTGTTGCAGATGTTTATGCCTTTCGGC	1308
DDBJ	TACCATCTGCCACAGGAGTTTGGTGATCAGGATTGTTGCAGATGTTTATGCCTTTCGGC	1320
	*****	
Probe	AACGTCATCTCTGCCAAGGTCTTTATTGACAAACAGACCAACCTTAGCAAGTGTTTTGGC	1368
DDBJ	AACGTCATCTCTGCCAAGGTCTTTATTGACAAACAGACCAACCTTAGCAAGTGTTTTGGC	1380
	*****	
Probe	TTTGTAAGTTACGACAATCCAGTTTCGTCCAGGCAGCCATTCAGTCAATGAACGGTTTT	1428
DDBJ	TTTGTAAGTTACGACAATCCAGTTTCGTCCAGGCAGCCATTCAGTCAATGAACGGTTTT	1440
	*****	
Probe	CAGATTGGAATGAAGCGGCTGAAGGTGCAACTTAAACGATCTAAAAATGACAGCAAGCCA	1488
DDBJ	CAGATTGGAATGAAGCGGCTGAAGGTGCAACTTAAACGATCTAAAAATGACAGCAAGCCA	1500
	*****	

Probe	TACTGA	1494
DDBJ	TACTGA	1506
	*****	

\*DDBJ corresponds to previously reported *cugbp1* cDNA sequence by Suzuki *et al.* (2000), Accession number AB032726. Probe refers to the sequence of *cugbp1* cDNA used to make antisense and sense probes for the *in situ* hybridization assay.

**Annex 4.** Amino acid sequence from *cugbp1* cDNA used for probe synthesis

```

1   M N G S L D H P D Q P D I D S I K M F V
1   ATGAATGGGTCTCTGGACCACCCAGACCAGCCCGACATTGATTCTATAAAGATGTTTGTG
21  G Q I P R T W S E D Q L R E L F E P Y G
61  GGTCAGATCCCTCGGACGTGGTCAGAGGATCAGCTGCGTGAGCTGTTTGAGCCCTATGGT
41  A V Y E I N V L R D R S Q N P P Q S K G
121 GCAGTTTATGAAATCAATGTTCTTCGTGACAGGAGTCAAAACCCCCACAGAGTAAAGGT
61  C C F V T Y Y T R K S A L E A Q N A L H
181 TGTGTTTTGTACATATTACACCCGTAAGTCTGCATTAGAAGCACAAAATGCCCTTCAC
81  N M K I L P G M H H P I Q M K P A D S E
241 AACATGAAGATTCTTCCAGGGATGCATCATCCCATACAAAATGAAACCTGCAGACAGTGAG
101 K N N A V E D R K L F V G M I S K K C N
301 AAAACAATGCGGTAGAAGATAGAAAGCTGTTTGTGGAAATGATTTCAAAGAAGTGAAT
121 E N D I R L M F S P Y G Q I E E C R I L
361 GAGAACGACATCAGACTCATGTTTTCTCCATATGGTCAAATCGAGGAGTGCCCATATTG
141 R G P D G L S R G C A F V T F T A R Q M
421 AGAGGTCCAGACGGACTAAGCCGTGGCTGTGCCTTCGTACATTACAGCGAGACAGATG
161 A Q S A I K S M H Q S Q T M E G C S S P
481 GCCCAGTCTGCCATCAAATCCATGCACCAGTACAGACTATGGAGGGCTGTTCTTCTCCC
181 I V V K F A D T Q K D K E Q K R I A Q Q
541 ATCGTGGTGAAGTTTGCAGACACACAGAAGGATAAAGAACAGAAACGCATCGCCCAGCAG
201 L Q Q Q M Q Q L N A A S M W G N L T G L
601 CTGCAGCAACAGATGCAACAGCTCAATGCTGCCTCCATGTGGGAAACSTTACAGGGGCTG
221 N S L G P Q Y L A L L Q Q S A S S G N A
661 AACTCACTGGGCCACAGTACCTTGCACTTCTACAGCAGTCTGCTTCTCTGAAATGCG
241 L N N L H P M S G L N A M Q N L A A L A
721 CTCAACAATCTCCATCCAATGTCAGGTCTGAATGCCATGCAAAATCTGGCTGCATTAGCA
261 A A A S A T Q A T P T G S S A L T T S S
781 GCAGCAGCGAGTGCTACACAGGCCACACTACAGGTAGCAGTGCGCTGACCACCTCCAGC
281 S P L S V L T S S G T P S G Q P A Q S A
841 TCCCCTCAGCGTCTCACCAGTACAGGTACGCCCTCCGGACAGCCTGCTCAATCTGCC
301 W D A Y K A G S S P T S S T S S S V N P
901 TGGGATGCCTACAAGGCAGGTTCTCTCCCACCTCCAGTACTAGTTCTTCTGTGAACCC
321 M A S L G A L Q S L A A G A G A G L N M
961 ATGGCATCTTTAGGTGCTCTTCAGTCTCTGCTGCGGGCGCTGGAGCAGGTCTCAACATG
341 S S L A S M A A L N G G L G S G G L S N
1021 AGTTCCTTAGCAAGCATGGCTGCTCTAAATGGTGGTCTGGGCAGCGGAGGTCTCTCCAAC
361 G S G S T M E A L T Q A A Y S G I Q Q Y
1081 GGCTCTGGAAGCACTATGGAGGCTCTGACTCAGGCGCCTATTCTGGGATCCAGCAGTAT
381 A A A A L P S L Y S Q S L L S Q Q N V S
1141 GCAGCTGCCGCTCTGCCAAGCCTCTACAGTCAGAGTTTACTGTCCCAGCAGAACGTTAGC
401 A A G S Q K E G P E G A N L F I Y H L P
1201 GCTGTGGCAGCCAAAAAGAAGGCCCTGAAGGAGCAAACCTGTTTCATCTACCATCTGCCA
421 Q E F G D Q D L L Q M F M P F G N V I S
1261 CAGGAGTTTGGTGATCAGGATTTGTTGCAGATGTTTATGCCTTTCGGCAACGTCATCTCT
441 A K V F I D K Q T N L S K C F G F V S Y
1321 GCCAAGGTCTTTATTGACAAACAGACCAACCTTAGCAAGTGTGTTTGGCTTTGTAAGTTAC
461 D N P V S S Q A A I Q S M N G F Q I G M
1381 GACAATCCAGTTTTCGTCCAGGCAGCCATCAGTCAATGAACGGTTTTTCAGATTGGAATG
481 K R L K V Q L K R S K N D S K P Y - (497aa)
1441 AAGCGGCTGAAGGTGCAACTTAAACGATCTAAAAATGACAGCAAGCCATACTGA (1494bp)

```

\***RED** refers to amino acids, **BLUE** refers to nucleotides.

## Annex 5. Protocol for *cugbp1* probe synthesis

**DIG-labeled, single stranded RNA antisense and sense probes were generated according to: DIG RNA Labeling Mix, 10 x conc. Cat No. 11 277 073 910 (Roche Applied Science).**

[https://e-labdoc.roche.com/LFR\\_PublicDocs/ras/11277073910\\_en\\_21.pdf](https://e-labdoc.roche.com/LFR_PublicDocs/ras/11277073910_en_21.pdf)

### **Reagents:**

1. DIG RNA Labeling Mix, 10X conc. 10mM ATP, 10mM CTP, 10mM GTP, 6.5mM UTP, 3.5mM DIG-11-UTP, pH 7.5 (20°C).
2. Transcription buffer, 10X conc. 400mM Tris-HCl, pH 8.0 (20°C); 60mM MgCl<sub>2</sub>, 100mM dithiothreitol (DTT), 20mM spermidin.
3. RNase inhibitor 20U/μl
4. DNase I. 10U/μl

### **Methods:**

Note: Make sure to work under RNase-free conditions.

1. Add the following to a microfuge tube on ice:
  - 2μl (1μg) linearized plasmid DNA.
  - 2μl DIG RNA labeling mix, 10X
  - 2μl Transcription buffer, 10X.
  - 1μl RNase inhibitor (adding this reagent is not mentioned in the original protocol).
  - 2μl (20U/μl) RNA polymerase T7 or SP6 for antisense or sense probes, respectively.
  - 11μl sterile RNase free double distilled water to a final volume of 20μl.
2. Mix and centrifuge briefly.
3. Incubate for 2 hours at 37°C.
4. Add 2μl DNase I, RNase-free to remove template DNA.
5. Incubate for 15 minutes at 37°C.
6. Add 2μl 0.2M EDTA (pH 8.0) to stop the reaction.

## Annex 6. Whole mount RNA *in situ* hybridization protocol

### A. Fixation and permeabilization

#### Fixation

Dechorionate embryos prior to fixing

Fix embryos in 4% PFA, overnight at 4°C

Wash 3X with PSB 5 min at RT

Add 100% MEOH, sit RT 5 min and then aliquot embryos (12-15) into tubes with fresh 100% MEOH. Store at -20 for at least 30 min.

#### Rehydration (all at RT)

5 min 50% MEOH/PBST

5 min 30% MeOH/PBST

2X 5 min PBST

Collagenase (1mg/ml PBST) (in Tupperware at bottom of -20 5.5hrs b/f PK)

2 DAY 1 HOUR

3 DAY 2 HOUR

#### PK Treatment

PK stocks 2 mg/mL (add 5 µL/ml PBST for 10 µg/mL)

Digest with PK (10µ g/mL PBST) at RT

Developmental period	Digestion time
> 10HRS	7 min
1 somite	10 min
24 hpf	12 min
33 hpf	14 min
36 hpf	15 min
48-50 hpf	20 min
60 hpf	27 min
72 hpf	30 min

Rinse 2X 5 min PBST at RT

Refix in PFA 25 min at RT

Wash 2X 5 min PBST at RT

### B. Hybridization

Prehyb in Hyb solution at 55°C for 3-5 hours

#### Hybridization

Remove prehyb and add Hyb with probe

Heat Hyb+probe solution 10 min at 68°C before adding. (10 µl of synthesized probe in 1ml of Hyb buffer = Hyb+probe solution). 500 µl per tube is recommended.  
Incubate overnight at 55 °C

### **Washes**

Make solutions for washes before starting:

Solution 1:

2X SSCT from stock 20X SSC (1:10)

$$V_1 C_1 = V_2 C_2$$

Add 50µl Tween

Solution 2:

0,2X SSCT (1:100)

$$V_1 C_1 = V_2 C_2$$

$$V_1 20X = 50ml * 0,2X$$

$$V_1 = 0,5ml = 500\mu l$$

Add 50µl Tween

Solution 3:

50% formamide /2X SSCT

25ml formamide + 25ml 2X SSCT

Heat every solution before using in the following indicated temperatures

Remove Probe and save at -20°C (can reuse 3-4 times)

Wash 20 min at 55°C in 50% formamide/2XSSCT

Wash 3X 10 min at 37°C in 2X SSCT

Wash 2X 15 min at 55°C in 0,2X SSCT

Wash 5 min at 37°C in PBST

Wash 5 min at RT in PBST

### **C. Anti-digoxigenin alkaline phosphatase (AP) labeling**

#### **Detection**

Block 1 (or more) at RT in Block

Remove block and add primary Ab/block (preincubated)

Leave for 4 hours at room temperature or overnight at 4°C

#### **D. Colorization**

##### **Washes**

4X 20 min at RT with PBST

If Ab added for 4 hours at RT, can leave in last PBST overnight at 4°C

3X 5 min RT in Staining buffer

5ml 1M Tris 9,5

2,5ml 1M MgCl<sub>2</sub>  
5ml 1M NaCl  
50µl T-20 + to 50ml with H<sub>2</sub>O  
Incubate in NBT/BCIP stain (500µl) at RT in dark. Check embryos every 30 min  
Wash 3X after desired staining level in PBS, RT.  
Fix in PFA at 4°C to preserve

#### **E. Solutions**

**4% PFA:** 2g PFA in 50ml PBS. Cover with foil, stir and heat to dissolve. Takes about 10-15min, cool on ice. Store at 4°C for 7days.

**PBST:** 1X PBS with 0.1% Tween20.

**SSCT:** SSC with 0.1% Tween20, 20X Stock.

**HYB:** 50ml: 50% formamide 25ml, 5X SSC (12.5ml of 20X), 0.1% Tween20 50µl, 5mg/ml yeast tRNA, 50µg/ml heparin. Can store at -20°C for years.

**Block:** 500µl NGS into 10ml of 1X PBTD.

Other: 2g BSA, 2ml DMSO, 600µl Triton X-100, 500µl Tween20, 4ml NGS, 1X PBS.

**Staining Buffer:** 50ml, store at 4°C for 2 weeks. 100mM, Tris 9.5 (5ml, 1M), 50mM MgCl<sub>2</sub> (2.5ml 1M), 100mM NaCl (5ml 1M). 0.1% Tween20 (50µl), H<sub>2</sub>O to 50ml.

**NBT/BCIP:** 1 tablet /10ml H<sub>2</sub>O plus 10 µl Tween20. Freeze in 1ml aliquots at -20 °C in dark.

## **Annex 7. Immunohistochemistry protocol**

From Uribe and Gross (2007).

### **Materials:**

- **Reagents**

1. DMSO (Dimethylsulfoxide may be harmful if absorbed through the skin or if its fumes inhaled). Safety directions: wear appropriate gloves and safety glasses. Use in a chemical fume hood to prevent inhalation. Store in a tightly closed container, DMSO is combustible. Keep away from heat, sparks, and open flame.
2. Normal Goat Serum (NGS)
3. Paraformaldehyde, 4% dissolved in 1X PBS
4. Phosphate Buffered Solution (PBS), 1X
5. Primary Antibody
6. Secondary Antibody
7. Sucrose, 25% and 35% both dissolved in 1X PBS
8. Tween-20
9. Vectashield Mounting Medium (Vector Labs)

- **Equipment**

1. Coverslips, No. 1 thickness
2. Cryostat
3. Cryomolds (Tissue Tek)
4. Eppendorf Tubes, 1.5 ml
5. Humid Chamber: A Tupperware container with air-sealed lock and wet paper towels or kimwipes inside to provide moisture
6. Microslides, 1.0 mm thick, pre-cleaned and gelatin-coated
7. PAP pen (Sigma)
8. Razor Blade
9. Slide jar or Coplin jar
10. Tissue Freezing Medium (Triangle Biomedical Sciences (TBS))

### **Methods:**

- **Fixation**

1. Collect and fix whole zebrafish embryos or surgically removed adult eyes in 4% Paraformaldehyde (PFA) at 4°C overnight (or for more time) or at room temperature

for 4-6 hours in eppendorf tubes. If collecting embryos before 48hpf, make sure to remove the chorion with forceps prior fixation.

2. Remove 4% PFA by using a pipette to gently remove solution. Rinse in 1x PBS 3 times, 5 minutes each for total time of 15 minutes.
3. Soak specimen in 25% Sucrose dissolved in 1x PBS at room temperature until embryos or eyes sink to the bottom of the tube (time varies, but may take up to 2.5 hours).
4. Remove 25% sucrose and add 35% sucrose dissolved in 1x PBS. Soak at room temperature until embryos or eyes sink to the bottom of the tube (again, time varies). Pause point: may leave in 35% sucrose at 4 °C for up to a week.

- **Cryosectioning**

5. To line fish up in cryomolds:
  - a. Prepare desired amount of cryomolds by filling cryomolds with Tissue Freezing Medium (TFM) at room temperature. Take care not to get any bubbles in the molds.
  - b. Using one TFM-filled mold as a transfer dish, remove specimen(s) from Eppendorf tube and stir gently around in TFM-filled mold to wash out 35% Sucrose.
  - c. Transfer specimen(s) to a new TFM-filled cryomold. With a blunt needle, submerge embryos in the TFM and move embryos into a row that faces one side of the mold: line up fish head first such that their tails are facing center of mold and their heads are against the wall. Keep embryos as close to one another as possible and in a straight line. For adult eye, orient in mold with lens facing outward. If not interested in lens tissue, one may remove the lens during this step for easier cryosectioning.
  - d. Carefully transfer to -80 °C to freeze. Pause point: may store at -80°C indefinitely.
6. To prepare for cryosectioning:
  - a. Set Cryostat to -20 °C. Remove specimen block from cryomold inside the cryostat. Using a razor blade, carefully trim away all excess frozen medium around specimen.
  - b. Place TFM on center of chilled cryostage to which your sample will be placed. Carefully place trimmed specimen onto this TFM with side to be sectioned facing up. Ensure that specimen block is as straight as possible. Add more TFM around periphery of sample on stage. Freeze for 1-2 minutes prior to sectioning.
  - c. Transfer cryostage to cryostage holder.

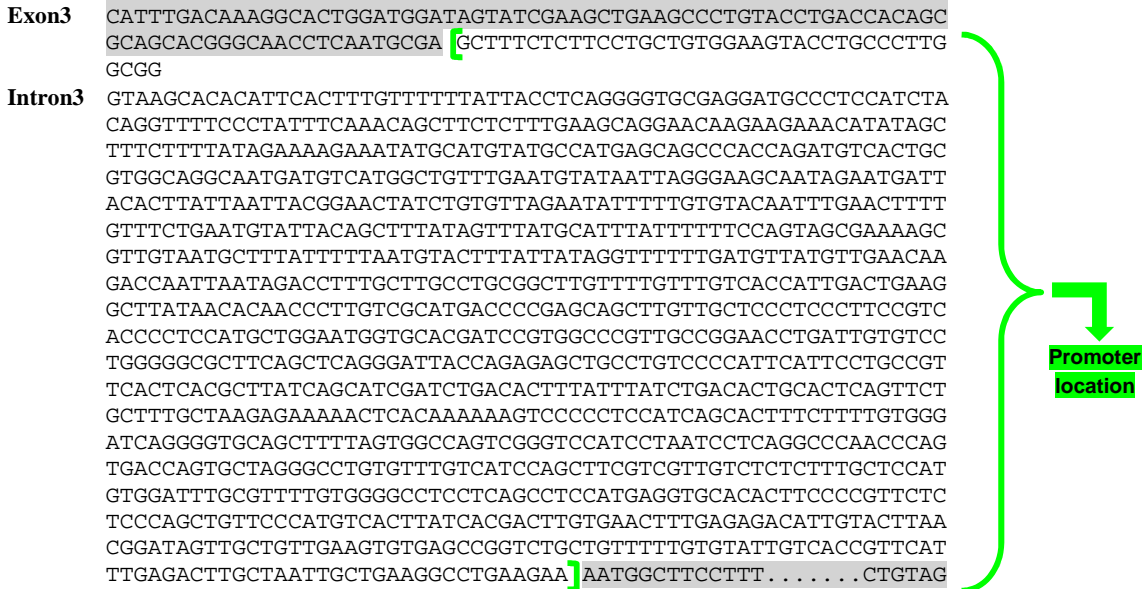
7. Using the trim function on the cryostat set to between 30-60 microns, trim through block until a uniform section is made in the appropriate part of the sample. Quickly transfer section to room temperature gelatin-coated slide by allowing cryosection to gently melt onto slide. Be careful not to section past the area of interest by checking sections using a basic light microscope.
8. Continue to section at 8-12 micron thickness. Gently transfer each section to room temperature gelatin-coated slide by allowing section to melt onto slide.
9. Allow sections to adhere to slide at room temperature for at least 2 hours prior to immunostaining. Pause point: slides may be stored at -20 °C for up to a month. In this case, slides should be brought to room temperature prior to beginning immunostaining.

- **Immunostaining**

10. Circle area of interest on slides with hydrophobic PAP pen. This will form a well to hold block and antibody solutions. Be careful not to touch sections. Rehydrate slides in PBTD, [0.1% Tween-20, 1% DMSO in 1 X PBS] at room temperature for 2-3 min in Coplin Jar.
11. Remove slides from PBTD, drain excess off slide and place slides in humid chamber. From this point forward, it is critical to not let the slides dry.
12. Gently pipette ~200-300 microliters of Block [5% NGS in PBTD] onto slides (Note: solution volume depends on how large area of interest).
13. Incubate at room temperature for 1-2 hours.
14. Remove Block from slides by draining off excess onto kimwipes
15. Add ~200-300 microliters of primary antibody diluted in block.
16. Incubate in humid chamber overnight at 4 °C.
17. Remove primary antibody by rinsing slides in PBTD 3 times at room temperature for 10 minutes each.
18. Drain excess PBTD, return slides to humid chamber and place 200-300 microliters of appropriate concentration of secondary antibody diluted in block.
19. Incubate at room temperature for 1-2 hours.
20. Remove secondary antibody by rinsing slides in PBTD 3 times at room temperature for 10 minutes each.
21. Drain as much PBTD from slide as possible. Add one drop of Vectashield mounting medium directly onto sections.
22. Carefully place no. 1 thickness coverslip on slide. Allow Vectashield to harden at room temperature for at least 3 hours before imaging. Pause point; may place slides in 4°C for up to 1 week until ready to image.
23. Image on confocal or fluorescent microscope.

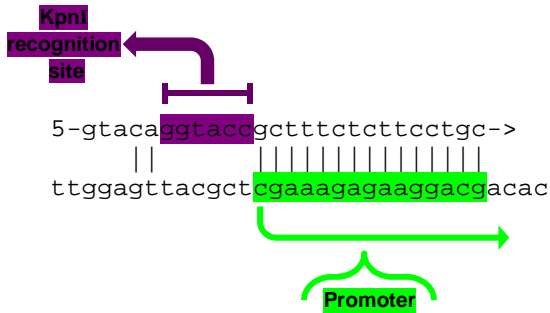
## Annex 8. *cugbp1* promoter sequence and location

Gene ID: ENSDARG0000005315  
 Transcript ID: ENSDART00000018448

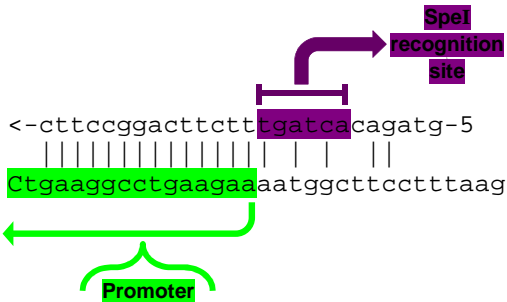


### Primers used to amplify the 1152bp *cugbp1* promoter

Primer 1: 5'-gtacaggtaccgctttctcttctcctgc



Primer 2: 5'-gtagacactagtttcttcaggccttc



## Annex 9. RT-PCR Morpholino Activity

### A. Morpholino disrupted splicing by removing exon4

Exon 4 (188bp)

AAGCAAGAAG **ATGAATGGGTCTCTGGACCAC**CCAGACCAGCCCGACATTGATTCTATAAA  
GATGTTTGTGGGTCAGATCCCTCGGACGTGGTCAGAGGATCAGCTGCGTGAGCTGTTTGA  
GCCCTATGGTGACGTTTATGAAATCAATGTTCTTCGTGACAGGAGTCAGAACCCCCACA  
GAGTAAAG

Region recognized by primer for RT-PCR

Intron 4 (289bp)

gtactttacagatgggettccaacttaatacagtttgttccaaateccagtgagcaeatg  
 eatatgeatacacaattgtgeagttataaaaactatgcttaaaaaagttgtcttgggatg  
 eaggatacttcagttgectectttttggaaacagtecccatagtggaatgtgcaaatgat  
 ttctcgtagagatgctcaactggtgtttggaaactgtgttctagagagtggtctctgtgga  
 aatggttgcatecttggacgtgattcatagaccatttattgcatttgeag

Exon5 is excised from mature mRNA

Exon 5 (83bp)

GTTGTTCTTTTCTCACATATTACACCCGTAAGTCTGCATTAGAAGCACAAAATGCCCTTC  
 ACAACATGAAC **ATTCTTCCAGGG**

Intron 5 (240bp)

**gtgagaaaatgtt**tttattttattatatcaataatecattaattctctgtgtgtgtea  
 aatgacctggcatctetaceaatttatgtgttttaaaatacaatcatatataaageaeata  
 tgagataatttcataatagcattttcagtaacccaaaggagctgtggaagatgttccaga  
 tttctcatgaggggtgggaaatgtcageattaagteacataattttatttttttcttcag

Regions recognized and where MO binds

Splice junction of exon5/intron5

Exon 6 (49)

ATGCATCATCCCATACAAATGAAA**CCTGCAGACAGTGAGAAAAACAATG**

Region recognized by primer for RT-PCR

In silico PCR Primer(s) search for: 2

1 5'-atgaatgggtctctggaccac

Position: 11->31 21bp 100%

5-atgaatgggtctctggaccac->  
 |||  
 tctacttaccagagacctggtgggtc

2 5'-cattgtttttctcactgtctgcagg

Position: 213<-237 25bp 100%

<-ggacgtctgtcactctttttgttac-5  
 |||  
 aacctgcagacagtgagaaaaacaatg

1 5'-atgaatgggtctctggaccac

2 5'-cattgtttttctcactgtctgcagg

PCR product size: 227bp

\***Blue Outlines:** regions amplified by RT-PCR.  
**Cross out:** regions deleted by splicing.

## Annex 9. RT-PCR Morpholino Activity

### B. Mismatch morpholino did not disrupt splicing

Exon 4 (188bp) Region recognized by primer for RT-PCR

AAGCAAGAAG **ATGAATGGGTCTCTGGACCAC**CCAGACCAGCCCGACATTGATTCTATAAA  
GATGTTTGTGGGTGAGATCCCTCGGACGTGGTCAGAGGATCAGCTGCGTGAGCTGTTTGA  
GCCCTATGGTGCAGTTTATGAAATCAATGTTCTTCGTGACAGGAGTCAGAACCCCCACA  
GAGTAAAG

Intron 4 (289bp)

gtactttaacagatgggettccaacttaatacagtttgttccaaateccagtgageaeattg  
 eatatgcatacacaattgtgcagttataaaaactatgcttaaaaaagttgttettgggatg  
 eaggatacttcagttgeectctttttggaaecagteccatagtggaatgtgceaatgat  
 ttctegttagagatgeteactgggtgtttggaaactgtgttctagagagtggtctctgtgga  
 aatgttgcatecttggacgtgattcatagaeattttattgeatttgcag

Exon 5 (83bp)

GTTGTTGTTTTGTACATATTACACCCGTAAGTCTGCATTAGAAGCACAAAATGCCCTTC  
ACAACATGAAGATPCTTCCAGGG

Intron 5 (240bp)

**gtgagaaaatgctt**tttattttattataatecaataatecattaattctctctgtgtgctea  
 aatgacctggcattctaceaatatttattgcttttaaaaatacateatataaageacataat  
 tgagataattteataatageattttteagtaeaeceaaaggagetgtggaagatgtteaga  
 tttctcatgaggggtgggaaatgceageattaagteacataattttatttttttctteag

Exon 6 (49bp)

ATGCATCATCCCATACAAATGAAA**CCTGCAGACAGTGAGAAAAACAATC**

In silico PCR Primer(s) search for: 1

```

1 5'-atgaatgggtctctggaccac
Position: 11->31      21bp   100%

5-atgaatgggtctctggaccac->
 |||||
tctacttaccagagacctggtgggtc

2 5'-cattgtttttctcactgtctgcagg
Position: 296<-320   25bp   100%

<-ggacgtctgtcactctttttgttac-5
 |||||
aacctgcagacagtgagaaaaacaatg
    
```

```

1 5'-atgaatgggtctctggaccac
2 5'-cattgtttttctcactgtctgcagg
    
```

PCR product size: 310bp

\***Blue Outlines:** amplified regions by RT-PCR.  
**Cross out:** regions deleted by splicing.

**Annex 10. BrdU+ cell counts**

Eye	Section n = 27	24 to 26hpf Number of BrdU+ cells		72 to 74hpf Number of BrdU+ cells	
		<i>cugbp1</i> -MM	<i>cugbp1</i> -MO	<i>cugbp1</i> -MM	<i>cugbp1</i> -MO
<b>1</b>	1	9	5	14	6
	2	7	5	13	7
	3	6	5	10	7
<b>2</b>	1	8	7	13	7
	2	8	9	12	8
	3	6	6	10	7
<b>3</b>	1	8	9	10	7
	2	8	7	3	7
	3	4	6	9	9
<b>4</b>	1	7	8	8	7
	2	9	10	8	7
	3	7	7	7	8
<b>5</b>	1	7	7	8	8
	2	8	9	9	9
	3	7	7	9	12
<b>6</b>	1	8	8	15	8
	2	8	9	13	12
	3	2	9	15	14
<b>7</b>	1	8	11	5	8
	2	7	13	7	8
	3	5	10	5	10
<b>8</b>	1	13	9	7	7
	2	14	6	8	6
	3	7	4	5	6
<b>9</b>	1	12	9	8	7
	2	13	11	9	8
	3	11	9	9	9
Mean ± SEM		8.037 ± 0.5188	7.963 ± 0.4117	9.222 ± 0.6047	8.111 ± 0.3711